

Galactic Globular Cluster Metallicity Scale From the Ca II Triplet I. Catalog

Glen A. Rutledge, James E. Hesser¹, and Peter B. Stetson

National Research Council of Canada, Herzberg Institute of Astrophysics,
Dominion Astrophysical Observatory, 5071 W. Saanich Rd., RR5, Victoria, BC V8X 4M6, Canada
Electronic mail: firstname.lastname@hia.nrc.ca

Mario Mateo¹

Department of Astronomy, University of Michigan, 821 Dennison Bldg. Ann Arbor, MI
48109-1090
Electronic mail: mateo@astro.lsa.umich.edu

Luc Simard

Department of Physics and Astronomy, University of Victoria, P.O. Box 3055, Victoria, BC
V8W 3P6, Canada
Electronic mail: simard@beluga.phys.uvic.ca

Michael Bolte

UCO/Lick Observatory, University of California, Santa Cruz, CA 95064
Electronic mail: bolte@lick.ucsc.edu

Eileen D. Friel

Maria Mitchell Observatory, 3 Vestal St. Nantucket, MA 02554
Electronic mail: efriel@mmo.org

and

Yannick Copin

Ecole Normale Supérieure de Lyon, 46, allée d'Italie, 69364 Lyon cedex 07
Electronic mail: Yannick.Copin@ens.ens-lyon.fr

ABSTRACT

We have obtained 2640 CCD spectra with resolution $\sim 4 \text{ \AA}$ in the region 7250–9000 \AA for 976 stars lying near the red giant branches in color-magnitude diagrams of 52 Galactic globular clusters. Radial velocities of $\sim 16 \text{ km s}^{-1}$ accuracy per star determined from the spectra are combined with other criteria to assess quantitative membership probabilities. Measurements of the equivalent widths of the infrared

¹Visiting Astronomer, Las Campanas Observatory.

calcium triplet lines yield a relative metal-abundance ranking with a precision that compares favorably to other techniques. Regressions between our system and those of others are derived. Our reduction procedures are discussed in detail, and the resultant catalog of derived velocities and equivalent widths is presented. The metal abundances derived from these data will be the subject of a future paper.

1. Introduction

The absolute and relative ages of globular clusters in the Galaxy and in the nearest Local Group galaxies provide unique constraints on cosmology and early epochs of galaxy formation. However, the ages of globular clusters cannot be determined, even in a differential sense, without knowledge to high precision of their chemical composition (or metallicity). An error of 0.3 dex in the overall heavy element abundance of a cluster — usually denoted by $[\text{Fe}/\text{H}]$ — corresponds to an error of about 3 Gyr in the age derived from fitting an otherwise absolutely correct isochrone to main-sequence photometry of perfect accuracy. Even for some bright, nearby clusters, recent careful abundance measurements differ by more than this amount, which reflects the challenges of detailed analyses from stellar spectra. Without reliable metallicity determinations for many clusters, and especially for the crucial clusters near the Galactic center, we cannot hope to test models of Milky Way formation in a compelling fashion.

In 1989 we carried out a photometric and spectroscopic program at Las Campanas Observatory that was aimed at developing a highly precise relative ranking of globular cluster abundances from measurements of the Ca II triplet lines in the near infrared spectra of 12-15 probable red giant members of each of 52 clusters. The early work of Armandroff and Zinn (1988, hereafter AZ88) used the Ca II triplet lines formed in the integrated light of Galactic globular clusters, from which it appeared that an internal precision of 0.15 dex per star was possible provided chromospherically active stars were avoided. Moreover, by working in the infrared, sensitivity would be reduced to the high and variable reddening towards many clusters of great interest for the evaluation of formation scenarios for the Galaxy. At the time the project began, it was a relatively unexplored empirical approach which had been applied primarily to integrated or composite light, and our goal was to acquire data of such quality on individual giants that we could assess thoroughly and independently the optimum procedures and relative merits of this technique.

Since we undertook this project, several others have exploited with great effect the Ca II triplet technique applied to individual giants for estimating abundances of globular clusters, with particular emphasis upon distant and/or sparse objects (see, e.g., Armandroff and Da Costa 1991 [hereafter AD91], Olszewski et al. 1991, Armandroff, Da Costa and Zinn 1992 [hereafter ADZ92], Da Costa, Armandroff and Norris 1992 [hereafter DAN92], Suntzeff et al. 1992 [hereafter S92], 1993 [hereafter S93], Da Costa and Armandroff 1995 [hereafter DA95], Geisler et al. 1995 [hereafter G95], and Suntzeff and Kraft 1996 [hereafter SK96]). While these programs have

provided numerous results of widespread interest, the original motivation of our program remains. In this paper we describe how we optimized our reduction of the spectral data (§3) to provide radial velocities (§4) and equivalent widths (§5), compare our prescriptions and results with those of other workers (§5.5), and present a catalog of the individual stellar results (§7). Following the AD91 prescription, the cluster reduced equivalent widths, W' , are calculated (§6). A companion paper discusses the calibration of our cluster W' values to $[\text{Fe}/\text{H}]$ values, and the astrophysical implications of our results.

2. Observations

Spectra were obtained at the Las Campanas Observatory’s 2.5m Dupont telescope equipped with the modular spectrograph and the Canon 85mm f/1.2 camera. A GG495 filter was used to block the second and higher spectral orders. The TI#2 detector (800×800 thinned CCD; readout noise = $11 e^- \text{ pix}^{-1}$; gain = $1.35 e^-$ per ADU; scale = $0.85'' \text{ pix}^{-1}$) was used with an 831 l mm^{-1} (8000 \AA blaze) grating, which produced a dispersion of $2.19 \text{ \AA pix}^{-1}$ and spectral coverage from $7250\text{--}9000 \text{ \AA}$. The $8' \times 1.25''$ slit provided an instrumental spectral resolution of $\sim 4 \text{ \AA}$.

Observations were obtained on two 1989 runs: 1) April 13–20 and 2) July 13–21. Of the 52 clusters observed, 23 were observed during the first run only, 26 were observed during the second run only, and three were observed during both runs to check the consistency of our results. In each cluster, spectra were obtained for 10 to 20 stars selected from published color-magnitude diagrams (CMDs) to lie on the red giant branch (RGB) and, if proper motion data were available, to be likely proper-motion members. Probable asymptotic branch (AGB) stars were avoided, as were horizontal branch (HB) stars, and known variable stars near the RGB tip. Slit positions were chosen to contain at least two stars per spectrograph rotation.

Each star was observed two or three times consecutively, with an Fe–Ar arc taken before and after each sequence for the wavelength calibration. Occasionally the same star was observed on different nights, or with a different slit orientation, to check for systematic effects in our results. Exposure times for a single frame ranged from 2 min to 17 min.

The adopted data for the clusters we observed are presented in Table 1, where the columns are, respectively: 1) the running cluster identification number used in Figure 4; 2,3,4) the NGC, other cluster, and IAU names; 5,6) Galactic longitude and latitude in degrees; 7) the visual magnitude of the horizontal branch level, V_{HB} ; 8,9) the radial velocity and associated uncertainty, v_H and $\sigma(v_H)$; 10) the mean reddening for the cluster; 11) the central velocity dispersion from Pryor and Meylan (1993, hereafter PM93); 12,13) the metallicity and associated uncertainty of the cluster taken from Zinn and West (1984, hereafter ZW84); 14) the standard deviation adopted for the V photometry, which is used in §6 during the robust line fitting technique to determine the reduced equivalent width, W' , of the cluster (this value is estimated from the scatter in the CMDs published by the authors from which we adopted the photometry [see Appendix A], and represents

a combination of both the photometric errors and differential reddening within the cluster). The data from columns 5-10 were taken from a 1994 version of the Harris (1996) electronic MWGC catalog (hereafter referred to as the MWGC catalog), and references can be found in Appendix A.

3. Extractions and Calibrations

Since there was not an overscan region on our detector, the bias level of each frame was estimated from the mean level of the bias frames. This was a satisfactory approach for run one, where the bias level remained constant at ~ 550 ADU. However, due to a CCD electronics problem, the bias level in run two varied between 540 and 650 ADU on timescales of a few hours.

The illumination response along the slit resulted in a $\sim 21\%$ reduction in transmission from one end of the slit to the other. This effect was independent of slit rotation, and was found in both the object and flat field frames. By normalizing the flat field frames along the dispersion axis only (with the IRAF² task **response**), we could use them to remove the illumination response. For run two, where the bias level of each frame was uncertain, the illumination response may not have been removed correctly by this procedure. For these data we chose sky windows on both sides of, and immediately adjacent to, the stellar spectrum being extracted so that a low-order fit between the windows would account satisfactorily for any residual errors in the illumination response and bias level. Spectra in crowded fields were not extracted from run two data when windows appropriate for accurate sky subtraction could not be identified adjacent to a spectrum.

We removed cosmic rays were removed with the IRAF task **cosmicrays**, while any remaining cosmic rays seen in a visual inspection of the two-dimensional images we removed using IRAF’s **imedit**. We rectified residual distortion in the images (manifested by curved night sky lines near the edges of the frames) with the IRAF tasks **fitcoords** and **transform**.

Several bad columns and pixels were noted before the observations were taken, and stars were placed on the slit to avoid them. Several other unreliable sections of the CCD were mapped and avoided during spectral extractions. Charge skimmed columns, in which the percentage of electrons skimmed varied with time, were also discovered during the reductions; no stars were extracted which fell on these columns.

Spectral extractions were made with IRAF’s **apextract** tasks. Two sky windows, with a minimum of 15 pixels each, were chosen on either side of the star, and a linear fit between the median values in the two windows was used to define the sky level at the position of the stellar spectrum. The windows were chosen to be as close to the star as possible, while still adhering to the run two constraints mentioned earlier. To facilitate the placement of the sky windows, a maximum of one bad column or charge skimmed column was permitted to lie in a window and be

² IRAF is distributed by the National Optical Astronomy Observatories, which is operated by the Association of Universities for Research in Astronomy, Inc., under cooperative agreement with the National Science Foundation.

dealt with by the medianing process. The arc spectra were extracted with the identical parameters used for the stellar extractions. The two arc exposures associated with a given star were averaged and the resultant digital spectra were logically connected to the appropriate extracted stellar spectrum.

We calculated the dispersion solution for each spectrum with a FORTRAN program (similar to IRAF’s World Coordinate System, which was unavailable at the time of the reductions) that did not alter the pixel binning or the pixel values, but rather wrote the coefficients of the dispersion solution to the headers of the individual spectra. For each arc, the program found every line above a threshold value and separated from all other lines by at least two pixels, and fit each with a Moffat function of exponent four to establish an accurate pixel center. A Legendre polynomial with five terms was fit to give the wavelength dispersion solution. This was done consecutively for all the spectra of a given run, and the mean and σ of the residual ($\lambda_{calc} - \lambda_{lab}$) for each line was calculated. If the mean residual was greater than 0.5 \AA , then the line was not used for the final dispersion solution. The remainder of the lines were weighted such that

$$w = 1.0 \quad \text{if} \quad \sigma \leq 0.02 \text{ \AA},$$

$$w = 0.02/\sigma \quad \text{if} \quad \sigma > 0.02 \text{ \AA}.$$

We applied these new weights in the final dispersion solution calculation for each spectrum. In the end, 16 lines in the wavelength interval 7272 \AA – 8668 \AA were used.

To estimate the S/N of each spectrum, we used two wavelength windows: $8580\text{--}8620 \text{ \AA}$ and $8700\text{--}8800 \text{ \AA}$. These windows were chosen such that none of the globular cluster Ca II triplet lines would be velocity shifted into them. In each of these regions a robust line fitting technique was used to fit a straight line to the pixel values, where the absolute deviation was minimized in the fit rather than the square of the deviation. Let N_i be the pixel value divided by its fitted value, and let the mean and average deviation of all N_i in a window be denoted as N_{mean} and N_{dev} (after clipping by $3 \times N_{dev}$). The S/N for each window was then estimated to be N_{mean}/N_{dev} , and the S/N for the spectrum in the relevant Ca II triplet region was taken to be the average S/N calculated for the two windows. Figure 1 shows a plot of the Ca II triplet region for four of our program spectra having S/N values ranging from 12 to 125. The distribution of S/N values for all of our program spectra can be found in Figure 2. The $\sim 1\%$ of the spectra with $S/N \lesssim 15$ were not analyzed further.

4. Radial Velocities

Radial velocities aid in identifying *bona fide* cluster members, particularly for those clusters projected against populous star fields. While for membership assessment only relative radial velocities are required, experimentation suggested that our data could be used for independent velocity determinations. The procedures adopted are described below.

4.1. Cross Correlations

We used a FORTRAN program to determine velocities by cross correlation against a template spectrum. NGC 6809 star 2441 (II-4-41), $S/N = 180$, served as our template. All spectra were continuum normalized and rebinned to a $\log \lambda$ scale. The correlation function, $C(\Delta\lambda)$, between the program spectra (P) and the template spectrum (T) was calculated to be the sum of $T(\lambda) \times P(\lambda - \Delta\lambda)$ between $\lambda_{template} = 8350 \text{ \AA}$ to 8750 \AA (which corresponds to $\lambda_{rest} \sim 8345 \text{ \AA}$ to 8745 \AA) for a large range of $\Delta\lambda$ values. These limits were chosen to avoid telluric H_2O features between $\sim 8100\text{--}8300 \text{ \AA}$, and $\gtrsim 8800 \text{ \AA}$. The maximum value of $C(\Delta\lambda)$ and the adjoining $\pm 3 \Delta\lambda$ values were then fit by a parabola whose center provided the initial velocity estimate. The program spectra were then Doppler shifted by the initial velocity estimate and the cross correlation repeated to get an additional velocity shift which ensured that the same wavelength region in each spectrum was being used in the correlation; this process was repeated until the velocity shift was stable to well within our errors. The final velocity was used to shift the spectra to the template velocity, so that the band windows used in §5 to calculate the EW s were aligned properly.

4.2. Velocity Errors

Given a stable Cassegrain spectrograph insensitive to rotation angle and changing gravity vector, the uncertainties in our velocities will be dominated by slit centering errors. In order to achieve maximum throughput as well as reliable relative velocities, considerable care was spent in the slit rotation process to ensure that the prime pair of stars was well centered on the $1.25''$ wide slit. This width corresponded to 1.47 pixels on the image plane, or $3.22 \text{ \AA} \sim 97 \text{ km s}^{-1}$ at 8500 \AA . As shown below, our velocities per star appear to be accurate to $\sim \pm 16 \text{ km s}^{-1}$, after centering and other uncertainties are considered.

4.2.1. Internal Errors

Our observational procedure ensured a large sample of stars for each run that were observed at least twice consecutively with the same exposure time. From these, the standard deviation of the velocity measurement could be determined and compared to the mean S/N of the spectrum. The results are found in Figure 3. The median standard deviation for run one, 7.7 km s^{-1} , and for run two, 8.0 km s^{-1} , are indicative of the internal precision and correspond to measuring shifts between the program spectra and the template spectrum at the ~ 0.1 pixel level, which is typical for cross correlation techniques.

4.2.2. External Errors

Several tests enable us to characterize the external accuracy of our data; these include comparison of observations on different nights within a run, observations on different runs, and observations with different spectrograph rotations. We generally have three consecutive spectra for every slit position, so comparisons below are made between the median of each group taken under the different conditions. The absolute value of the difference between two observations, each with standard error σ , has an expectation value of $\sqrt{2}\sigma$; this formulae was used below to estimate the standard error where appropriate.

Star 3204 in NGC 3201 (see Table 9) was observed consecutively 19 times during run one at positions ranging over the entire length of the slit. The standard deviation of the velocity was 14.2 km s^{-1} , and no significant trend of derived velocity was found as a function of position along the slit. There were 223 and 37 stars observed on more than one night of runs one and two, respectively; there were no significant differences found from night to night, and the standard errors derived from the mean absolute value of the star differences were $16 \pm 14 \text{ (s.d.) km s}^{-1}$, and $12 \pm 12 \text{ (s.d.) km s}^{-1}$, respectively. Fourteen and seven stars were observed in runs one and two, respectively, with different spectrograph rotation angles. The standard errors derived from the mean absolute differences were, respectively, $14 \pm 9 \text{ (s.d.) km s}^{-1}$ and $22 \pm 10 \text{ (s.d.) km s}^{-1}$; in neither case was a trend observed as a function of rotation angle. From 15 stars observed in common between the two runs, the mean difference between the velocities (run two–run one) was $-3.5 \pm 10.1 \text{ (s.d.) km s}^{-1}$.

An independent estimate of our uncertainties taking into account the internal velocity dispersion of the clusters was made by comparing our velocities with results from §4.4. Our calculated dispersion, σ_{calc} , for each cluster for which we had 10 or more stars was compared to the internal velocity dispersion, σ_{int} , as given by Pryor and Meylan (1993). The mean excess in dispersion for 25 such clusters is $\sigma_e = (\sigma_{calc}^2 - \sigma_{int}^2)^{0.5} = 16.0 \pm 5.7 \text{ (s.d.) km s}^{-1}$.

In summary, while the internal precision of an individual stellar velocity appears to be $\sim 8 \text{ km s}^{-1}$, the more relevant external uncertainties (arising from centering errors, flexure, etc.) are $\sim 16 \text{ km s}^{-1}$. The velocity of each star relative to its cluster velocity given in the MWGC catalog is presented in Table 9.

4.3. Template Velocity Zero Point and Cluster Velocities

As noted earlier, star 2441 (II-4-41) of NGC 6809 (M55) was chosen as our template for the cross correlations. Since we did not observe radial velocity standard stars, its ex post facto choice was based upon it being a relatively high S/N observation of a globular cluster giant from a cluster with a well determined radial velocity and velocity dispersion. To produce velocities on the standard system we need to assign a velocity to 2441. We could have chosen to use the

MWGC catalog value ($174.9 \pm 0.4 \text{ km s}^{-1}$) for the cluster, and ignore the possibility that this star might have a detectable offset therefrom. The latter possibility seems ruled out by the unpublished measurements of Pryor and collaborators who used the radial velocity scanner on the Canada-France-Hawaii Telescope, where the velocity of 2441 was found to be $177.6 \pm 0.5 \text{ km s}^{-1}$ relative to the cluster mean velocity (for a 20 star dataset), $176.6 \pm 0.9 \text{ km s}^{-1}$, and a cluster velocity dispersion of 3.8 km s^{-1} . We chose, however, to set the template velocity zero point by minimizing the difference between our cluster velocity estimates and those given in the MWGC catalog, as we now describe.

Our initial cluster velocity estimate was the median velocity after five iterations of 3σ clipping. Our final cluster velocity estimate also accounted for the central internal velocity dispersion, σ_{int} , of each cluster. The latter values, listed in Table 1, are from Pryor and Meylan (1993). If the cluster was not listed by Pryor and Meylan, then a typical value of 5 km s^{-1} was used. Using our estimate of the external error in the measurement of the velocity of a single observation of a single star, $\sigma_e = 16 \text{ km s}^{-1}$ (see §4.2) for our measurement error, the observed dispersion for each cluster should be $\sigma_{obs} = (\sigma_{int}^2 + \sigma_e^2)^{0.5}$. The mean of all stars within $3\sigma_{obs}$ of our initial velocity estimate form our final cluster velocity estimate, v . If these stars are drawn from a normal distribution with $\sigma = \sigma_{obs}$, then the variance in v can be estimated as $\sigma^2(v) \sim const^2 \times \sigma_{obs}^2/N$, where N is the number of stars entering the mean, and $const$ is a constant that is determined below.

To obtain the template velocity zero point, we compared our velocity determinations of 16 clusters for which the MWGC catalog quotes velocity errors $< 1 \text{ km s}^{-1}$, and for which our estimate was based upon > 10 stars. Let v_H and v be the catalog and our values, respectively. For each cluster, the difference, $\Delta v = v - v_H$, and the variance, $\sigma^2(\Delta v) = \sigma^2(v) + \sigma(v_H)^2$, were calculated (where the value of $const$ in $\sigma^2(v)$ was set to 1 in this analysis). The velocity of the template, $v_{template}$, was taken to be the weighted mean ($w_i = 1/\sigma^2(\Delta v_i)$) of Δv_i , 172 km s^{-1} . The mean error of unit weight (*m.e.1*) was calculated as follows:

$$m.e.1 = \left[\left(\sum \frac{(\Delta v_i - v_{template})^2}{\sigma^2(\Delta v_i)} \right) / \nu \right]^{\frac{1}{2}} = 2.3,$$

where the sum is over the 16 clusters used and $\nu = 15$. The uncertainty in our template velocity zero point is then taken to be $\sigma(v_{template}) = m.e.1 \times (\sum 1/\sigma^2(\Delta v_i))^{-0.5} = 2.2 \text{ km s}^{-1}$. If we accept the cluster velocity errors given in the MWGC catalog, then the *m.e.1* value above indicates that $const \sim 2.3$, in the definition of $\sigma(v)$, will give a realistic external error estimate for v . It is unclear why *m.e.1* is 2.3 rather than 1; either the normal error estimate, σ_{obs}/\sqrt{N} , is not appropriate for our error distribution, or the errors quoted in the MWGC catalog are underestimated (e.g., perhaps the quoted errors are more correct estimates of internal errors, rather than external errors).

In summary, we assign a velocity of $172 \pm 2.2 \text{ km s}^{-1}$ to star 2441, and our external uncertainties for the cluster velocities are, $\sigma(v) \sim 2.3 \times \sigma_{obs}/\sqrt{N}$, where N is the number of stars entering the mean.

4.4. Velocity Results

Our cluster results are presented in Table 2, where the columns are respectively, 1,2,3) as in Table 1; 4,5,6) our mean cluster velocity, v , external error, $\sigma(v)$, and the number of stars used to estimate the mean velocity, N ; 7,8) the difference $\Delta v = v - v_H$, and $\sigma(v - v_H) = (\sigma^2(v) + \sigma^2(v_H))^{0.5}$, where the v_H values can be found in Table 1; 9,10,11) the reduced equivalent width, W' of the cluster, its associated uncertainty, $\sigma(W')$, and the mean error of unit weight, m.e.1, in the fit of the cluster as described in §6. The difference between each star’s velocity and the cluster velocity given in the MWGC catalog is plotted in Figure 4, and the individual stellar velocities are tabulated in Table 9 in §7, below.

While the goal of this project was not to determine accurate cluster velocities, it is reassuring that our cluster velocity estimates generally agree well with the estimates given in the MWGC catalog, with only five clusters having differences greater than 3σ : NGCs 2298, 5897, 6101, 6553, and 6981. For NGCs 2298, 5897 and 6101, G95 recently reported velocities of $150.4 \pm 1.3 \text{ km s}^{-1}$, $102.9 \pm 1.0 \text{ km s}^{-1}$ and $364.3 \pm 1.9 \text{ km s}^{-1}$, respectively. In all three cases the differences between our velocities and theirs are less than 1σ .

Finally, NGCs 6235, 6528 and 6681 presented particular challenges when identifying stars to define the initial velocity estimate. For NGC 6235, there was no obvious grouping of velocity measures in our sample; therefore, the catalog velocity was used as the first estimate of this cluster’s velocity and only five stars satisfied the iterative clipping procedures to determine our velocity, which differs from the catalog value by 0.1σ . NGC 6528, with $(l, b) = (1.1^\circ, -4.2^\circ)$, is projected onto the dense star fields of the Galactic center. However its high radial velocity made it reasonable to reject all the stars with velocities near 0 km s^{-1} , which are most likely bulge stars, when determining the initial estimate; eight stars survived the clipping to enter our final velocity, which differs from the catalog value by 3.4σ . However, membership remains something of a concern for any cluster with such contamination problems. Similarly, NGC 6681 is close to the bulge, but has a high radial velocity. Since there was a group of stars close to the velocity quoted in the catalog, and a scattering of stars with velocities closer to 0 km s^{-1} , the median velocity of the five stars close to the catalog velocity was used as a first estimate of this cluster’s velocity, which produced a final cluster velocity estimate that differs from the catalog value by 0.1σ . Due to these problems, the cluster velocities we obtain, and our assignment of membership probabilities for stars from these three clusters, are less reliable than those for the other 49 clusters.

4.5. Cluster Membership Probabilities

For each cluster, a Gaussian probability distribution function (PDF) was defined, $P_G(v_{star}, v, \sigma)$, which represents the probability that a star with velocity v_{star} was drawn from the assumed cluster Gaussian velocity distribution with mean v and $\sigma = [\sigma_{obs}^2 + \sigma^2(v)]^{0.5}$ as defined in §4.3. A field star population was defined by selecting all stars which differed from their cluster

velocity by more than 2σ . Of the 976 stars in our sample, 158 fit this criterion. These presumed field stars form a symmetrical distribution about $v = 0 \text{ km s}^{-1}$, and are satisfactorily fit by a Gaussian with $\sigma_{field} = 75 \text{ km s}^{-1}$. Therefore, the field PDF was defined as $P_G(v_{star}, 0, \sigma_{field})$. To define accurately the probability of a star being a velocity member of a given cluster, it is also necessary to know the relative number density of cluster stars and field stars for each cluster at the radii where we observed. To first order, this number can be estimated as the total number of cluster stars in our sample over the total number of field stars, as defined above (i.e. $N_{c/f} = 818/158$). The probability that a star is a cluster member on the basis of its velocity relative to the cluster mean is,

$$P_v = \frac{N_{c/f} P_G(v_{star}, v, \sigma_{obs})}{N_{c/f} P_G(v_{star}, v, \sigma_{obs}) + P_G(v_{star}, 0, \sigma_{field})}.$$

This approach to assigning individual star membership probabilities offers at least two advantages compared to simple σ -clipping. First, it allows for the greater ease of distinguishing between field and cluster stars when the cluster has a high velocity. Second, a star whose velocity deviates from the cluster mean in the direction of $v = 0 \text{ km s}^{-1}$ is more likely to be a field star than one that deviates in the opposite direction. These two effects are reflected in our probability scheme since the field star population is centered on $v = 0 \text{ km s}^{-1}$, and the cluster population is centered on v . Membership probabilities thus calculated are listed for each star in Table 9.

5. Ca II Triplet Equivalent Widths

Measurement of the EW of an absorption feature is usually done by defining continuum bandpasses on each side of the feature, and linearly interpolating the average or median intensities in each of the bandpasses to define the continuum at the feature wavelength. The EW is then the integral over the feature bandpass of the difference between the continuum and the feature (see §5.2). The feature is defined either directly by the spectral intensities or by some analytical function fitted to them (see §5.1). For Ca II triplet work, it is also necessary to combine the three lines in some manner to get a net Ca II index, which we will denote as ΣCa (see §5.3). Table 3 summarizes the approaches used by previous practitioners of Ca II triplet work, where the columns are, respectively: 1) the referenced paper; 2) the method used to combine the three Ca II triplet lines into a single Ca II index for the star, ΣCa ; 3) the method used to define the line feature in the spectrum; 4) the reference for bandpass limits used to define the continuum and feature regions. Table 4 defines the bandpasses that were adopted by other authors and by ourselves³, where the columns are, respectively: 1) the paper where the bandpasses are defined; 2) the Ca II triplet line name defined by its rest wavelength; 3) the line center adopted by other authors and

³ Note that the instrumental resolution (usually defined by the FWHM of the arc lines) was $\sim 3 \text{ \AA}$ for the earlier studies, with values ranging from 2.5 \AA (Olszewski et al. 1991) to 4.8 \AA (Armandroff and Zinn 1988), compared to our $3.4\text{--}4.8 \text{ \AA}$ (see § 5.2).

derived by ourselves; 4) the limits of integration for the line; 5,6) the limits used to define the continuum on the blue and red side of the line.

Since there were many multiply observed stars in our sample, a series of tests were performed to determine the optimum method of calculating ΣCa . In these tests, the mean, $\langle EW \rangle$, and standard deviation, $\sigma(EW)$, of the EW was calculated for each line in every star that was observed at least twice consecutively with the same exposure time⁴. A diagnostic, α , defined as the median $\sigma(EW)$ divided by the median $\langle EW \rangle$, provides essentially an estimate of the inverse S/N for the EW . A technique was then developed to minimize α . Table 5 presents the α values for the various tests described below, where the columns are respectively, 1) the technique used to calculate the equivalent widths; 2) the run that the test was performed on; 3,4,5) the α values for each of the three Ca II triplet lines.

5.1. Line Fitting Technique

Three different techniques were tested for measuring equivalent widths: direct numerical integration, fitting the line with a Gaussian function, and fitting the line with a Moffat function of exponent 2.5. Initially the AZ88 line bandpasses were used, and for the continuum bandpasses the AZ88 definition was used for λ_{8498} , and the AD91 definition was used for λ_{8542} and λ_{8662} (see Table 4), which we will refer to as the AZ88/AD91 continuum bandpasses⁵. Between both runs, there was a total of 600, 764, and 750 stars used for λ_{8498} , λ_{8542} , and λ_{8662} , respectively. The first six rows of Table 5 show that compared to the Numerical method, the Gaussian method shows an improvement in α of $\sim 10\%$ on average, and compared to the Gaussian method, the Moffat method shows an improvement of $\sim 4\%$ on average. In addition, when plotting the deviations from the fitted profile for *all* our spectra, it is clear that the Moffat fit shows no obvious systematic differences from the observed profile⁶, except for slightly underestimating the wings. On the other hand, the Gaussian fit underestimates the depth of the line by $\sim 5\%$, overestimates the FWHM by $\sim 10\%$, and grossly underestimates the depth of the wings. We have therefore adopted the Moffat fitting technique for the remainder of our analysis. To quantify the differences between the line fitting techniques, we performed a spectrum-by-spectrum comparison for 1866 spectra to relate the Ca index (see § 5.3) calculated with the Numerical method, $\Sigma Ca(N)$, the Gaussian

⁴In §5.1 and §5.2, the sample was also restricted to stars with successful EW calculations for all three line fitting methods to avoid bias arising from one method having a higher success rate than another. For the remaining tests, we restricted the samples to stars which had successful EW calculations from the Moffat line fitting technique for all three Ca II triplet lines, which was necessary for our ΣCa to be calculated.

⁵ AD91 significantly modified the continuum bandpasses defined by AZ88 for λ_{8542} and λ_{8662} to optimize their equivalent width calculations.

⁶ The exponent for the Moffat function was chosen to be 2.5 since, from a visual inspection, it was found to fit our observed line profile the best.

method, $\Sigma Ca(G)$, and the Moffat method, $\Sigma Ca(M)$. A least squares fit results in,

$$\Sigma Ca(N) = 1.005(\pm 0.003) \cdot \Sigma Ca(M) - 0.047(\pm 0.013) \quad rms = 0.12 \text{ \AA}$$

$$\Sigma Ca(G) = 0.995(\pm 0.003) \cdot \Sigma Ca(M) - 0.084(\pm 0.005) \quad rms = 0.04 \text{ \AA},$$

which indicates that there are slight zero point shifts between the techniques, but the slopes are consistent with unity. The larger *rms* value for the Numerical technique is consistent with its larger α value (*c.f.* Table 5).

5.2. Line and Continuum Bandpass Windows

Next, we optimized the continuum bandpasses for the line bandpasses of Armandroff. Our continuum bandpasses, listed in Table 4, were chosen to be as large as possible, while still avoiding the telluric H_2O features between ~ 8100 – 8300 \AA and $\gtrsim 8800 \text{ \AA}$. As seen in rows 7 and 8 of Table 5, our new continuum windows reduced α by $\sim 9\%$ for the λ_{8498} line, while the λ_{8542} and λ_{8662} lines were insignificantly affected. We quantified the differences between the two sets of continuum windows by making a star-by-star comparison for 764 stars. This allowed us to relate the Ca index calculated with the Armandroff continuum windows, $\Sigma Ca(A)$, and with our larger continuum windows, $\Sigma Ca(L)$. A least squares fit results in,

$$\Sigma Ca(A) = 1.071(\pm 0.004) \cdot \Sigma Ca(L) - 0.19(\pm 0.02) \quad rms = 0.13 \text{ \AA},$$

which indicates that a small scaling factor and zero-point offset exists between the two methods. All stars that lie significantly off this relation were previously noted to have strong TiO absorption, and were not further included in our analysis.

Finally, we adopted the new continuum bandpasses and tested a variety of line bandpasses that ranged from $\pm 3.5 \text{ \AA}$ to $\pm 10 \text{ \AA}$ about each line center. Our line fitting technique simultaneously fit the amplitude, function-width parameter, and central wavelength, λ_c , for each line of each spectrum. The median λ_c for each line from all spectra are listed in Table 4, which are almost identical to the laboratory wavelengths defined for these lines. The feature bandpasses were defined around these median λ_c values. In general, we found, as one might expect, that α decreases monotonically from the larger to the smaller bandpasses. The effect is strongest for λ_{8498} , which ranges from $0.082 (\pm 10 \text{ \AA})$ to $0.063 (\pm 3.5 \text{ \AA})$ for run one, and $0.091 (\pm 10 \text{ \AA})$ to $0.074 (\pm 3.5 \text{ \AA})$ for run two. For bandpasses $\lesssim \pm 4.5 \text{ \AA}$, the change in α becomes insignificant. Thus, for each line, the largest bandpass for which there was no significant increase in α from the $\pm 3.5 \text{ \AA}$ band was analyzed further. The values chosen for λ_{8498} , λ_{8542} and λ_{8662} , $\pm 4 \text{ \AA}$, $\pm 4.5 \text{ \AA}$, and $\pm 4.5 \text{ \AA}$, respectively, are about half the size of the original Armandroff line bandpasses. The α values for these line bandpasses represent a 16.5% reduction, on average, from the Armandroff line bandpasses.

Although smaller line bandpasses significantly decrease the α values, they also dramatically increase sensitivity to changes in the instrumental profile, which in turn, induce systematic errors in our calculated equivalent widths. Unfortunately, from an analysis of the arc lines associated with each spectrum, the FWHM were essentially constant for run one at ~ 3.4 Å, while for run two, the FWHM was ~ 4.9 Å for night one, ~ 4.4 Å for nights two to six, and ~ 3.8 Å for the remainder of the nights. The changes in run two are attributed, *ex post facto*, to changes in the spectrograph focus. To quantify the effects of these changes in the FWHM of the instrumental profile on our choice of line and continuum bandpasses, a group of 532 pairs of spectra were collected, such that i) the spectra were of the same star, and ii) the FWHM of the arc lines associated with the two spectra differed by more than 0.1 Å (the maximum difference was 0.8 Å). Let ΔEW be the difference between ΣCa calculated from the spectra with the larger arc FWHM and the smaller arc FWHM, and let $|\Delta FWHM|$ be the absolute value of the difference between the FWHM of each of the arc lines. When we use the AZ88 line bandpasses and our continuum bandpasses (see the TP bandpasses in Table 4), a least squares fit results in,

$$\Delta EW = 0.008(\pm 0.10) \cdot |\Delta FWHM| - 0.04(\pm 0.03),$$

so no significant trend is present. However, when we make the same comparison with the the narrow line bandpasses and our continuum windows, we obtain,

$$\Delta EW = -0.57(\pm 0.07) \cdot |\Delta FWHM| + 0.05(\pm 0.02),$$

which clearly shows that the EW of a line is underestimated as the FWHM of the instrumental profile increases, as one would expect. Had our instrumental resolution remained constant throughout the two runs, it is clear from the final α diagnostic in Table 5 that the narrower line bandpasses derived herein would have represented improvements over the AZ88 values. With the data available, however, it is evident that the larger line bandpasses are preferable, and thus they were adopted for the remainder of our work. Our final bandpasses (TP) are presented in Table 4.

5.3. Combining the Ca II Triplet Lines: ΣCa

In their original work, AZ88 measured Ca II indices from integrated cluster light and they defined ΣCa to be the sum of the three triplet lines. When AD91 used individual cluster giants, they determined that inclusion of the λ_{8498} line added more noise than signal to ΣCa , and thus excluded it from the sum. Since we have a large sample of multiply observed stars, we revisited this issue.

Our goal is to determine a weighted mean for ΣCa , $\Sigma Ca = w_1 EW(\lambda_{8498}) + w_2 EW(\lambda_{8542}) + w_3 EW(\lambda_{8662})$, where the weights minimize α for ΣCa . For each line in each star in our sample we calculated the mean, variance and covariance, $(m1, m2, m3)$, $(v1, v2, v3)$, and $(c12, c13, c23)$, respectively. The median of these values was calculated for a sample and respectively denoted as

$m1_0, m2_0, m3_0, v1_0, v2_0, v3_0, c12_0, c13_0$, and $c23_0$. A value equivalent to α defined earlier was then calculated as

$$\tilde{\alpha} = \frac{(w_1^2 v1_0 + w_2^2 v2_0 + w_3^2 v3_0 + 2w_1 w_2 c12_0 + 2w_1 w_3 c13_0 + 2w_2 w_3 c23_0)^{\frac{1}{2}}}{w_1 m1_0 + w_2 m2_0 + w_3 m3_0}.$$

Even though the covariances were less than the variances by at least a factor of ten, they were retained. We proceeded as follows. We set the value of w_2 to 1, and we minimize $\tilde{\alpha}$ with a downhill simplex method (Press et al. 1992) by letting w_1 and w_3 vary. For observing run one, the minima found were $w_1 = 0.55$ and $w_3 = 0.62$, while for run two they were $w_1 = 0.48$, and $w_3 = 0.68$. The average, rounded to the nearest tenth, for each weight was taken to give final weights of $w_1 = 0.5$, $w_2 = 1.0$, and $w_3 = 0.6$. These weights yield a final α value for ΣCa of 0.032 for run one, and 0.034 for run two. If, on the other hand, both w_3 and w_2 were 1.0 and w_1 was 0.0, the respective α values would be 0.035 for run one, and 0.037 for run two. It thus appears that in our data, inclusion of the λ_{8498} feature increases the S/N of ΣCa , and we therefore include it with the weights just defined.

5.4. EW errors

In order to combine observations with varying S/N in the most effective way, and to measure the uncertainty in ΣCa for single observations, the standard deviation in the ΣCa , $\sigma(\Sigma Ca)$, was computed for 594 stars that were consecutively observed with identical configurations and exposure times, and compared to the mean signal to noise, $\langle S/N \rangle$, for each star. These values are plotted in Figure 5. The solid line overplotted on these data represents our estimate of the single observation internal σ as a function of the S/N of the spectra, and was calculated as follows. A running median over 20 stars for both $\sigma(\Sigma Ca)$ and $\langle S/N \rangle$ was calculated, and a quadratic fit was performed which is taken to be the error estimate for $\langle S/N \rangle$ less than 100, and for $\langle S/N \rangle$ greater than 100, a constant $\sigma(\Sigma Ca) = 0.067 \text{ \AA}$ was assumed. We assume our errors are approximately Gaussian, and weight the observations as $1/\sigma^2$ when calculating the mean ΣCa for a star that was observed multiple times. The σ listed for each star in Table 9 is the error in the weighted mean, $[\sum 1/\sigma^2(\Sigma Ca_i)]^{-0.5}$, where the sum is over the number of spectra per star.

A number of tests for systematic effects in ΣCa determinations were possible, which also allowed us to estimate the external errors in ΣCa . From 15 stars observed in common between runs one and two, the mean difference in ΣCa was found to be $\Sigma Ca(\text{run two}) - \Sigma Ca(\text{run one}) = 0.007 \pm 0.15(\text{s.d.}) \text{ \AA}$. NGC 3201 star 3204 was observed consecutively 19 times at different slit positions. The standard deviation in ΣCa was 0.17 \AA for a mean S/N of 62, which is $\sim 1.4 \times \sigma(\Sigma Ca)$; no trend in ΣCa was seen as a function of position on the slit. There were 223 and 37 stars observed on different nights of run one and run two, respectively. No significant offsets were found between any of the nights, and the standard errors derived from the overall absolute value of the differences between nights was $0.12 \pm 0.12 \text{ \AA}$ [$S/N = 61 \pm 23$; $\sim 1.0 \times \sigma(\Sigma Ca)$] and $0.09 \pm 0.07 \text{ \AA}$ [$S/N = 71 \pm 15$; $\sim 0.9 \times \sigma(\Sigma Ca)$] for runs one and two, respectively. Fourteen stars

from run one and seven stars from run two were observed with different spectrograph rotation angles. The standard errors derived from the mean absolute value of the difference in ΣCa were 0.16 ± 0.09 (s.d.) Å and 0.17 ± 0.10 (s.d.) Å, respectively. For their respective mean S/N of 53 and 43, these correspond to error excesses of $\sim 1.1 \times \sigma(\Sigma Ca)$ and $\sim 1.0 \times \sigma(\Sigma Ca)$.

In summary, our external EW errors appear to be consistent with our internal errors.

5.5. Transformations

We have derived transformations between our ΣCa system, TP, and those of others. Observations of individual stars in common with various sources are plotted in Figure 6. The error bars for the abscissa represent our external error estimates, while the error bars for the ordinate represent the errors quoted by the other authors. The dotted lines on the graph represent a one to one correlation, while the solid line represents our least squares fit to the data, which allows for errors in both directions (Stetson 1989). The regression coefficients for the fit $\Sigma Ca(other) = m \cdot \Sigma Ca(TP) + b$, are listed in Table 6, where the columns are respectively, 1) the data source; 2,3) the slope of the fit and its corresponding uncertainty; 4,5) the intercept of the fit and its corresponding uncertainty; 6) the mean error of unit weight for the fit; 7,8) the approximate minimum and maximum $\Sigma Ca(TP)$ for which the regression is valid; and 9) the number of stars in common, N. The *m.e.1* value was calculated as, $m.e.1 = (\sum \epsilon^2 / \sigma^2)^{0.5} \nu^{-0.5}$, where the sum is over all the stars used, ϵ is the deviation along the ordinate of a star from the fitted relation, σ is calculated for each star as $(m^2 \sigma^2[\Sigma Ca(TP)] + \sigma^2[\Sigma Ca(other)])^{0.5}$, and ν is the number of stars used minus two. The uncertainties listed for the coefficients are the formal uncertainties from the fit multiplied by the *m.e.1* value for the fit. The fit to the SK96 data was done excluding the star with the largest ΣCa , NGC 104 L5622, since this star has weak TiO bands present, and SK96 suggest that the line strengths may be varying in this star.

If we assume that our estimates for $\sigma(\Sigma Ca)$ reflect our true external errors, then the *m.e.1* values for S92, S93, G95, and SK96, which are greater than one, suggest that they have underestimated their errors. For G95, the *m.e.1* value reduces from 1.75 to 1.18 if the two most deviant points are removed. DA95 compared their ΣCa values to those of other authors as well, but did not publish regressions. Their results are qualitatively in agreement with ours, which suggests that the DA95 and S93 ΣCa values are on the same system, the AD91 ΣCa values show a positive slope with respect to the DA95/S93 system (i.e., the difference between AD91 ΣCa and DA95/S93 ΣCa becomes larger as ΣCa increases), and the ADZ92 ΣCa show a small excess of ~ 0.25 Å over the DA95/S93 ΣCa for the small range of ΣCa in common. DA95 found a small positive slope between the DAN92 ΣCa and the DA95/S93 system, whereas we find that all three systems are essentially the same.

We attribute the differences in slope and zero point between studies to a combination of continuum window definitions (see §5.2), line fitting techniques (see §5.1), ΣCa definitions

(see §5.3), and slight changes in the instrumental resolution and throughput properties of the spectrograph and detector used (see §5.2).

6. Cluster Reduced Equivalent Widths: W'

As demonstrated by AD91, the change in ΣCa as a function of $V_{HB} - V$ for stars within a cluster has a constant slope, $\Delta(\Sigma Ca)/\Delta(V_{HB} - V)$, for all clusters. This result was corroborated by subsequent studies for stars with $V_{HB} - V \gtrsim 0$, where the mean slopes from the various papers are presented in Table 7; the columns are respectively, 1) paper reference, 2) mean slope from the paper, and 3) the uncertainty in the slope. In most cases, a standard slope of $0.62 \text{ \AA mag}^{-1}$ was adopted, which allows for the calculation of a reduced equivalent width, W' , for a cluster, where the ΣCa of each star in the cluster is corrected to the level of the horizontal branch by subtracting $0.62(V_{HB} - V)$, and the mean of all cluster members is taken. Since our method of calculating ΣCa differs from the previous studies, we do not expect, *a priori*, that our slope will be the same as theirs. Since SK96, and S92 showed that the slope reduces to ~ 0.35 for RGB stars with $V_{HB} - V \lesssim 0$, we have calculated W' for each cluster excluding these stars, which represents only $\sim 4\%$ of our total sample. We have also excluded stars which appear to be AGB stars, HB stars, have an uncertain ID, or lie significantly off the locus defined by the other stars in the ΣCa , $V_{HB} - V$ plot. Furthermore, the weight of a star in the fitting procedure is dependent on its radial velocity and proper motion, as described below.

The technique we chose to calculate W' for each cluster uses an iterative, robust algorithm to fit one slope and 52 intercepts simultaneously to all our data. The intercepts represent the value of ΣCa at the level of the horizontal branch for each cluster, and thus are equivalent to W' . The analytic function fit to our data by an iterative least squares technique, allowing for errors in both directions, is $y_{i,j} = mx_{i,j} + b_j$, where $y_{i,j}$ is the ΣCa value of star i in cluster j ; $x_{i,j}$ is the $V_{HB} - V$ value of star i in cluster j ; m is the slope, $\Delta(\Sigma Ca)/\Delta(V_{HB} - V)$, which is assumed to be constant for all clusters; and b_j is the intercept or reduced equivalent width, W' , of cluster j . The errors, σ_x , assigned to the x_i values were assumed to be constant for a cluster, and are listed in Table 1 as $\sigma(V)$. They represent our estimate of the errors in V from a combination of photometric errors, and errors due to differential reddening within the cluster. The errors, σ_y , assigned to the y_i values are our estimates of the external errors in the ΣCa of the star, and are listed in Table 9 as $\sigma(\Sigma Ca)$.

The weight of each star in the fit is $w = f_p f_r \sigma^{-2}$, where the final w , f_p , and f_r are listed for each star in Table 9. The f_p value for a star is a constant throughout the iterative fitting, and is calculated as,

$$\begin{aligned} f_p &= P_v & \text{if } P_\mu \text{ is not available,} \\ f_p &= P_v & \text{if } P_\mu > 0.2, \\ f_p &= 0 & \text{if } P_\mu \leq 0.2, \end{aligned}$$

where the P_μ and P_v values for each star are the probabilities of membership based on proper motions and velocities (see §4.5), respectively (listed in Table 9). Since stars were selected to be close to the RGB of the cluster, and are found as close to the cluster center as the published photometry, finder charts, and stellar density permitted, (both of which increase their probability of being cluster members), the proper motion probabilities were used conservatively to assess membership. The σ attached to each star is calculated as $\sigma = (m_0^2 \sigma_x^2 + \sigma_y^2)^{0.5}$, where m_0 is the estimate of the slope from the previous iteration. The f_r value assigns lower weight to stars which lie significantly off the locus defined by the other stars in the cluster, and is calculated as,

$$f_r = \frac{1}{1 + [|\epsilon|/(\gamma \sigma m.e.1)]^\beta},$$

where ϵ is the star’s ΣCa deviation from its cluster fit in the previous iteration; σ is calculated as described above; γ and β are constants discussed below; and $m.e.1$ is the mean error of unit weight for the cluster which is calculated as $m.e.1 = (\sum \epsilon^2 / \sigma^2)^{0.5} \nu^{-0.5}$, where the sum is over the number of stars in the cluster with $f_p \geq 0.75$, and ν is one less than this. The constants γ and β were set to 3 and 4, respectively, which assigns equal values of f_r to all stars within $\sim 2 \sigma m.e.1$ of the cluster fit, while f_r drops rapidly to 1/2 when the star is $\sim 3 \sigma m.e.1$ from the cluster fit. The iterations were continued until there was no significant change in $m.e.1$ for any cluster. For each cluster, the final intercept, W' , its uncertainty, $\sigma(W')$, and the $m.e.1$ value are listed in Table 2, where $\sigma(W')$ is the formal uncertainty in the intercept from the fitting technique multiplied by $m.e.1$ for the cluster. An $m.e.1$ value greater than one indicates that the scatter about the best fit line is larger than what would be expected from the adopted errors in ΣCa and V alone. Since we are generally confident in our error estimates for ΣCa (see §5.4), the excess scatter in most clusters is likely due to underestimating the errors in V , including non-cluster members in our sample, including non-RGB stars in our sample, differential reddening within a cluster, or, as a remote possibility, a Ca spread in the cluster. The inhomogeneous nature of the photometry used to establish the ordinate in Figure 7 seems likely to be the dominant source of scatter.

The slope that we obtain from this technique is $0.64 \pm 0.02 \text{ \AA mag}^{-1}$, with $m.e.1 = 1.6$, where the uncertainty quoted is the formal uncertainty from the fitting technique multiplied by $m.e.1$. The $m.e.1$ value here is calculated as it was for individual clusters, except the sum is over the number of stars in *all* clusters with $f_p \geq 0.75$, and ν is this number minus 53 (i.e., the number of clusters used plus one). This slope is consistent with the slopes that previous authors have found, even though our transformation results (§5.5) suggest that our slope should be slightly shallower. This is most likely due to the fact that other authors have not allowed for errors in V when calculating the slope, which causes the fitting technique to underestimate the true slope (Stetson 1989). This method of calculating the mean slope is more effective than simply taking the mean of slopes fit independently, since clusters with stars having a small range in $V_{HB} - V$, and therefore possessing little slope information, simply add noise to the latter method, whereas they do not affect the former. The final fit for each cluster is plotted in Figure 7.

We performed two experiments to investigate whether the slope, $\Delta(\Sigma Ca)/\Delta(V_{HB} - V)$, is

a function of $[\text{Fe}/\text{H}]$. In the first, every cluster was fit by our technique independently, and the resultant slopes of each cluster were plotted against their respective $[\text{Fe}/\text{H}]$ from ZW84, which are listed in Table 1. The mean slope was $0.62 \pm 0.02 \text{ \AA mag}^{-1}$, and no significant trend with $[\text{Fe}/\text{H}]$ was observed, although there was some indication that the slope may become steeper for the more metal-rich clusters. To examine further any possible $[\text{Fe}/\text{H}]$ dependence of the slope, the clusters were split into four metallicity bins, with each subset analyzed following the precepts described above for the full sample. The results are presented in Table 8, where the columns are respectively, 1) the $[\text{Fe}/\text{H}]$ range as defined by ZW84 (see Table 1), 2) the number of clusters in that $[\text{Fe}/\text{H}]$ range, 3,4) the slope, $\Delta(\Sigma Ca)/\Delta(V_{HB} - V)$, and uncertainty in the slope, derived for the clusters in the bin, and 5) the *m.e.1* value for the fit. As seen in Table 8, none of the slopes for the metallicity bins differs significantly from the $0.64 \pm 0.04 \text{ \AA mag}^{-1}$ found for the whole sample, nor is there compelling evidence that more metal-rich clusters differ in this regard. Accordingly, we will continue to assume that the slope is constant for all metallicities. With better photometry and membership information, this point would be well worth revisiting in the future.

7. The Catalog

The results for individual stars are given in Table 9, where the columns are, respectively: 1) the star name; 2) the difference between our calculated velocity of the star (see §4), and the cluster velocity given in the MWGC catalog; 3) the V magnitude of the star above the horizontal branch; 4) the de-reddened $B - V$ color of the star determined with $E(B - V)$ from the MWGC catalog; 5) the weighted mean ΣCa of the star, calculated according to §5; 6) the external error of the weighted mean ΣCa ; 7) the probability of cluster membership from proper motion data; 8) the probability of cluster membership from our calculated velocities (see § 4.5); 9,10,11) the f_p, f_r values and final weight, w , respectively, used in our fitting technique to calculate the reduced equivalent width, W' , of the cluster (see §6 for technique, and Table 2 for W' values); the weight has been scaled in each cluster so that the highest weight star in the cluster has $w = 1$; 12) the number of spectra analyzed for the star; 13) the nights that the star was observed, where the first number indicates the observing run, and the other numbers indicate the specific night of observation. Therefore, 1-1 represents April 13, 1989, 1-2 represents April 14, 1989 ..., and 2-1 represents July 13, 1989, ... If a star was observed on more than one night for a given run, then it will have more than one number following the dash. Finally, column 14) indicates when notes are found at the bottom of the table.

The values of v_H , V_{HB} , and $E(B - V)$ for each cluster can be found in Table 1. The references for these values, as well as the references for the Table 9 star names, photometry, and the proper motions (in columns 1,3,4 and 7, respectively) can be found in Appendix A. Notes for a given cluster, or stars in the cluster, can also be found in Appendix A. In Figure 7, the $V_{HB} - V$ magnitudes are plotted against the ΣCa values in the left panel. The light line represents the robust line fit (see §6) to the cluster stars, while the bold lines represent the line fits to three well

studied clusters spanning a large range in $[\text{Fe}/\text{H}]$ and each having low reddening. The CMD of the same stars is plotted in the right panel to give an indication of possible non-RGB stars, and to allow assessment of the photometry, where a large scatter is likely indicative of sizable photometric errors, differential reddening, inclusion of undetected non-members, or some combination thereof. The RGBs of the same three fiducial clusters used in the left panels are plotted in the right panels with bold lines. The relative placement, with respect to the fiducial lines, of the cluster line fit in the left panels, and the RGB stars in the right panels give an indication of the accuracy of the $E(B - V)$ values listed in the MWGC catalog. The details for these figures are given in the figure caption. The interpretation of the data compiled in this paper will be presented in subsequent publications.

We thank Las Campanas night assistants Angel Guerra and Fernando Peralta for their cheerful, effective support, and W.E. Kunkel for setting up the spectrograph and instructing JEH in its use for run one. The large quantity of photographic work required to prepare the extensive, large-scale finding charts essential to the observations was ably performed by Dave Duncan at DAO. We thank Gianni Marconi, Hugh Harris, Don Terndrup, and Sergio Ortolani for sending us ASCII copies of their photometry, in some cases before publication. Thanks also to Bill Harris for compiling the MWGC catalog, for insightful discussions, and for a helpful referee’s report. GAR would like to thank the NRC for funding during this project.

A. The Program Clusters

The reference cluster data (see Table 1) were taken from the June 1994 version of the Harris (1996) electronic MWGC catalog. Since this is a dynamic catalog, the reference sources for the data we adopted are listed below for each cluster. The cluster coordinates were taken from Djorgovski and Meylan (1993). The sources for the $E(B - V)$ measurements were from Reed et al. (1988), Webbink (1985), and Zinn (1985). The catalog documentation states, “In addition to the three major sources listed above, measurements of $E(B - V)$ from the individual color-magnitude studies (sources given for V_{HB}) were employed whenever they appeared to be well calibrated... The final adopted reddenings are the straight averages of the given sources (up to 4 per cluster)”. The cluster radial velocities were mainly taken from Armandroff and Zinn (1988), Hesser, Shawl and Meyer (1986), Webbink (1981), and Zinn and West (1984). Again, the catalog documentation states, “However, numerous more recent sources are also available for smaller lists of objects; in many cases these are based on large samples of stars from CORAVEL or multi-object echelle spectra with very high precision ($\pm 1 \text{ km s}^{-1}$ or less) and almost totally supersede any previous data. The adopted v_r for each cluster is the average of the available measurements, each one weighted inversely as the published uncertainty.” These more recent sources are listed below for individual clusters in the form v_H : author, author....

More generally, for each cluster we list individually the relevant data sources, as follows.

Horizontal-branch magnitudes (V_{HB}): these were measured from the sources, which are cited in the form V_{HB} : type of data-author, type of data-author, ..., where the type of data is one of: 1) CCD for photometry done with a charged coupled device, 2) PG for photometry done with a photographic plate, and 3) RR Lyrae if the determination is specifically referred to them.

Proper motion data (P_μ): values listed in Table 9 are cited in the notes here in the form P_μ : author.

Stellar identifications and photometric zero points: sources are cited in the form ID: author[letter], author[letter], ..., where the letter is used to preface the star ID in Table 9 and for discussion of any photometric zero-point adjustments. Because a 0.1 V magnitude zero-point offset between photometry used for the HB and RGB stars would lead to a systematic shift in the calculated $[\text{Fe}/\text{H}]$ of ~ 0.025 dex for metal-poor clusters, and more for metal-rich clusters, zero-point offsets larger than ~ 0.1 mag between photometric systems were always applied to the RGB stars to bring them onto the V_{HB} system. These adjustments are listed below as $V_{HB} - V_{\text{letter}} = \dots$; in more complicated scenarios, they are explicitly given. When star-by-star comparisons were performed, the \pm refers to the standard deviation of the sample. We also indicate how the photometry from different sources was combined to give the V values listed in Table 9. If there are no comments for a cluster, then the photometry was taken unchanged from the single source listed.

NGC 104 = M 12 = 47 Tuc - v_H : Armandroff and Da Costa (1986), Meylan et al. (1991), Meylan and Mayor (1986); V_{HB} : CCD - Hesser et al. (1987); P_μ : Tucholke (1992a); ID: Lee (1977b)[L]. Hesser et al. (see their Figure 11, and Appendix E) found that their V photometry agrees with L to within ± 0.02 mag, so no corrections were applied.

NGC 288 - v_H : Peterson et al. (1986), Pryor et al. (1991), Pryor and Meylan (1993); V_{HB} : CCD - Bergbusch (1993); ID: Alcaïno and Liller (1980c)[A], Olszewski et al. (1984)[O]. Using 10 stars, the V photometry of A was brighter than O's by -0.08 ± 0.09 mag, so the straight mean was taken for these stars for both V and $B-V$. No stars from A or O were in common with the Bergbusch study, but Bolte (1992, see his Figure 6) finds good agreement between his photometry and O. Bergbusch found that his V photometry was ~ 0.064 mag fainter than Bolte, so no corrections were applied.

NGC 362 - v_H : Fischer et al. (1993); V_{HB} : PG - Harris (1982); P_μ : Tucholke (1992b); ID: Harris (1982)[H].

NGC 1261 - V_{HB} : CCD - Ferraro et al. (1993); ID: Ferraro et al. (1993)[F], Alcaïno (1979b)[A]. All photometry was taken from F.

NGC 2298 - V_{HB} : CCD - Janes and Heasley (1988); ID: Alcaïno and Liller (1986a)[A]. No stars from A were in common with the Janes and Heasley study, but V_{HB} in both studies indicates that there is not a significant zero-point difference.

NGC 2808 - V_{HB} : CCD - Ferraro et al. (1990); ID: Harris (1975)[H], Harris (1978). The photometry was taken from Harris (1975), and recalibrated according to Harris (1978). We could not reproduce Ferraro et al.’s comparison to the Harris (1978) data, so from our comparison of 14 stars, the V photometry of Ferraro et al. was brighter than Harris (1978) by 0.06 ± 0.04 mag, and the $B-V$ photometry was redder by 0.09 ± 0.06 . Ferraro et al. photometry was used for stars when available, and otherwise Harris (1978) data was used with no corrections.

NGC 3201 - v_H : Coté et al. (1995); V_{HB} : CCD - Brewer et al. (1993); ID: Lee (1977c)[L]. Star 2405 was listed in both the PE and PG data of L; we assumed that the PG value was correct. Brewer et al. find systematic differences with the photometry of L, but this effect was $\lesssim 0.1$ mag in V , for the central part of the cluster, and less severe in the outskirts. Since our stars were selected far from the center, no corrections were applied.

NGC 4372 - V_{HB} : CCD - Alcaïno et al. (1991); ID: Alcaïno (1974a)[A]. Alcaïno et al. find no systematic differences with the A photometry.

NGC 4590 = M 68 - v_H : Pryor and Meylan (1993); V_{HB} : CCD - McClure et al. (1987); ID: Harris (1975)[H], Alcaïno (1977a)[A]. Using 12 stars, the V photometry of H was brighter than A by -0.03 ± 0.01 , so no adjustments were made. McClure et al. (see their Figure 3) overplotted the CMD of H on their data; no significant difference in V_{HB} was found. We obtained two spectra of HI184 with low S/N ~ 20 . Although we determine this star to be a 94% probable velocity member, S93, who obtained higher precision velocity data, showed that this star is not a velocity member, and thus it was not used in our W' analysis.

NGC 4833 - V_{HB} : PG - Menzies (1972); ID: Menzies (1972)[M].

NGC 5286 - V_{HB} : PG - Harris et al. (1976); ID: PG - Harris et al. (1976)[H].

NGC 5897 - V_{HB} : CCD - Ferraro et al. (1992); ID: Sandage and Katem (1968)[S]. Ferraro et al. (see their Figure 3) found that their V photometry was ~ 0.1 mag fainter than S, so $V_{HB} - V_S = 0.1$.

NGC 5904 = M 5 - v_H : Olszewski et al. (1986), Peterson et al. (1986), Rastorguev and Samus (1991); V_{HB} : CCD photometric RR Lyrae - Storm et al. (1991); P_μ : Cudworth (1979); ID: Buonanno et al. (1981)[B]. From the level of V_{HB} in the CMD of B, there does not appear to be a systematic V offset from Storm et al.

NGC 5927 - V_{HB} : CCD - Sarajedini and Norris (1994), CCD - Friel and Geisler (1991); ID: Menzies (1974b)[M]. Sarajedini and Norris found that their V photometry was on average 0.2 mag fainter than M, so $V_{HB} - V_M = 0.2$.

NGC 5986 - V_{HB} : CCD - Bond et al. (1994); ID: Harris et al. (1976)[H]. From the level of V_{HB} in the CMD of H, there does not appear to be a systematic V offset from Bond et al.

NGC 6093 = M 80 - V_{HB} : PG - Harris and Racine (1974); ID: PG - Harris and Racine (1974)[H].

NGC 6101 - V_{HB} : CCD - Sarajedini and Da Costa (1991) ID: Alcaïno (1974b)[A] Marconi (private communication)[M] M found that the V photometry of Sarajedini and Da Costa was on average 0.08 mag brighter than M, so $V_{HB} - V_M = -0.08$.

NGC 6121 = M 4 - v_H : Clementini et al. (1994), Peterson and Latham (1986), Peterson et al. (1986), Rastorguev and Samus (1991); V_{HB} : PG - Cudworth and Rees (1990); P_μ : Cudworth and Rees (1990); ID: Lee (1977a)[L]. Photometry was taken from Cudworth and Rees.

NGC 6144 - V_{HB} : PG - Alcaïno (1980); ID: Alcaïno (1980)[A].

NGC 6171 = M 107 - v_H : Da Costa and Seitzer (1989), Piatek et al. (1994), Pryor et al. (1987); V_{HB} : PG - Cudworth et al. (1992); P_μ : Cudworth et al. (1992); ID: Sandage and Katem (1964)[S]. Photometry taken from Cudworth et al.

NGC 6218 = M 12 - v_H : Harris et al. (1983), Pryor et al. (1987), Rastorguev and Samus (1991); V_{HB} : PG - Racine (1971); ID: Racine (1971)[R - private communication].

NGC 6235 - V_{HB} : PG - Liller (1980a); ID: Liller (1980a)[L].

NGC 6254 = M 10 - v_H : Rastorguev and Samus (1991); V_{HB} : CCD - Hurley et al. (1989); ID: Harris et al. (1976)[H]. Hurley et al. found that their V magnitudes were 0.18 mag fainter than H, so $V_{HB} - V_H = 0.18$

NGC 6266 = M 62 - V_{HB} : CCD BV - Caloi et al. (1987); ID: Alcaino (1978)[A]. Using 14 stars the V photometry of Caloi et al. was fainter than A by 0.14 ± 0.04 mag, so $V_{HB} - V_A = 0.14$

NGC 6273 = M 19 - V_{HB} : PG - Harris et al. (1976); ID: Harris et al. (1976)[H].

NGC 6304 - V_{HB} : CCD - Davidge et al. (1992); ID: Hesser and Hartwick (1976)[H]. Our estimate of the V_{HB} level in H was 16.15, whereas the estimate from Davidge et al. was 16.25, so $V_{HB} - V_H = 0.1$

NGC 6352 - V_{HB} : CCD - Sarajedini and Norris (1994); ID: Sarajedini and Norris (1994)[S], Alcaino (1971)[A], Hartwick and Hesser (1972)[H]. Using 17 stars, the V photometry of A was fainter than H by only 0.03 ± 0.09 , and the $B-V$ photometry of A was redder than H by only 0.006 ± 0.1 . Using 10 stars, the V photometry of S was fainter than H by 0.25 ± 0.09 , and the $B-V$ photometry of S was bluer than H by -0.21 ± 0.28 . Photometry was taken from S when available. Otherwise, the mean of H and A was used or, for the cases where H photometry was not available, A was used. When photometry was taken from H and A, 0.25 was added to V , and -0.2 was added to $B-V$.

NGC 6366 - v_H : Da Costa and Seitzer (1989); V_{HB} : CCD - Harris (1993); ID: Pike (1976)[P]. From the level of V_{HB} in the CMD of P, there does not appear to be a systematic V offset from Harris.

NGC 6362 - v_H : Pryor and Meylan (1993); V_{HB} : CCD - Alcaino and Liller (1986b); ID: Alcaino (1972)[A]. Using 12 stars, the V photometry of Alcaino and Liller was fainter than A by only 0.08 ± 0.1 mag, so no correction was applied.

NGC 6397 - V_{HB} : digitized PG - Alcaino et al. (1987); ID: Alcaino (1977b)[A], Cannon (1974)[C] Alcaino et al. (1987)[AB]. Photometry taken from AB.

NGC 6496 - V_{HB} : CCD - Sarajedini and Norris (1994); ID: Armandroff(1988)[A], Richtler(1995)[R]. Photometry was taken from R. Due to the high quality photometry in both studies, it is evident that the V_{HB} in the CMD of Sarajedini and Norris was ~ 0.05 mag brighter than R, so $V_{HB} - V_H = -0.05$. Note that the star A68 = R111/112 was listed as one star in A's

photometry, but was resolved into two stars in the photometry of R. Stars R111 and R112 have identical magnitudes ($V = 15.19$) and almost identical colours ($B - V = 1.40$ and 1.39 for R111 and R112, respectively). We assumed it was one star with $V = 15.19$, since we did not resolve these two stars. This will not affect our results since the surface gravity and temperature of both stars should be very similar.

NGC 6522 - V_{HB} : CCD - Terndrup and Walker (1994, private communication; photometry without star names), ID: Arp (1965)[A]. Photometry was taken from Terndrup and Walker, except for star A15, which did not have a $B - V$ mag listed, so the value given in A was used. The star A116 was resolved into three fainter stars by Terndrup and Walker, and was not used in our analysis. The photometry for this star is from A.

NGC 6535 - v_H : Pryor and Meylan (1993); V_{HB} : CCD - Sarajedini (1994); ID: Liller(1980)[L], Sarajedini (1994)[S]. Photometry was taken from Sarajedini.

NGC 6528 - V_{HB} : CCD - Ortolani et al. (1992); ID: van den Bergh and Younger (1979)[VY], Ortolani et al. (1992)[O (private communication)]. Photometry was taken from O, except VYII-42, which was taken from VY. Using four stars fainter than $V = 16.5$, the V photometry of O was fainter than VY's by 0.05 ± 0.04 , and the $B - V$ photometry was redder by 0.24 ± 0.03 , so a correction of $(0, +0.24)$ was applied to $(V, B - V)$ for the VY photometry of VYII-42.

NGC 6544 - V_{HB} : PG - Alcaïno (1983); ID: Alcaïno (1983)[A].

NGC 6541 - V_{HB} : PG - Alcaïno (1979a); ID: Alcaïno (1979a)[A].

NGC 6553 - V_{HB} : CCD - Ortolani et al. (1990); ID: Hartwick (1975)[H], Ortolani et al. (1990)[O (private communication)]. Photometry was taken from O. Star HII-3 = O140 was not used in this analysis, since it is part of the RGB turn over as shown in Figure 3b of O. Star HII-59 was not used due to strong TiO bands (the photometry for this star was taken from H).

NGC 6624 - v_H : Pryor et al. (1989), Pryor and Meylan (1993); V_{HB} : CCD - Sarajedini and Norris (1994); ID: Liller and Carney (1978)[L], Richtler (1995)[R]. Photometry was taken from R for all stars except LIV150 and LI102, for which L's photometry was used. Sarajedini and Norris, as well as R, found systematic differences with L which were correlated with V . Using Figure 2 and 3 of R, a $(V, B - V)$ correction of $(+0.2, -0.2)$ was applied to LIV150, and $(+0.1, -0.1)$ was applied to LI102. From the level of V_{HB} in the CMD of R, there do not appear to be systematic differences with the V photometry of Sarajedini and Norris.

NGC 6626 - v_H : Pryor et al. (1989), Pryor and Meylan (1993); V_{HB} : PG - Rees and Cudworth (1991); ID: Alcaïno (1981)[A - written A(ring#)-(star#)]. Photometry was taken from Rees and Cudworth, except A1-80, and A2-125, for which A’s photometry was used. Using 11 stars, the V photometry of Rees and Cudworth was fainter than A by 0.1 ± 0.08 mag, and the $B-V$ photometry was bluer by 0.03 ± 0.02 mag, so the $(V, B-V)$ corrections applied to the A stars was $(+0.1, 0)$.

NGC 6638 - V_{HB} : PG - Alcaïno and Liller (1983), spectroscopy of C-type RR Lyrae - Smith and Stryker (1986); ID: Alcaïno and Liller (1983)[A].

NGC 6637 = M 69 - V_{HB} : CCD - Sarajedini and Norris (1994); ID: Hartwick and Sandage (1968)[H -note that ‘n’ implies the star is from the inner circle], Richtler (1995)[R], Sarajedini and Norris (1994)[S]. Photometry was taken from either R or S as indicated by the star names. Stars that only had photometry from H were not used due to their photometric uncertainties (see Figure 13 of S, and Figure 4 of R). From the level of V_{HB} in the CMD of R, the V photometry of Sarajedini and Norris was ~ 0.1 mag fainter than R, so 0.1 was added to the V photometry of R.

NGC 6681 = M70 - v_H : Pryor et al. (1989); V_{HB} : CCD - Mittermeier et al. (1994); ID: Harris (1975)[H]. From the level of V_{HB} in the CMD of H, there does not appear to be a systematic V offset from Mittermeier et al.

NGC 6712 - v_H : Grindlay et al. (1987); V_{HB} : PG - Cudworth (1988); P_μ : Cudworth (1988); ID: Sandage and Smith (1966)[S]. Photometry of Cudworth was used for all stars except SB67 and SA34, for which the photometry of S was used. Using 8 stars, the V photometry of Cudworth was fainter than S by 0.12 ± 0.04 mag, and the $B-V$ photometry was bluer by 0.02 ± 0.06 mag, so the $(V, B-V)$ corrections applied to the S stars was $(+0.12, 0)$.

NGC 6717 = Pal 9 - V_{HB} : CCD - Jensen et al. (1994); ID: Goranskii (1979)[G]. From the level of V_{HB} in the CMD of G, the V photometry of Jensen et al. was ~ 0.7 mag fainter than G, so $V_{HB} - V_R = 0.7$. All the G photometry was measured by eye except stars G16, G23, G15, and G24, which were measured with an iris-diaphragm photometer. Star G35 has an uncertain ID.

NGC 6723 - V_{HB} : CCD - Fullton and Carney (1993); ID: Menzies (1974a)[M]. From the level of V_{HB} in the CMD of M, there does not appear to be a systematic V offset from Fullton and Carney. The star MII-7 was not used in our analysis since it appears to be a blue HB star.

NGC 6752 - V_{HB} : PG - Buonanno et al. (1986); ID: Alcaïno (1972)[A], Cannon and Stobie (1973)[C], Buonanno et al. (1986)[B]. Using 12 stars, the V photometry of C was fainter than B by 0.03 ± 0.05 , so the V magnitudes were taken to be the straight mean of C and B, while the $B-V$ magnitudes were simply taken from C. The star A9 = B2403 was not used as it is most likely a variable, or was contaminated in B’s study, who obtained a V magnitude 0.35 mag fainter than A and C.

NGC 6809 - v_H : Pryor et al. (1991), Pryor and Meylan (1993); V_{HB} : PG - Lee (1977d); ID: Lee (1977d)[L].

NGC 6981 - V_{HB} : PG - Dickens (1972a); ID: Dickens (1972a)[D].

NGC 7089 - v_H : Armandroff and Da Costa (1986); V_{HB} : PG - Harris (1975); P_μ : Cudworth and Rauscher (1987) ID: Harris (1975)[H]. Using 9 stars, the V photometry of H was fainter than Cudworth and Rauscher by 0.004 ± 0.07 mag, so the V magnitudes were taken to be the straight mean of H and Cudworth and Rauscher, while the $B-V$ magnitudes were simply taken from H.

NGC 7099 - v_H : Pryor and Meylan (1993); V_{HB} : CCD - Bolte (1987); ID: Dickens (1972b)[D - PG magnitudes, DP - PE magnitudes], Alcaïno and Liller (1980b)[A]. Photometry was taken from D, or DP. No stars were in common between Bolte and D, but Buonanno et al. (1988) find no significant difference between their photometry and D, and since $V_{HB} = 15.1$ for both the photometry of Buonanno et al. and Bolte, no correction was applied to D. DP17 has an uncertain ID.

NGC 7492 - V_{HB} : CCD - Côté et al. (1991); ID: Buonanno et al. (1987)[B], Cuffey (1961)[C]. Photometry was taken from B. The star CR has an uncertain ID.

Pal 12 - v_H : Armandroff and Da Costa (1991); V_{HB} : CCD - Stetson et al. (1989); ID: Stetson et al. (1989)[S], Harris and Canterna (1980)[H]. Photometry was taken from S, except H4122, which was taken from H.

REFERENCES

- Alcaino, G. 1972, A&A, 16, 220
- Alcaino, G. 1974a, A&AS, 13, 345
- Alcaino, G. 1974b, A&AS, 18, 9
- Alcaino, G. 1977a, A&AS, 29, 9
- Alcaino, G. 1977b, A&AS, 29, 397
- Alcaino, G. 1978, A&AS, 32, 379
- Alcaino, G. 1979a, A&AS, 35, 233
- Alcaino, G. 1979b, A&AS, 38, 61
- Alcaino G. 1980, A&AS, 39, 315
- Alcaino G. 1981, A&AS, 44, 191
- Alcaino G. 1983, A&AS, 52, 105
- Alcaino, G., and Liller, W. 1980a, AJ, 85, 680
- Alcaino, G., and Liller, W. 1980b, AJ, 85, 1330
- Alcaino, G., and Liller, W. 1980c, AJ, 85, 1592
- Alcaino, G., and Liller, W. 1983, AJ, 88, 1166
- Alcaino, G., and Liller, W. 1986a, A&A, 161, 61
- Alcaino, G., and Liller, W. 1986b, AJ, 91, 303
- Alcaino, G., Buonanno, R., Caloi, V., Castellani, V., Corsi, C.E., Ianniccolo, G., and Liller, W. 1987, AJ, 94, 917
- Alcaino, G., Liller, W., Alvarado, F., and Wenderoth, E. 1991, AJ, 102, 159
- Armandroff, T.E. 1988, AJ, 96, 588
- Armandroff, T.E., and Zinn, R. 1988, AJ, 96, 92 (AZ88)
- Armandroff, T.E., and Da Costa, G.S. 1986, AJ, 92, 777
- Armandroff, T.E., and Da Costa, G.S. 1991, AJ, 101, 1329 (AD91)
- Armandroff, T.E., Da Costa, G.S., and Zinn, R. 1992, AJ, 104, 164 (ADZ92)
- Arp, H. 1965, ApJ, 141, 43
- Bergbusch, P.A., 1993, AJ, 106, 1024
- Bolte, M. 1987, ApJ, 319, 760
- Bolte, M. 1992, ApJS, 82, 145
- Bond, H., Harris, W.E., Harris, G.L.H., Mittermeier, R., and Palmer, K. 1994, in preparation

- Brewer, J.P., Fahlman, G.G., Richer, H.B., Searle, L., and Thompson, I. 1993, *AJ*, 105, 2158
- Buonanno, R., Corsi, C.E., and Fusi Pecci, F. 1981, *MNRAS*, 196, 435
- Buonanno, R., Caloi, V., Castellani, V., Corsi, C., Fusi Pecci, F., and Gratton, R. 1986, *A&AS*, 66, 79
- Buonanno, R., Corsi, C.E., Ferraro, I., and Fusi Pecci, F. 1987, *A&AS*, 67, 327
- Buonanno, R., Caloi, V., Castellani, V., Corsi, C.E., and Ferraro, I. 1988, *A&AS*, 74, 353
- Caloi, V., Castellani, V., and Piccolo, F. 1987, *A&AS*, 67, 181
- Cannon, R.D., and Stobie, R.S. 1973, *MNRAS*, 162, 227
- Cannon, R.D. 1974, *MNRAS*, 167, 551
- Clementini, G., Merighi, R., Pasquini, L., Cacciari, C., and Gouiffes, C. 1994, *MNRAS*, 267, 83
- Coté, P., Richer, H.B., and Fahlman, G.G. 1991, *AJ*, 102, 1358
- Coté, P., Welch, D.L., Fischer, P., and Gebhardt, K. 1995, *ApJ*, 454, 788
- Cudworth, K.M. 1979, *AJ*, 84, 1866
- Cudworth, K.M. 1988, *AJ*, 96, 105
- Cudworth, K.M., and Rauscher, B.J. 1987, *AJ*, 93, 856
- Cudworth, K.M., and Rees, R. 1990, *AJ*, 99, 1491
- Cudworth, K.M., Smetanka, J.J., and Majewski, S.R. 1992, *AJ*, 103, 1252
- Cuffey, J. 1961, *MNRAS*, 122, 363
- Da Costa, G.S., and Seitzer, P. 1989, *AJ*, 97, 405
- Da Costa, G.S., and Armandroff, T.E. 1995, *AJ*, 109, 2533 (DA95)
- Da Costa, G.S., Armandroff, T.E., and Norris, J.E. 1992, *AJ*, 104, 154 (DAN92) 109, 2533
- Davidge, T.J., Harris, W.E., Bridges, T.J., and Hanes, D.A. 1992, *ApJS*, 81, 251
- Dickens, R.J. 1972a, *MNRAS*, 157, 281
- Dickens, R.J. 1972b, *MNRAS*, 157, 299
- Djorgovski S., and Meylan G. 1993, in *Structure and Dynamics of Globular Clusters*, ASP Conf.Series 50, ed.G.Meylan and S.Djorgovski (San Francisco: A.S.P.), 325
- Ferraro, F.R., Clementini, G., Fusi Pecci, F., Buonanno, R., and Alcaïno, G. 1990, *A&AS*, 84, 59
- Ferraro, F.R., Fusi Pecci, F., and Buonanno, R. 1992, *MNRAS*, 256, 376
- Ferraro, F.R., Clementini, G., Fusi Pecci, F., Vitiello, E., and Buonanno R. 1993, *MNRAS*, 264, 273
- Ferraro, F.R., Fusi Pecci, F., Guarnieri, M.D., Moneti, A., Origlia, L., Testa, V. 1994, *MNRAS*, 266, 829

- Fischer, P., Welch, D.L., Mateo, M., and Cote, P. 1993, *AJ*, 106, 1508
- Friel, E.D., and Geisler, D. 1991, *AJ*, 101, 1338
- Fullton, L.K., and Carney, B.W. 1993, *BAAS*, 25, 1407
- Geisler, D., Piatti, A.E., Clariá, J., and Minniti, D. 1995, *AJ*, 109, 605 (G95)
- Goranskii, V.P. 1979, *Soviet Astronomy*, 23, 284
- Grindlay, J., Bailyn, C., Mathieu, R., and Latham, D. 1987, in *Globular Cluster Systems in Galaxies*, IAU Symposium 126, ed. J.Grindlay and A.G.D.Philip (Dordrecht: Reidel), 659
- Harris, H.C. 1993, *AJ*, 106, 604
- Harris, H.C., Nemec, J.M., and Hesser, J.E. 1983, *PASP*, 95, 256
- Harris, W.E. 1975, *ApJS*, 29, 397
- Harris, W.E. 1978, *PASP*, 90, 45
- Harris, W.E. 1982, *ApJS*, 50, 573
- Harris, W.E. 1996, *AJ*, 112, 1487
- Harris, W.E., and Racine R., 1974, *AJ*, 79, 472
- Harris, W.E., and Canterna, R. 1980, *ApJ*, 239, 815
- Harris, W.E., Racine, R., and de Roux, J. 1976, *ApJS*, 31, 13
- Hartwick, F.D.A., and Hesser, J.E. 1972, *ApJ*, 175, 77
- Hartwick F.D.A. 1975, *PASP*, 87, 77
- Hartwick, F.D.A., and Sandage, A. 1968, *ApJ*, 153, 715
- Hesser, J.E., and Hartwick, F.D.A. 1976, *ApJ*, 203, 113
- Hesser, J.E., Shawl, S.J., and Meyer, J.E. 1986, *PASP*, 98, 403
- Hesser, J.E., Harris, W.E., VandenBerg, D.A., Allwright, J.W.B., Shott, P., and Stetson, P.B. 1987, *PASP*, 99, 739
- Hurley, D.J.C., Richer, H.B. and Fahlman, G.G. 1989, *AJ*, 98, 2124
- Janes, K.A., and Heasley, J.N. 1988, *AJ*, 95, 762
- Jensen, N., Harris, W.E., and Bond, H. 1994, in preparation
- Lee, S-W. 1977a, *A&AS*, 27, 376
- Lee, S-W. 1977b, *A&AS*, 27, 381
- Lee, S-W. 1977c, *A&AS*, 28, 408
- Lee, S-W. 1977d, *A&AS*, 29, 1
- Liller, M.H. 1980a, *AJ*, 85, 673
- Liller, M.H. 1980b, *AJ*, 85, 1480

- Liller, M.H., and Carney, B.W. 1978, *ApJ*, 224, 383
- McClure, R.D., VandenBerg, D.A., Bell, R.A., Hesser, J.E., and Stetson, P.B. 1987, *AJ*, 93, 1144
- Menzies, J. 1972, *MNRAS*, 156, 207
- Menzies, J. 1974a, *MNRAS*, 168, 177
- Menzies, J. 1974b, *MNRAS*, 169, 79
- Meylan, G., and Mayor, M. 1986, *A&A*, 166, 122
- Meylan, G., Dubath, P., and Mayor, M. 1991, *ApJ*, 383, 587
- Mittermeier, R., Harris, G.L.H., Bond, H., Harris, W.E., and Palmer, K. 1994, in prep
- Olszewski, E.W., Canterna, R., and Harris, W.E. 1984, *ApJ*, 281, 158
- Olszewski, E.W., Peterson, R.C., and Aaronson, M. 1986, *ApJ*, 302, L4
- Olszewski, E.W., Schommer, R.A., Suntzeff, N.B., and Harris, H. 1991, *AJ*, 101, 515
- Ortolani, S., Barbuy, B., and Bica, E. 1990, *A&A*, 236, 362
- Ortolani, S., Bica, E., and Barbuy, B. 1992, *A&AS*, 92, 441
- Peterson, R.C., and Latham, D.W. 1986, *ApJ*, 305, 645
- Peterson, R.C., Olszewski, E.W., and Aaronson, M. 1986, *ApJ*, 307, 139
- Piatek, S., Pryor, C., McClure, R.E., Fletcher, J.M., and Hesser, J.E. 1994, *AJ*, 107, 1397
- Pike, C.D. 1976, *MNRAS*, 177, 257
- Press, W.H., Teukolsky, S.A., Vetterling, W.T. and Flannery, B.P. 1992, *Numerical Recipes in Fortran*, second edition, Cambridge University Press.
- Pryor, C., McClure, R.D., Fletcher, J.M., and Hesser, J.E. 1987, in *Globular Cluster Systems in Galaxies*, IAU Symposium 126, ed. J.Grindlay and A.G.D.Philip (Dordrecht: Reidel), 661
- Pryor, C., McClure, R.D., Fletcher, J.M., and Hesser, J.E. 1989, *AJ*, 98, 596
- Pryor, C., McClure, R.D., Fletcher, J.M., and Hesser, J.E. 1991, *AJ*, 102, 1026
- Pryor, C.. and Meylan, G. 1993, in *Structure and Dynamics of Globular Clusters*, ASP Conf. Series 50, ed. G. Meylan and S. Djorgovski (San Francisco:ASP), 357 (PM93)
- Racine, R. 1971, *AJ*, 76, 331
- Rastorguev, A.S., and Samus, N.N. 1991, *Sov.Astron.Letters*, 17, 388
- Reed B.C., Hesser J.E., and Shawl S.J. 1988, *PASP*, 100, 545
- Rees, R.F., and Cudworth, K.M. 1991, *AJ*, 102, 152
- Richtler, T. 1995, *A&AS*, 109, 1
- Sandage, A., and Katem, B. 1964, *ApJ*, 139, 1080
- Sandage, A., and Katem, B. 1968, *ApJ*, 153, 569

- Sandage, A., and Smith, L.L. 1966, *ApJ*, 144, 886
- Sandquist, E.L., Bolte, M., Stetson, P.B., and Hesser, J.E. 1996, *ApJ*, 470, 910
- Sarajedini, A. 1994, *PASP*, 106, 404
- Sarajedini, A., and DaCosta, G.S. 1991, *AJ*102, 628
- Sarajedini, A., and Norris, J.E. 1994, *ApJS*, 93, 161
- Smith, H.A., and Stryker, L.L. 1986, *PASP*, 98, 453
- Stetson, P.B. 1989, *Image and Data Processing*, eds. B Barbuy, E. Janot-Pacheco, A. M. Magalhães, S.M. Viegas, published by Departamento Astronomia, Instituto Astronomico e Geofísico, Universidade de São Paulo, C.P. 9638, São Paulo 01065, Brazil.
- Stetson, P.B., Vandenberg, D.A., Bolte, M., Hesser, J.E., and Smith, G.H. 1989, *AJ*, 97, 1360
- Storm, J., Carney, B.W., and Beck, J. 1991, *PASP*, 103, 1264
- Suntzeff, N.B., Schommer, R.A., Olszewski, E.W., Walker, A.R. 1992, *AJ*, 104 (5), 1743 (S92)
- Suntzeff, N.B., Mateo, M., Terndrup, D.M., Olszewski, E.W., Geisler, D., and Weller, W. 1993, *ApJ*, 418, 208 (S93)
- Suntzeff, N.B., and Kraft, R.P. 1996, *AJ*, 111, 1913 (SK96)
- Terndrup, D., and Walker, A. 1994, *AJ*, 107, 1786
- Tucholke, H.J. 1992a, *A&AS*, 93, 293
- Tucholke, H.J. 1992b, *A&AS*, 93, 311
- van den Bergh, S., and Younger, F. 1979, *AJ*, 84, 1305
- Webbink, R.F. 1981, *ApJS*, 45, 259
- Webbink R.F. 1985, in *Dynamics of Star Clusters*, IAU Symposium 113, ed. J.Goodman and P.Hut (Dordrecht: Reidel), 541
- Zinn, R. 1977, *ApJ*, 218, 96
- Zinn, R. 1985, *ApJ*, 293, 424
- Zinn, R., and West, M.J. 1984, *ApJS*, 55, 45 (ZW84)

Fig. 1.— Comparison of spectra with different S/N values (estimated as explained in the text) illustrate the degradation as the S/N values drop below ~ 15 .

Fig. 2.— A histogram of the distribution of the S/N for the 2640 spectra analyzed.

Fig. 3.— The standard deviation of the velocity measurements for stars observed consecutively at least twice with the same exposure times are compared to the mean S/N values for each set of multiple observations of the same star.

Fig. 4.— The difference between the median velocity calculated for each star and the cluster velocity given in the Harris (1994) MWGC catalog is plotted for each of the 52 clusters observed. The numbers on the abscissa are linked with NGC numbers in Table 1.

Fig. 5.— As in Figure 3, but for the standard deviation of the ΣCa measurements for stars observed consecutively at least twice with the same exposure times.

Fig. 6.— A comparison of the ΣCa values in globular cluster stars from various sources. The regression coefficients are found in Table 6.

Fig. 7.— For each cluster, the V magnitude above the horizontal branch (V_{HB} values found in Table 1) is plotted against the ΣCa in the left panel, and the color-magnitude diagram is plotted in the right panel, where the $B-V$ values have been de-reddened by the cluster $E(B-V)$ given in Table 1. The *circles* represent stars that have f_p values greater than 0.75, while the *triangles* represent the remainder. The stars that were not used to compute the reduced equivalent width, W' , are labelled with a \times symbol. The slope in the left panel is $0.64 \pm 0.02 \text{ \AA mag}^{-1}$. The error bars in the left panel are calculated as $\sigma = (m^2 \sigma^2(V) + \sigma^2(\Sigma Ca))^{0.5}$, where $\sigma(V)$ is assumed to be constant for a cluster and is listed in Table 1, and $\sigma(\Sigma Ca)$ is listed for each star in Table 9 (plotted if $\sigma > 0.1 \text{ \AA}$). The light line in the left panel represents the robust line fit for the stars in the cluster (see § 6), while the bold lines represent the robust line fit for the three clusters (from left to right) NGC 4590 (M 68), NGC 5904 (M 5), and NGC 104 (47 Tuc), all of which have well determined $[\text{Fe}/\text{H}]$ and W' values and low $E(B-V)$ values. In the right panel, the RGB fiducials for each of these clusters is plotted (in the same order from left to right); they were taken, respectively, from McClure et al. (1987) [bright end from Harris(1975)], Sandquist et al. (1996), and Hesser et al. (1987).

Rutledge et al.: GGC CaII Metallicity Scale -- Figure 1

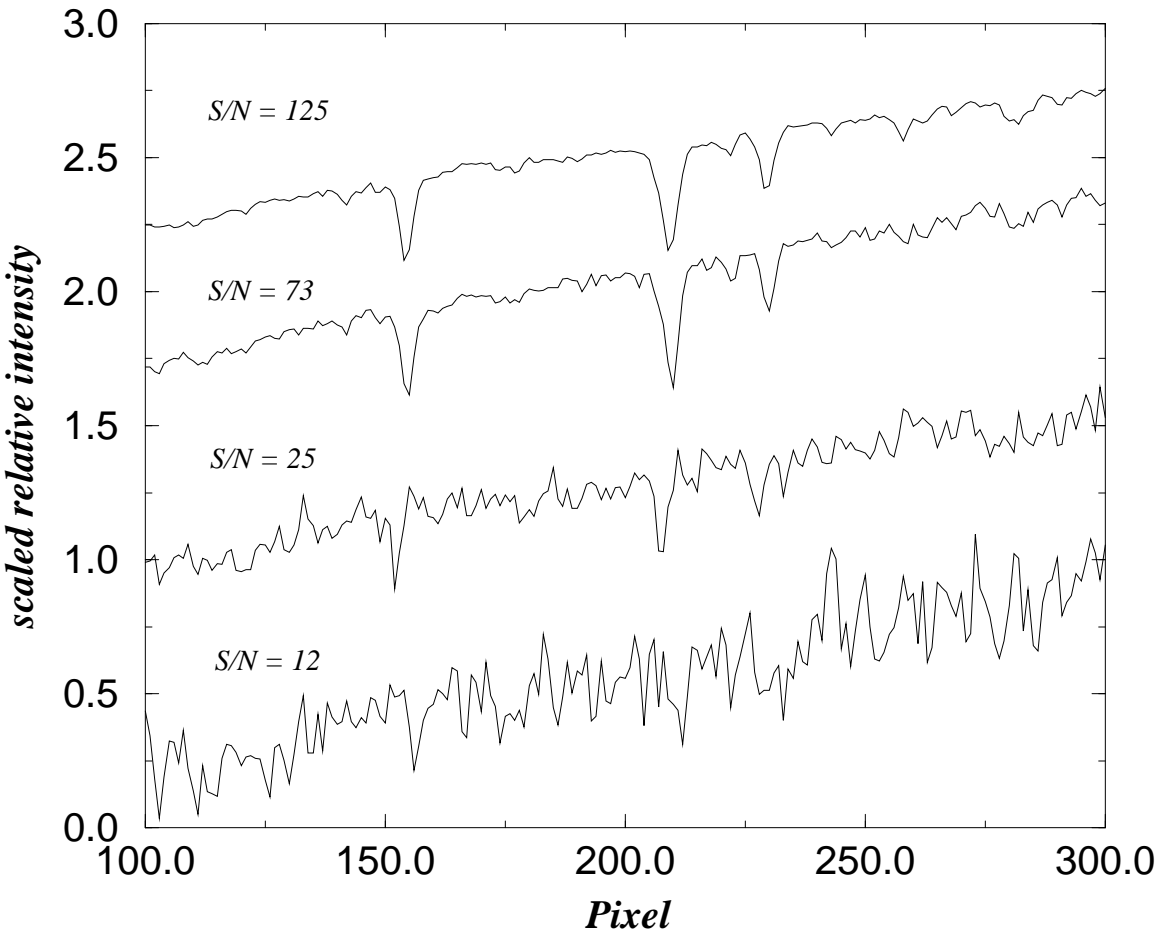


TABLE 1. Adopted Cluster Data

No.	NGC	Name	IAU	l^{II}	b^{II}	V_{HB} mag	v_H km s^{-1}	$\sigma(v_H)$ km s^{-1}	$E(B-V)$ mag	σ_{int} km s^{-1}	[Fe/H] dex	$\sigma([\text{Fe}/\text{H}])$ dex	$\sigma(V)$ mag
1	104	47 Tuc	C0021-723	305.9	-44.9	14.06	-18.7	0.2	0.04	11.5	-0.71	0.08	0.10
2	288		C0050-268	152.3	-89.4	15.38	-46.4	0.4	0.03	2.9	-1.40	0.12	0.10
3	362		C0100-711	301.5	-46.2	15.43	223.5	0.5	0.05	6.4	-1.27	0.07	0.10
4	1261		C0310-554	270.5	-52.1	16.70	53.3	9.1	0.01	...	-1.31	0.09	0.10
5	2298		C0647-359	245.6	-16.0	16.11	100.5	9.1	0.13	...	-1.85	0.11	0.15
6	2808		C0911-646	282.2	-11.3	16.19	99.7	2.9	0.23	13.4	-1.37	0.09	0.15
7	3201		C1015-461	277.2	8.6	14.80	494.6	0.2	0.21	5.2	-1.61	0.12	0.15
8	4372		C1223-724	301.0	-9.9	15.30	60.8	6.5	0.45	...	-2.08	0.15	0.20
9	4590	M 68	C1236-264	299.6	36.1	15.68	-95.1	0.6	0.04	2.5	-2.09	0.11	0.15
10	4833		C1256-706	303.6	-8.0	15.45	203.1	5.6	0.33	...	-1.86	0.09	0.20
11	5286		C1343-511	311.6	10.6	16.20	53.6	4.1	0.25	8.0	-1.79	0.11	0.20
12	5897		C1514-208	342.9	30.3	16.35	23.0	8.0	0.08	...	-1.68	0.11	0.15
13	5904	M 5	C1516+022	3.9	46.8	15.06	51.8	0.5	0.03	5.7	-1.40	0.06	0.10
14	5927		C1524-505	326.6	4.9	16.60	-100.5	5.3	0.47	...	-0.30	0.09	0.20
15	5986		C1542-376	337.0	13.3	16.50	92.3	5.9	0.27	...	-1.67	0.10	0.20
16	6093	M 80	C1614-228	352.7	19.5	15.86	7.3	4.1	0.18	12.4	-1.68	0.12	0.20
17	6101		C1620-720	317.7	-15.8	16.60	191.1	13.7	0.04	...	-1.81	0.15	0.10
18	6121	M 4	C1620-264	351.0	16.0	13.45	70.0	0.5	0.36	4.2	-1.33	0.10	0.20
19	6144		C1624-259	351.9	15.7	16.60	142.7	7.7	0.32	...	-1.75	0.15	0.20
20	6171	M 107	C1629-129	3.4	23.0	15.70	-33.8	0.3	0.33	4.1	-0.99	0.06	0.20
21	6218	M 12	C1644-018	15.7	26.3	14.90	-43.5	0.6	0.17	4.5	-1.61	0.12	0.20
22	6235		C1650-220	358.9	13.5	16.70	86.9	3.9	0.36	...	-1.40	0.15	0.20
23	6254	M 10	C1654-040	15.1	23.1	14.65	75.4	1.0	0.28	6.6	-1.60	0.08	0.20
24	6266	M 62	C1658-300	353.6	7.3	16.30	-68.0	3.2	0.47	14.3	-1.28	0.15	0.20
25	6273	M 19	C1659-262	356.9	9.4	16.40	129.4	6.9	0.37	...	-1.68	0.15	0.20
26	6304		C1711-294	355.8	5.4	16.25	-105.0	8.7	0.52	...	-0.59	0.23	0.20
27	6352		C1721-484	341.4	-7.2	15.28	-114.6	6.3	0.21	...	-0.51	0.08	0.20
28	6366		C1725-050	18.4	16.0	15.65	-122.6	0.5	0.69	1.3	-0.99	0.25	0.15
29	6362		C1726-670	325.6	-17.6	15.34	-13.0	0.6	0.09	2.8	-1.08	0.09	0.20
30	6397		C1736-536	338.2	-12.0	12.87	18.8	0.1	0.18	4.5	-1.91	0.14	0.10
31	6496		C1755-442	348.0	-10.0	16.47	-98.4	7.7	0.13	...	-0.48	0.15	0.10
32	6522		C1800-300	1.0	-3.9	16.85	-8.7	5.6	0.50	6.7	-1.44	0.15	0.20
33	6535		C1801-003	27.2	10.4	15.73	-215.1	0.5	0.32	2.4	-1.75	0.15	0.15
34	6528		C1801-300	1.1	-4.2	17.10	162.2	5.2	0.62	...	0.12	0.21	0.15
35	6544		C1804-250	5.8	-2.2	14.90	-16.6	6.5	0.74	...	-1.56	0.15	0.25

TABLE 1. (continued)

No.	NGC	Name	IAU	l^{II}	b^{II}	V_{HB} mag	v_H km s^{-1}	$\sigma(v_H)$ km s^{-1}	$E(B-V)$ mag	σ_{int} km s^{-1}	[Fe/H] dex	$\sigma([\text{Fe}/\text{H}])$ dex	$\sigma(V)$ mag
36	6541		C1804-437	349.3	-11.2	15.30	-153.8	3.1	0.12	8.2	-1.83	0.15	0.15
37	6553		C1806-259	5.2	-3.0	16.60	-26.9	4.1	0.84	...	-0.29	0.11	0.20
38	6624		C1820-303	2.8	-7.9	16.11	54.3	0.6	0.27	5.4	-0.35	0.15	0.15
39	6626		C1821-249	7.8	-5.6	15.70	15.2	1.2	0.41	8.6	-1.44	0.15	0.15
40	6638		C1827-255	7.9	-7.2	16.50	9.7	6.8	0.40	...	-1.15	0.15	0.20
41	6637	M 69	C1828-323	1.7	-10.3	16.00	39.6	4.7	0.17	...	-0.59	0.19	0.15
42	6681	M 70	C1840-323	2.9	-12.5	15.60	218.7	1.2	0.07	5.1	-1.51	0.14	0.15
43	6712		C1850-087	25.4	-4.3	16.25	-107.7	0.6	0.46	4.3	-1.01	0.14	0.15
44	6717	Pal 9	C1852-227	12.9	-10.9	16.60	1.8	7.1	0.21	...	-1.32	0.15	0.25
45	6723		C1856-367	0.1	-17.3	15.50	-81.9	6.3	0.06	...	-1.09	0.14	0.15
46	6752		C1906-600	336.5	-25.6	13.70	-27.4	2.7	0.04	4.5	-1.54	0.09	0.15
47	6809	M 55	C1936-310	8.8	-23.3	14.40	174.9	0.4	0.07	4.9	-1.82	0.15	0.15
48	6981	M 72	C2050-127	35.2	-32.7	16.90	-288.8	8.2	0.05	...	-1.54	0.09	0.15
49	7089	M 2	C2130-010	53.4	-35.8	16.05	-6.7	2.1	0.05	8.2	-1.62	0.07	0.15
50	7099	M 30	C2137-234	27.2	-46.8	15.10	-184.3	1.0	0.04	5.6	-2.13	0.13	0.15
51	7492		C2305-159	53.4	-63.5	17.63	-188.5	8.5	0.00	...	-1.82	0.30	0.15
52		Pal 12	C2143-214	30.5	-47.7	17.13	28.5	1.5	0.02	...	-1.14	0.20	0.10

Rutledge et al.: GGC CaII Metallicity Scale -- Figure 2.

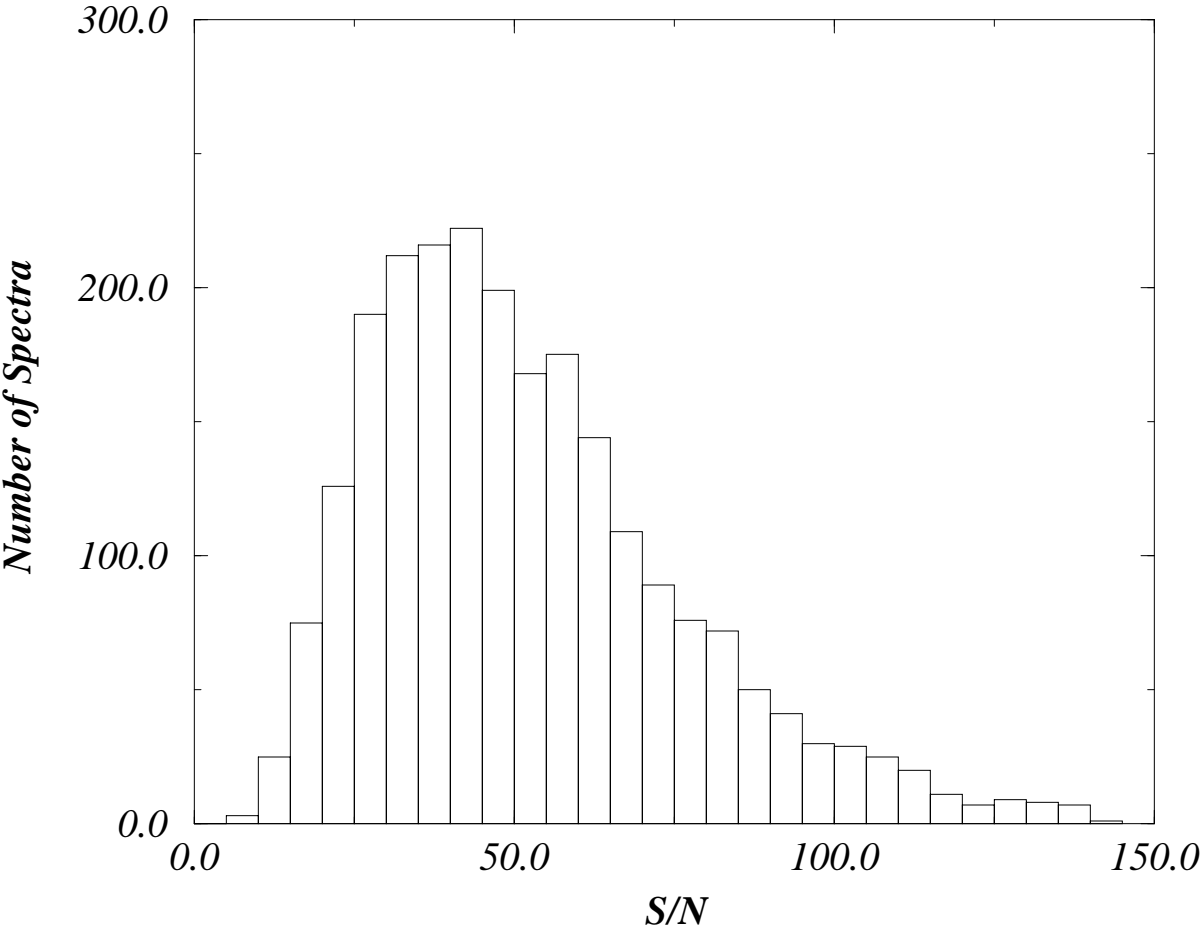


TABLE 2. Cluster Velocity and Reduced EW Results

No.	NGC	Name	v km s^{-1}	$\sigma(v)$ km s^{-1}	N	Δv km s^{-1}	$\sigma(\Delta v)$ km s^{-1}	W' \AA	$\sigma(W')$ \AA	$m.e.1$
1	104	47 Tuc	-26.5	8.1	31	-7.8	8.1	4.51	0.04	1.49
2	288		-65.7	10.3	13	-19.3	10.3	3.65	0.06	1.32
3	362		225.5	11.9	11	2.0	11.9	3.72	0.07	1.16
4	1261		73.2	12.1	10	19.9	15.1	3.77	0.09	1.86
5	2298		144.4	9.0	18	43.9	12.8	2.24	0.05	1.30
6	2808		80.1	9.9	23	-19.6	10.3	3.75	0.08	2.13
7	3201		499.6	7.0	30	5.0	7.0	3.41	0.03	1.14
8	4372		70.4	7.1	29	9.6	9.6	1.94	0.05	1.33
9	4590	M 68	-84.9	8.5	19	10.2	8.5	1.58	0.06	1.51
10	4833		194.1	7.5	26	-9.0	9.4	2.27	0.05	1.41
11	5286		65.7	11.8	12	12.1	12.5	3.03	0.08	1.45
12	5897		97.6	9.9	15	74.6	12.7	2.24	0.07	1.56
13	5904	M 5	58.6	5.9	43	6.8	5.9	3.75	0.06	1.93
14	5927		-123.8	8.8	19	-23.3	10.3	4.79	0.05	0.99
15	5986		86.7	11.0	12	-5.6	12.5	3.16	0.09	1.36
16	6093	M 80	11.8	10.6	19	4.5	11.4	2.86	0.06	1.20
17	6101		363.6	10.6	13	172.5	17.3	1.95	0.11	2.47
18	6121	M 4	70.1	6.6	33	0.1	6.6	3.83	0.05	1.52
19	6144		174.3	13.5	8	31.6	15.6	2.20	0.05	0.80
20	6171	M 107	-31.1	8.7	19	2.7	8.7	3.99	0.05	1.01
21	6218	M 12	-37.3	9.5	16	6.2	9.5	3.85	0.10	1.73
22	6235		88.7	17.1	5	1.8	17.6	3.54	0.11	1.52
23	6254	M 10	83.1	9.9	16	7.7	9.9	3.42	0.07	1.70
24	6266	M 62	-62.1	9.3	28	5.9	9.8	3.95	0.07	1.64
25	6273	M 19	138.0	11.5	11	8.6	13.4	2.69	0.10	1.99
26	6304		-107.8	9.0	18	-2.8	12.5	4.84	0.05	1.02
27	6352		-122.8	8.0	23	-8.2	10.2	4.73	0.07	1.55
28	6366		-113.7	9.5	15	8.9	9.5	4.70	0.05	1.09
29	6362		-16.0	9.6	15	-3.0	9.6	3.93	0.07	1.44
30	6397		17.8	8.7	19	-1.0	8.7	2.21	0.06	1.99
31	6496		-129.3	19.1	4	-30.9	20.6	4.70	0.08	1.10
32	6522		-18.3	9.3	18	-9.6	10.9	3.47	0.09	1.72
33	6535		-204.8	14.0	7	10.3	14.0	2.74	0.27	3.33
34	6528		212.2	13.5	8	50.0	14.5	5.41	0.14	2.57
35	6544		-33.0	11.0	12	-16.4	12.8	3.53	0.09	1.42
36	6541		-163.5	12.4	11	-9.7	12.8	2.72	0.05	1.02
37	6553		8.4	8.4	21	35.3	9.3	5.13	0.09	1.55
38	6624		38.6	8.4	21	-15.7	8.4	4.66	0.05	1.09
39	6626		42.3	10.4	16	27.1	10.4	4.05	0.08	1.51
40	6638		22.4	11.0	12	12.7	13.0	4.31	0.10	1.62
41	6637	M 69	40.4	8.2	22	0.8	9.4	4.48	0.07	1.59
42	6681	M 70	216.8	17.1	5	-1.9	17.2	3.14	0.05	0.66
43	6712		-105.5	10.9	12	2.2	10.9	4.11	0.06	1.49
44	6717	Pal 9	29.0	8.8	19	27.2	11.3	3.78	0.11	1.50
45	6723		-100.3	9.9	15	-18.4	11.7	4.07	0.08	1.73
46	6752		-21.9	10.1	14	5.5	10.5	3.42	0.04	1.03
47	6809	M 55	158.9	11.5	11	-16.0	11.5	2.69	0.05	1.30
48	6981	M 72	-359.6	9.6	16	-70.8	12.6	3.53	0.10	2.13

TABLE 2. (continued)

No.	NGC	Name	v km s^{-1}	$\sigma(v)$ km s^{-1}	N	Δv km s^{-1}	$\sigma(\Delta v)$ km s^{-1}	W' \AA	$\sigma(W')$ \AA	$m.e.1$
49	7089	M 2	4.1	12.4	11	10.8	12.6	3.28	0.10	1.76
50	7099	M 30	-177.2	15.8	6	7.1	15.8	1.72	0.12	2.08
51	7492		-214.2	11.5	11	-25.7	14.3	2.98	0.16	2.47
52		Pal 12	13.7	15.6	6	-14.8	15.7	4.57	0.15	2.34

Notes to Table 2.

The velocity results for NGCs 6235, 6528, and 6681 are affected by heavy field star contamination (see §4.4).

Rutledge et al.: GGC CaII Metallicity Scale -- Figure 3.

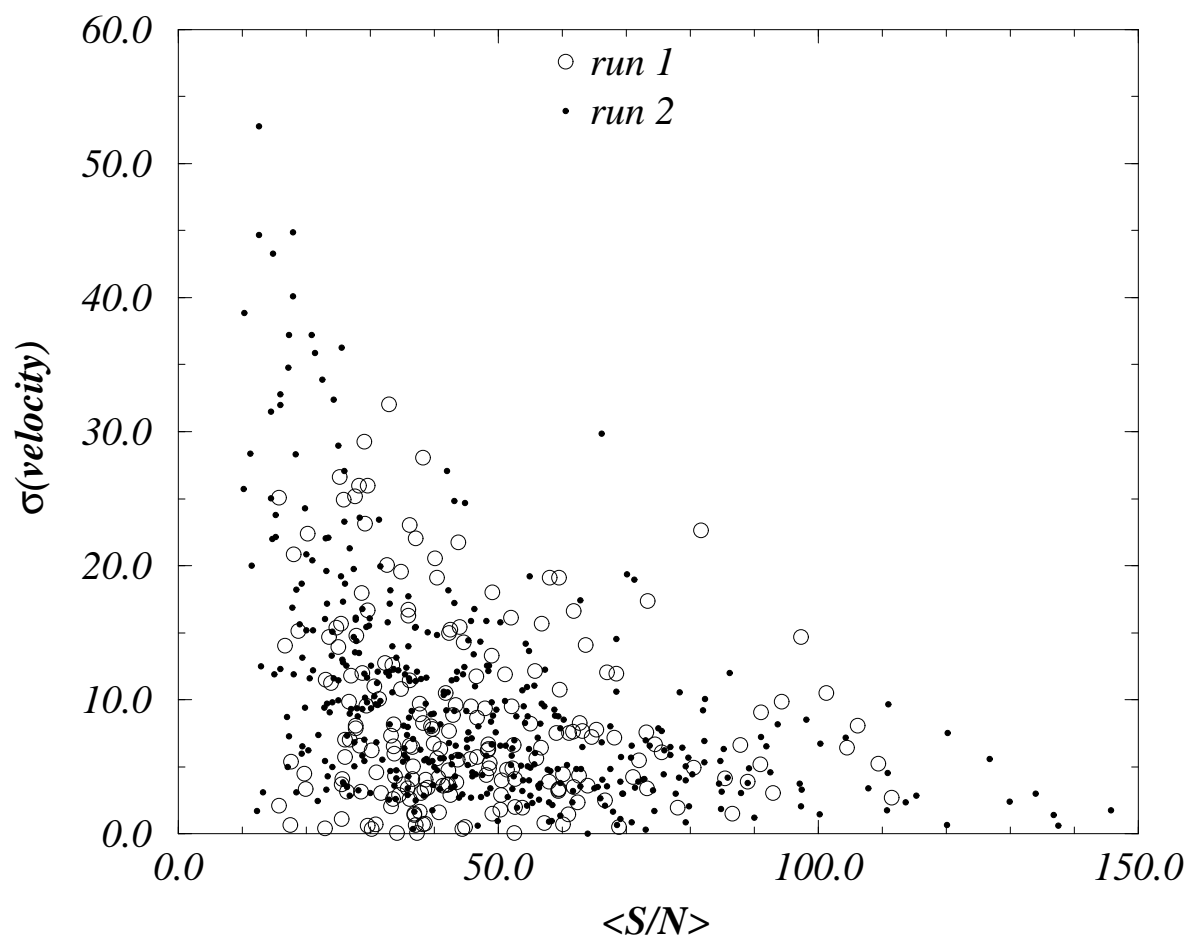


TABLE 3. Comparison of ΣCa calculation techniques

Paper	ΣCa	Line Fitting	Bandpasses ^a
AZ88	$\lambda_{8498} + \lambda_{8542} + \lambda_{8662}$	Numerical	AZ88
AD91	$\lambda_{8542} + \lambda_{8662}$	Gaussian	AD91
Olszewski et al. (1991)	$\lambda_{8498} + \lambda_{8542} + \lambda_{8662}$	Gaussian	AZ88
ADZ92	$\lambda_{8542} + \lambda_{8662}$	Gaussian	AD91
DAN92	$\lambda_{8542} + \lambda_{8662}$	Gaussian	AD91
S92 ^b	$\lambda_{8542} + \lambda_{8662}$	Gaussian	AZ88
S93	$\lambda_{8542} + \lambda_{8662}$	Gaussian	AZ88
G95	$\lambda_{8542} + \lambda_{8662}$	Numerical	AZ88
DA95	$\lambda_{8542} + \lambda_{8662}$	Gaussian	AD91
SK96	$\lambda_{8542} + \lambda_{8662}$	Gaussian	AZ88
This Paper (TP)	$0.5\lambda_{8498} + \lambda_{8542} + 0.6\lambda_{8662}$	Moffat	TP

^aSee Table 4 for the different bandpass limits

^bIn the original paper, the sum of all three lines was used, but in the Appendix of S93, the S92 ΣCa values were expressed as the sum of the two strongest lines; it is the latter values that we are referring to in this paper.

Rutledge et al.: GGC CaII Metallicity Scale — Figure 4.

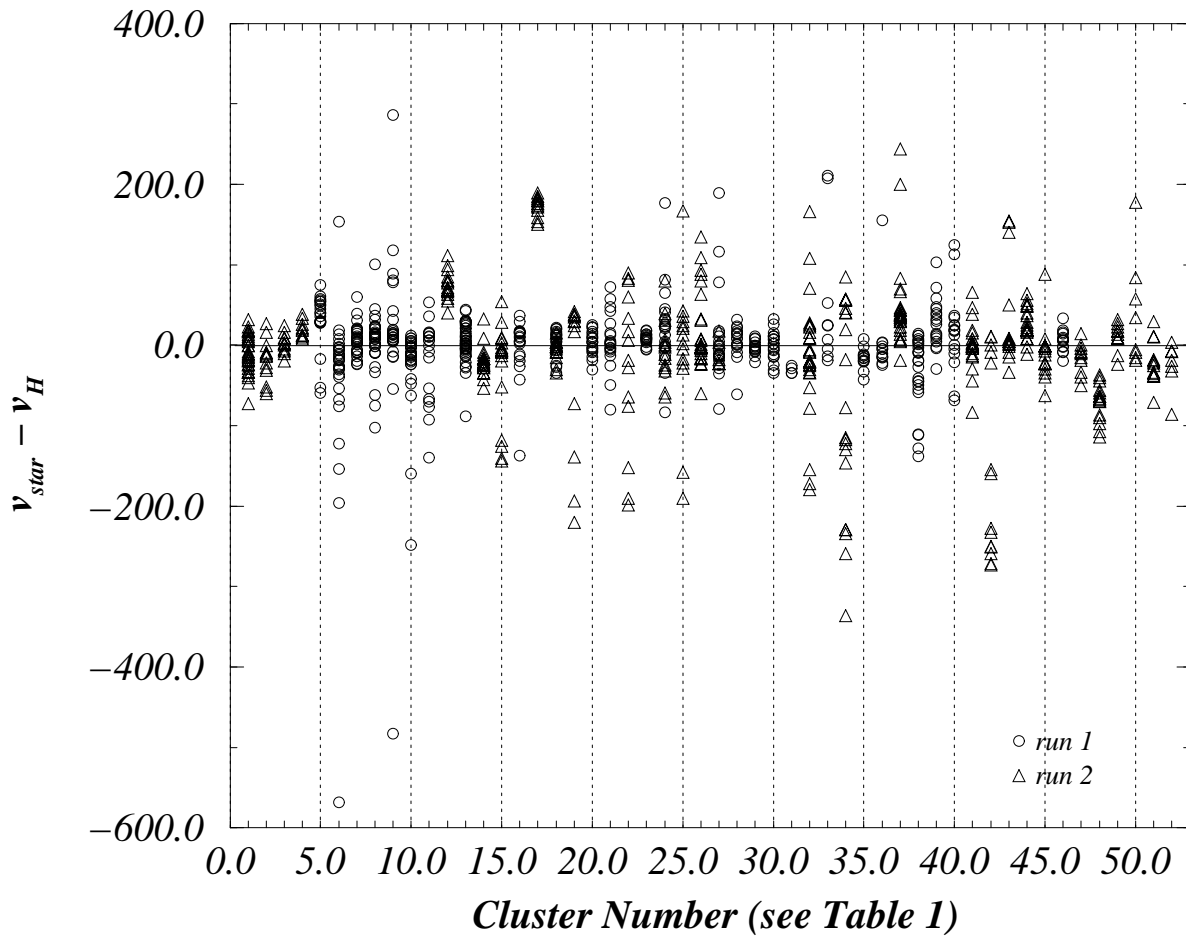


TABLE 4. Ca II triplet line and continuum bandpasses

Paper	Feature Name	Line Center (Å)	Line Bandpass (Å)	Blue Continuum Bandpass (Å)	Red Continuum Bandpass (Å)
AZ88	λ_{8498}	8498	8490–8506	8474–8489	8521–8531
	λ_{8542}	8542	8532–8552	8521–8531	8555–8595
	λ_{8662}	8662	8653–8671	8626–8650	8695–8725
AD91	λ_{8542}	8542	8532–8552	8474–8489	8559–8595
	λ_{8662}	8662	8653–8671	8626–8647	8695–8754
TP	λ_{8498}	8498.1	8490–8506	8346–8489	8563–8642
	λ_{8542}	8542.3	8532–8552	8346–8489	8563–8642
	λ_{8662}	8662.4	8653–8671	8563–8642	8697–8754

Rutledge et al.: GGC CaII Metallicity Scale -- Figure 5.

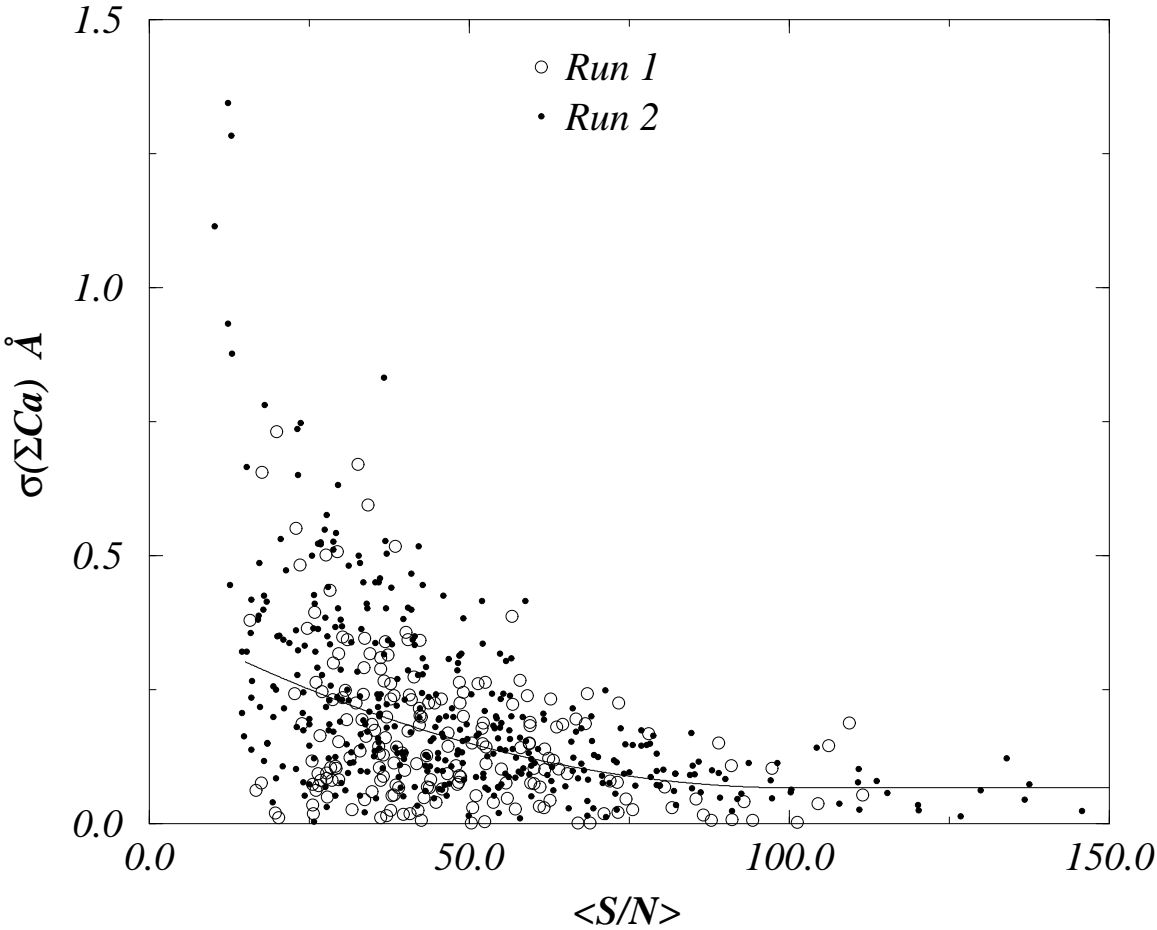


TABLE 5. Ca II triplet α diagnostic for different EW calculation techniques

Technique	Run	λ_{8498}	λ_{8542}	λ_{8662}
Numerical	1	0.118	0.042	0.067
	2	0.117	0.053	0.068
Gaussian	1	0.088	0.042	0.064
	2	0.101	0.051	0.073
Moffat	1	0.088	0.041	0.059
	2	0.101	0.049	0.069
Moffat (new cont.)	1	0.080	0.040	0.059
	2	0.092	0.047	0.070
Moffat (new cont. + new line)	1	0.065	0.034	0.050
	2	0.071	0.036	0.057

Rutledge et al.: GGC CaII Metallicity Scale -- Figure 6.

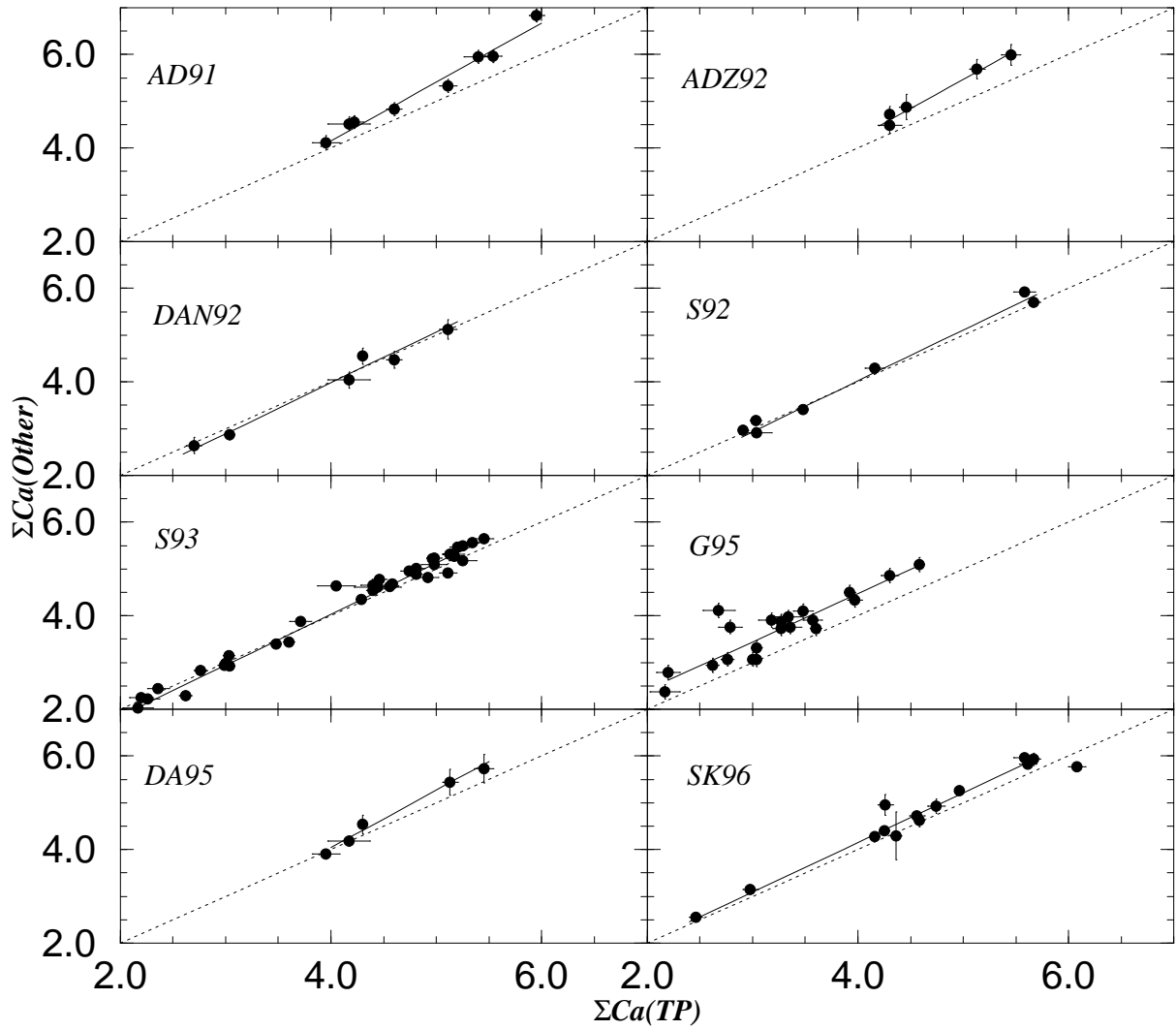


TABLE 6. Transformation Regressions

Paper	m	δm	b (Å)	δb (Å)	$m.e.1$	min (Å)	max (Å)	N
AD91	1.26	0.08	-0.89	0.06	0.92	3.9	6.0	8
ADZ92	1.24	0.10	-0.73	0.05	0.51	4.2	5.4	5
DAN92	1.09	0.07	-0.38	0.07	0.92	2.6	5.2	6
S92	1.04	0.04	-0.11	0.05	1.45	2.9	5.7	7
S93	1.10	0.02	-0.33	0.02	1.35	2.1	5.5	37
G95	1.03	0.10	0.35	0.07	1.75	2.2	4.6	21
DA95	1.23	0.10	-0.88	0.05	0.49	4.0	5.5	5
SK96	1.06	0.02	-0.09	0.03	0.94	2.4	5.7	14

Rutledge et al.: GGC CaII Metallicity Scale -- Figure 7.

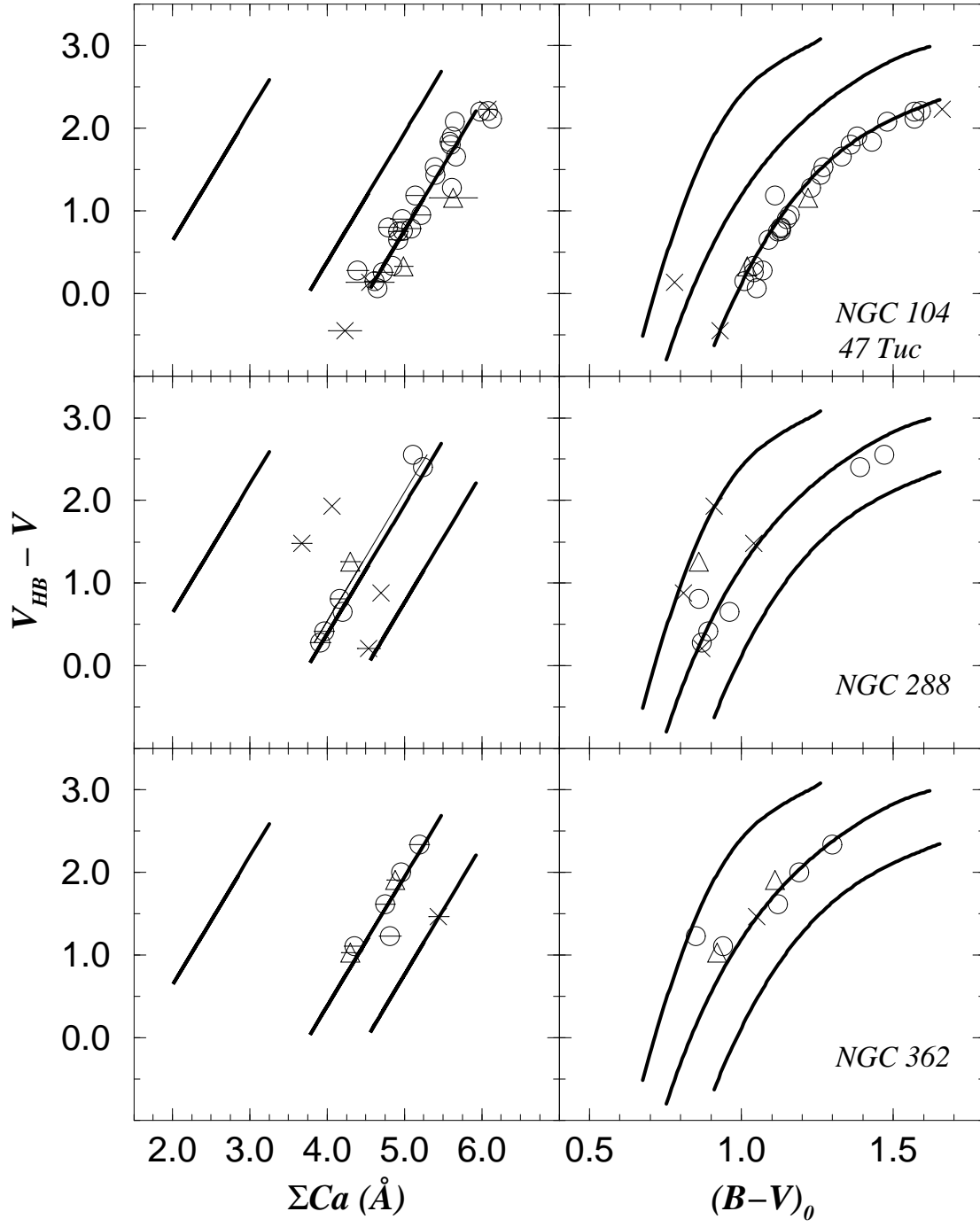


TABLE 7. Published $\Delta(\Sigma Ca)/\Delta(V_{HB} - V)$ slopes

Paper	m \AA mag^{-1}	δm \AA mag^{-1}
AD91	0.62	0.01
ADZ92	0.66	0.07
DAN92	0.72	0.04
S93	0.64	0.03
G95	0.61	0.04
DA95	0.61	0.03
TP	0.64	0.02

Rutledge et al.: GGC CaII Metallicity Scale -- Figure 7.

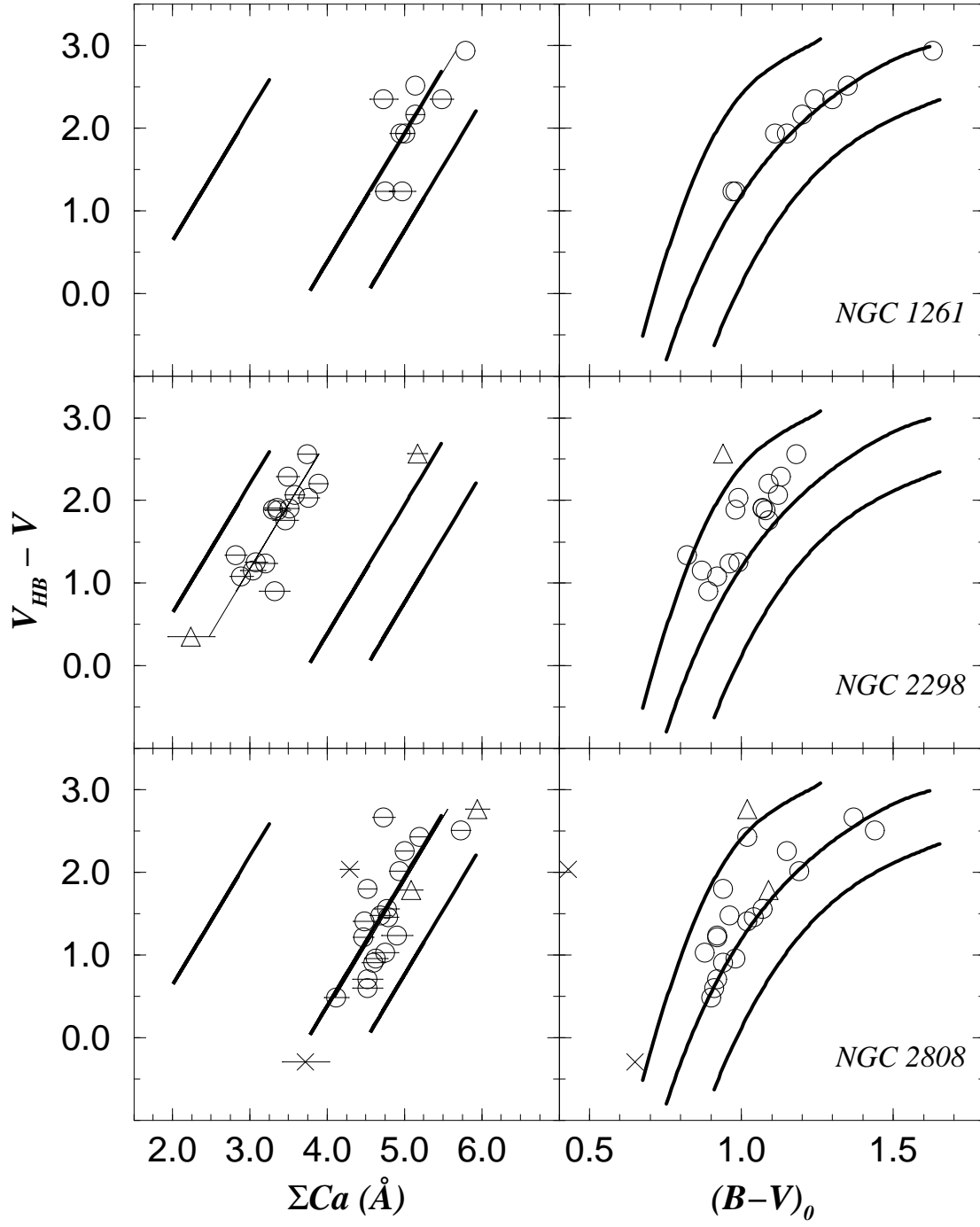


TABLE 8. Metallicity $\Delta(\Sigma Ca)/\Delta(V_{HB} - V)$ slopes

Metallicity Range	N	m \AA mag^{-1}	δm \AA mag^{-1}	$m.e.1$
$-0.8 < [\text{Fe}/\text{H}]$	9	0.73	0.10	1.4
$-1.2 < [\text{Fe}/\text{H}] \leq -0.8$	7	0.54	0.11	1.4
$-1.8 < [\text{Fe}/\text{H}] \leq -1.2$	26	0.62	0.06	1.6
$[\text{Fe}/\text{H}] \leq -1.8$	10	0.67	0.09	1.6
<i>all</i>	52	0.64	0.04	1.6

Rutledge et al.: GGC CaII Metallicity Scale -- Figure 7.

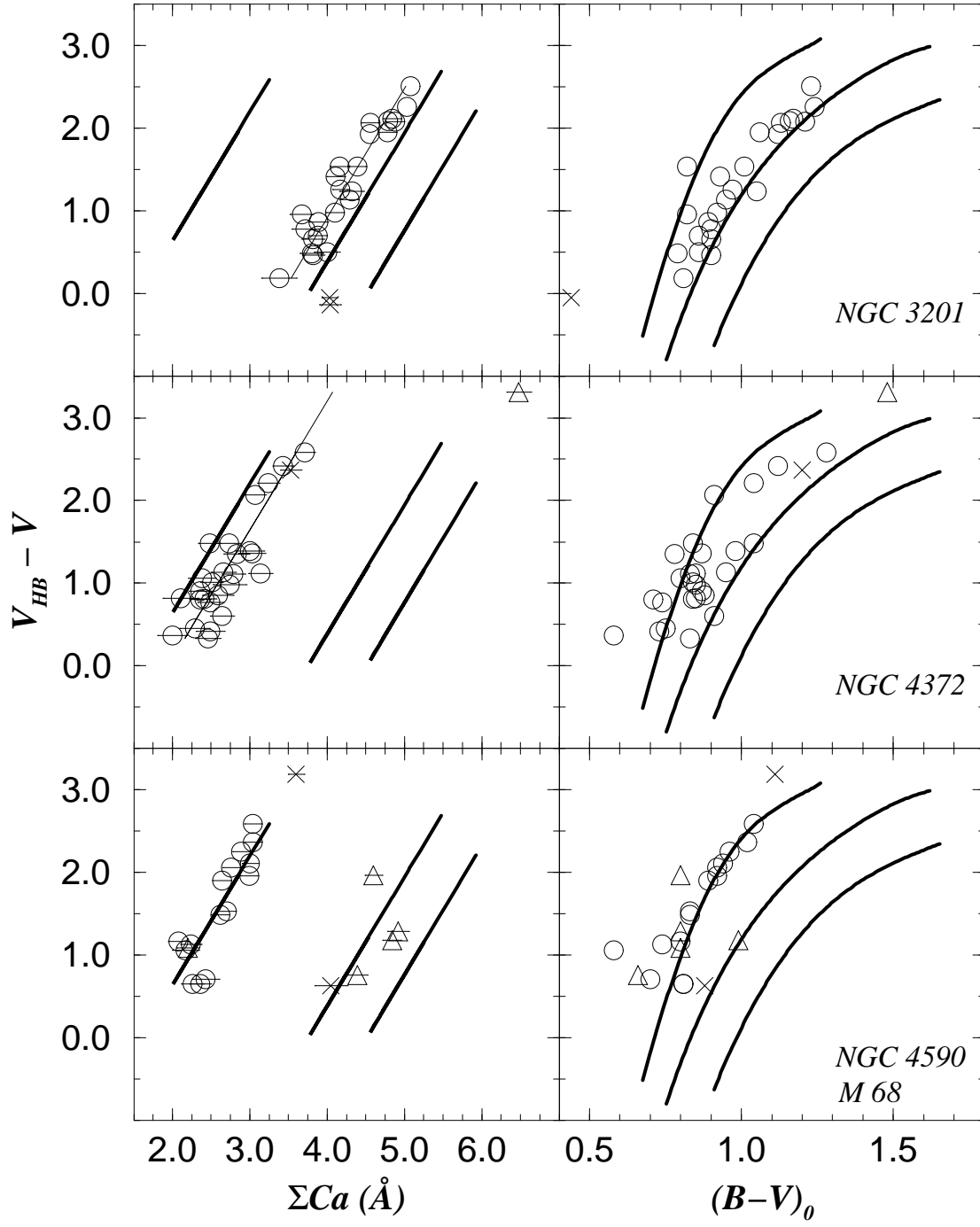


TABLE 9. Individual Star Data and Results

Star	$v_* - v_H$ km s ⁻¹	$V_{HB} - V$ mag	$(B-V)_0$ mag	ΣCa Å	$\sigma(\Sigma Ca)$ Å	P_μ	P_v	f_p	f_r	w	N	Run- Night	Notes
NGC 104 = 47 Tuc													
L5622	17	2.23	1.66	6.08	0.08	97	90	1	2-3	0,2,11
L3730	-11	2.21	1.59	6.08	0.05	96	95	0.95	0.98	0.67	4	2-258	
L8704	-1	2.20	1.57	5.98	0.03	98	95	0.95	1.00	1.00	6	2-3678	
L4741	-8	2.12	1.57	6.13	0.04	98	95	0.95	0.76	0.69	4	2-2356	
L4729	13	2.08	1.48	5.65	0.04	98	92	0.92	0.89	0.68	4	2-2356	
L4745	-33	1.90	1.38	5.61	0.06	97	92	0.92	0.99	0.50	3	2-2	
L5623	-15	1.84	1.43	5.58	0.10	97	95	0.95	1.00	0.25	1	2-3	
L8705	32	1.80	1.36	5.60	0.05	96	76	0.76	1.00	0.54	6	2-3678	
L5739	-19	1.66	1.33	5.67	0.06	98	95	0.95	1.00	0.57	3	2-3	
L4628	-1	1.53	1.27	5.39	0.05	98	95	0.95	0.99	0.62	3	2-2	
L6732	8	1.44	1.26	5.40	0.05	95	93	0.93	1.00	0.60	3	2-6	
L6728	5	1.28	1.23	5.61	0.08	...	94	0.94	0.88	0.33	3	2-6	
L6717	18	1.19	1.11	5.14	0.09	98	90	0.90	0.99	0.26	3	2-6	4
L4737	-73	1.16	1.22	5.63	0.30	98	26	0.26	0.99	0.01	2	2-2	
L4748	-33	0.95	1.16	5.22	0.08	98	92	0.92	1.00	0.34	3	2-2	
L4705	-40	0.90	1.15	4.97	0.14	95	89	0.89	1.00	0.13	3	2-2	
L4626	22	0.80	1.13	4.79	0.10	92	87	0.87	0.96	0.22	3	2-2	
L6727	11	0.79	1.13	5.09	0.10	98	92	0.92	1.00	0.22	3	2-6	
L4636	6	0.76	1.13	4.98	0.07	95	94	0.94	1.00	0.40	3	2-3	
L5743	-29	0.75	1.12	4.92	0.10	98	93	0.93	1.00	0.22	3	2-3	
L5702	18	0.65	1.09	4.92	0.10	96	90	0.90	1.00	0.25	3	2-2	
L6720	-18	0.34	1.04	4.84	0.07	95	95	0.95	1.00	0.44	6	2-57	
L4634	8	0.33	1.02	4.99	0.10	...	93	0.00	0.94	0.00	3	2-3	
L4717	-24	0.28	1.07	4.39	0.12	98	94	0.94	0.94	0.16	3	2-2	
L4731	17	0.26	1.04	4.72	0.12	89	90	0.90	1.00	0.17	3	2-2	
L4735	-25	0.15	1.01	4.61	0.11	97	94	0.94	1.00	0.21	3	2-2	
L4635	-13	0.14	0.78	4.55	0.30	...	95	1	2-3	0,5
L6707	-19	0.07	1.05	4.65	0.07	74	95	0.95	1.00	0.46	6	2-57	
L6723	-47	-0.45	0.93	4.23	0.20	59	83	2	2-5	

TABLE 9. (continued)

Star	$v_* - v_H$ km s ⁻¹	$V_{HB} - V$ mag	$(B-V)_0$ mag	ΣCa Å	$\sigma(\Sigma Ca)$ Å	P_μ	P_v	f_p	f_r	w	N	Run- Night	Notes
NGC 288													
A96,O403	0	2.55	1.47	5.11	0.04	...	94	0.94	0.89	0.82	3	2-3	
A78,O274	-14	2.40	1.39	5.24	0.04	...	96	0.96	1.00	1.00	3	2-3	
A100,O409	-12	1.93	0.91	4.06	0.05	...	96	3	2-3	0,4
A277,O525	-10	1.48	1.04	3.67	0.11	...	96	3	2-5	0,9
A206,O601	27	1.26	0.86	4.30	0.11	...	52	0.52	0.99	0.13	3	2-3	4
A179,O329	-9	0.88	0.81	4.70	0.06	...	96	3	2-5	0,4
A131	-52	0.81	0.86	4.16	0.09	...	92	0.92	1.00	0.30	3	2-3	4
A103	-22	0.65	0.96	4.20	0.06	...	97	0.97	0.98	0.62	3	2-3	
A104,O415	-56	0.42	0.89	3.96	0.11	...	89	0.89	1.00	0.22	3	2-3	
A154,O503	-28	0.28	0.87	3.91	0.12	...	97	0.97	1.00	0.22	3	2-5	
A166,O318	-31	0.21	0.87	4.54	0.13	...	97	3	2-5	0,10
NGC 362													
H1216	-7	2.34	1.30	5.19	0.11	...	99	0.99	1.00	0.42	3	2-6	
H2213	2	2.00	1.19	4.96	0.07	99	99	0.99	1.00	1.00	3	2-6	
H1422	10	1.91	1.11	4.88	0.08	2	99	0.00	1.00	0.00	3	2-6	
H1412	3	1.62	1.12	4.75	0.10	99	99	0.99	1.00	0.48	3	2-6	
H2302	-4	1.47	1.05	5.44	0.11	99	99	3	2-6	0,10
H2307	16	1.23	0.85	4.81	0.12	99	99	0.99	0.87	0.31	3	2-6	4
H1225	-11	1.11	0.94	4.35	0.11	...	99	0.99	1.00	0.43	3	2-6	
H1218	-19	1.03	0.92	4.30	0.10	3	99	0.00	1.00	0.00	3	2-6	
NGC 1261													
A27,F680	12	2.94	1.63	5.79	0.07	...	96	0.96	1.00	1.00	3	2-8	
A96,F619	18	2.52	1.35	5.14	0.07	...	97	0.97	0.96	0.94	3	2-7	
A105,F119	38	2.35	1.24	4.73	0.17	...	96	0.96	0.91	0.21	3	2-8	
A122,F402	8	2.35	1.30	5.48	0.13	...	96	0.96	1.00	0.36	3	2-7	
A100,F501	34	2.17	1.20	5.14	0.10	...	97	0.97	1.00	0.61	3	2-8	
A53,F49	12	1.94	1.11	5.01	0.09	...	96	0.96	1.00	0.70	5	2-8	
A106,F136	21	1.94	1.15	4.95	0.13	...	97	0.97	1.00	0.40	3	2-7	

TABLE 9. (continued)

Star	$v_* - v_H$ km s ⁻¹	$V_{HB} - V$ mag	$(B-V)_0$ mag	ΣCa Å	$\sigma(\Sigma Ca)$ Å	P_μ	P_v	f_p	f_r	w	N	Run- Night	Notes
A101,F328	26	1.24	0.97	4.75	0.11	...	97	0.97	1.00	0.51	5	2-8	
A102,F228	20	1.24	0.98	4.97	0.16	...	97	0.97	0.97	0.26	5	2-8	
NGC 2298													
A3	-53	2.57	0.94	5.17	0.08	...	0	0.00	0.02	0.00	2	1-5	
A4	58	2.56	1.18	3.74	0.08	...	99	0.99	0.99	0.74	4	1-56	
A6	28	2.29	1.13	3.49	0.11	...	98	0.98	0.98	0.45	1	1-6	
A7	45	2.20	1.09	3.89	0.06	...	99	0.99	0.94	0.88	2	1-5	
A8	75	2.07	1.12	3.58	0.08	...	99	0.99	1.00	0.70	3	1-56	
A9	40	2.03	0.99	3.76	0.10	...	99	0.99	0.98	0.54	1	1-6	
A10	60	1.91	1.07	3.35	0.13	...	99	0.99	1.00	0.38	1	1-6	
A11	28	1.90	1.07	3.51	0.07	...	98	0.98	1.00	0.83	3	1-56	
A13	56	1.89	0.98	3.30	0.06	...	99	0.99	0.98	1.00	8	1-56	
A12	29	1.88	1.08	3.36	0.13	...	99	0.99	1.00	0.38	1	1-5	
A14	54	1.76	1.09	3.46	0.13	...	99	0.99	1.00	0.38	2	1-5	
A16	40	1.34	0.82	2.82	0.10	...	99	0.99	0.93	0.51	4	1-56	
A15	30	1.25	0.99	3.08	0.11	...	99	0.99	1.00	0.49	4	1-56	
A17	36	1.24	0.96	3.20	0.12	...	99	0.99	0.99	0.44	3	1-56	
A18	49	1.15	0.87	3.04	0.13	...	99	0.99	1.00	0.38	4	1-56	
A19	28	1.08	0.92	2.89	0.12	...	98	0.98	1.00	0.42	3	1-56	
A21	30	0.90	0.89	3.32	0.17	...	99	0.99	0.85	0.20	4	1-56	
A32	-17	0.35	...	2.24	0.29	...	17	0.17	1.00	0.02	1	1-6	
NGC 2808													
H251	-76	2.77	1.02	5.94	0.12	...	47	0.47	0.97	0.15	1	1-8	
H120	-19	2.67	1.37	4.73	0.11	...	97	0.97	0.70	0.27	4	1-24	
H275	-7	2.51	1.44	5.73	0.07	...	97	0.97	0.95	0.58	3	1-8	
H129	-54	2.43	1.02	5.19	0.06	...	87	0.87	1.00	0.67	4	1-24	
H63	-2	2.26	1.15	5.00	0.04	...	97	0.97	0.99	1.00	7	1-248	
H82	-68	2.04	0.43	4.29	0.07	...	68	3	1-2	0,4,9
H269	-11	2.02	1.19	4.93	0.08	...	97	0.97	1.00	0.57	2	1-4	
H106	-5	1.80	0.94	4.52	0.05	...	97	0.97	0.91	0.85	3	1-2	
H315	154	1.79	1.09	5.09	0.11	...	0	0.00	1.00	0.00	2	1-4	

TABLE 9. (continued)

Star	$v_* - v_H$ km s ⁻¹	$V_{HB} - V$ mag	$(B-V)_0$ mag	ΣCa Å	$\sigma(\Sigma Ca)$ Å	P_μ	P_v	f_p	f_r	w	N	Run- Night	Notes
H321,F5777	-15	1.56	1.07	4.77	0.12	...	97	0.97	1.00	0.29	2	1-4	
H288	2	1.48	0.96	4.69	0.10	...	96	0.96	1.00	0.42	2	1-8	
H246	13	1.46	1.04	4.79	0.09	...	95	0.95	1.00	0.48	2	1-4	
H26	-39	1.41	1.02	4.48	0.10	...	94	0.94	1.00	0.37	5	1-248	
H258	-36	1.24	0.92	4.90	0.17	...	95	0.95	0.99	0.16	2	1-4	
H59	-19	1.22	0.92	4.47	0.09	...	97	0.97	1.00	0.50	7	1-248	
H297,F1637	-12	1.03	0.88	4.75	0.14	...	97	0.97	0.99	0.24	2	1-8	
H98	8	0.96	0.98	4.63	0.12	...	96	0.96	0.99	0.33	3	1-2	
H49	-27	0.91	0.94	4.60	0.11	...	96	0.96	0.99	0.33	6	1-248	
H173,F1685	-3	0.71	0.92	4.52	0.17	...	97	0.97	1.00	0.18	2	1-8	
H66,F118	-29	0.60	0.91	4.52	0.16	...	96	0.96	0.99	0.18	2	1-2	
H40	-30	0.49	0.90	4.12	0.12	...	96	0.96	1.00	0.29	2	1-2	
H307,F1656	18	-0.29	0.65	3.72	0.29	...	94	2	1-4	0,5
NGC 3201													
L3204	-9	2.51	1.23	5.08	0.03	...	99	0.99	1.00	1.00	19	1-18	
L4318	1	2.26	1.24	5.03	0.03	...	99	0.99	0.95	0.92	12	1-12478	
L2405	5	2.12	1.17	4.84	0.07	...	99	0.99	1.00	0.54	1	1-7	1
L3401	5	2.09	1.16	4.79	0.03	...	99	0.99	1.00	0.98	7	1-1247	
L4507	21	2.08	1.21	4.88	0.07	...	99	0.99	0.99	0.54	1	1-7	
L3522	17	2.07	1.13	4.56	0.07	...	99	0.99	0.96	0.52	1	1-7	
L1501	19	1.95	1.06	4.78	0.07	...	99	0.99	0.99	0.54	1	1-7	
L1410	20	1.93	1.12	4.55	0.03	...	99	0.99	0.99	0.97	6	1-1247	
L3504	7	1.54	1.01	4.39	0.05	...	99	0.99	1.00	0.68	2	1-2	
L1309	20	1.54	0.82	4.16	0.08	...	99	0.99	0.90	0.42	2	1-1	4
L3107	-9	1.42	0.93	4.11	0.07	...	99	0.99	0.93	0.48	4	1-1	
L1411	4	1.26	0.97	4.17	0.03	...	99	0.99	1.00	0.92	6	1-1247	
L4215	18	1.24	1.05	4.32	0.12	...	99	0.99	1.00	0.23	1	1-7	
L3101	-19	1.14	0.95	4.29	0.07	...	99	0.99	0.98	0.48	3	1-18	
L4403	4	0.98	0.92	4.10	0.06	...	99	0.99	1.00	0.58	2	1-47	
L2214	-14	0.96	0.82	3.67	0.11	...	99	0.99	0.81	0.22	2	1-1	
L3525	8	0.87	0.89	3.89	0.07	...	99	0.99	1.00	0.50	1	1-7	
L1416	14	0.78	0.90	3.72	0.15	...	99	0.99	0.99	0.17	2	1-2	
L3304	11	0.70	0.86	3.88	0.06	...	99	0.99	1.00	0.59	6	1-124	

TABLE 9. (continued)

Star	$v_* - v_H$ km s ⁻¹	$V_{HB} - V$ mag	$(B-V)_0$ mag	ΣCa Å	$\sigma(\Sigma Ca)$ Å	P_μ	P_v	f_p	f_r	w	N	Run- Night	Notes
L2321	-8	0.66	0.90	3.82	0.11	...	99	0.99	1.00	0.28	2	1-2	
L2207	4	0.50	0.86	4.00	0.13	...	99	0.99	0.95	0.20	2	1-1	
L3102	-23	0.49	0.79	3.80	0.11	...	99	0.99	1.00	0.26	4	1-1	
L4307	8	0.47	0.90	3.82	0.11	...	99	0.99	1.00	0.30	1	1-4	
L3413	39	0.19	0.81	3.38	0.20	...	99	0.99	1.00	0.10	1	1-4	
L1415	9	-0.05	0.44	4.03	0.03	...	99	6	1-247	0,5
L1201	-6	-0.13	0.05	4.04	0.10	...	99	2	1-1	0,5
NGC 4372													
A104	-76	3.31	1.48	6.48	0.09	...	0	0.00	0.00	0.00	2	1-1	
A13	14	2.58	1.28	3.71	0.04	...	97	0.97	1.00	1.00	3	1-157	
A20	11	2.42	1.12	3.43	0.04	...	97	0.97	1.00	0.98	3	1-157	
A141	100	2.37	1.20	3.53	0.04	...	0	3	1-17	0,1
A94	20	2.21	1.04	3.24	0.07	...	97	0.97	1.00	0.75	1	1-5	
A70	13	2.07	0.91	3.07	0.05	...	97	0.97	0.98	0.89	2	1-5	
A1	8	1.48	1.04	2.73	0.08	...	97	0.97	1.00	0.60	1	1-5	
A10	22	1.48	0.84	2.48	0.07	...	97	0.97	0.79	0.60	7	1-1257	
A81	13	1.39	0.98	3.00	0.14	...	97	0.97	1.00	0.33	1	1-7	
A67	13	1.36	0.87	3.03	0.12	...	97	0.97	0.99	0.42	1	1-5	
A57	10	1.35	0.78	2.83	0.10	...	97	0.97	1.00	0.49	2	1-2	
A74	8	1.13	0.95	2.66	0.10	...	97	0.97	1.00	0.53	1	1-5	
A76	-1	1.12	0.85	3.14	0.09	...	96	0.96	0.74	0.43	2	1-1	
A77	-9	1.11	0.83	2.79	0.08	...	94	0.94	1.00	0.65	2	1-1	
A60	9	1.06	0.80	2.38	0.12	...	97	0.97	0.99	0.39	2	1-2	
A14	23	1.01	0.84	2.51	0.07	...	97	0.97	1.00	0.75	5	1-127	
A105	-27	0.98	0.85	2.74	0.17	...	76	0.76	1.00	0.18	2	1-1	
A75	21	0.90	0.87	2.36	0.08	...	97	0.97	1.00	0.65	1	1-5	
A91	-9	0.85	0.88	2.59	0.15	...	94	0.94	1.00	0.28	2	1-2	
A95	14	0.82	0.85	2.11	0.19	...	97	0.97	0.98	0.19	2	1-2	
A89	1	0.81	0.84	2.41	0.09	...	96	0.96	1.00	0.54	2	1-5	
A16	14	0.80	0.71	2.36	0.06	...	97	0.97	1.00	0.82	9	1-127	
A100	23	0.77	0.74	2.49	0.11	...	97	0.97	1.00	0.46	2	1-7	
A84	2	0.60	0.91	2.64	0.08	...	97	0.97	0.93	0.58	2	1-5	
A71	16	0.45	0.75	2.29	0.15	...	97	0.97	1.00	0.29	1	1-5	

TABLE 9. (continued)

Star	$v_* - v_H$ km s ⁻¹	$V_{HB} - V$ mag	$(B - V)_0$ mag	ΣCa Å	$\sigma(\Sigma Ca)$ Å	P_μ	P_v	f_p	f_r	w	N	Run- Night	Notes
A12	-9	0.42	0.73	2.49	0.13	...	94	0.94	0.98	0.34	2	1-1	5
A85	-1	0.37	0.58	2.00	0.14	...	96	0.96	1.00	0.32	2	1-5	
A96	31	0.33	0.83	2.46	0.10	...	96	0.96	0.95	0.48	2	1-7	
NGC 4590 = M 68													
HZNG2	42	3.19	1.11	3.60	0.05	...	85	3	1-48	0,1
HI257	15	2.59	1.04	3.04	0.05	...	97	0.97	0.97	0.82	4	1-18	
HI10	18	2.37	1.02	3.04	0.05	...	97	0.97	1.00	0.91	3	1-48	
HI254	10	2.25	0.96	2.89	0.06	...	98	0.98	1.00	0.68	4	1-18	4
HQ	15	2.11	0.94	3.00	0.04	...	97	0.97	1.00	1.00	4	1-45	
HI119	-15	2.06	0.92	2.76	0.06	...	96	0.96	0.99	0.67	4	1-25	
A18	80	1.97	0.80	4.60	0.06	...	1	0.01	0.01	0.00	6	1-14568	4
HI128	7	1.96	0.92	2.99	0.06	...	98	0.98	0.99	0.71	5	1-15	
A81	9	1.90	0.89	2.64	0.07	...	98	0.98	0.99	0.61	2	1-5	
HI30	7	1.53	0.83	2.70	0.07	...	98	0.98	1.00	0.59	4	1-15	4
HI239	5	1.49	0.83	2.62	0.07	...	98	0.98	1.00	0.67	4	1-24	
HI179	118	1.29	0.80	4.92	0.10	...	0	0.00	0.00	0.00	4	1-24	
A29	287	1.18	0.99	4.84	0.07	...	0	0.00	0.00	0.00	6	1-124	4
A20	12	1.17	0.80	2.08	0.09	...	98	0.98	0.97	0.44	6	1-14568	
HI35	20	1.13	0.74	2.24	0.10	...	97	0.97	1.00	0.41	3	1-48	
HI74	-54	1.09	0.80	2.20	0.11	...	23	0.23	1.00	0.08	5	1-15	4
HI49	6	1.06	0.58	2.17	0.14	...	98	0.98	1.00	0.22	3	1-15	
A21	89	0.76	0.66	4.39	0.09	...	0	0.00	0.00	0.00	8	1-146	
A23	-14	0.71	0.70	2.43	0.14	...	96	0.96	0.94	0.21	6	1-124	4
HI147	13	0.65	0.81	2.36	0.10	...	97	0.97	0.90	0.34	7	1-245	
HI172	6	0.65	0.81	2.26	0.11	...	98	0.98	0.98	0.33	4	1-28	
HI184	32	0.63	0.88	4.05	0.19	...	94	2	1-2	0,1
NGC 4833													
MA75	-13	2.86	1.48	4.35	0.07	...	99	0.99	0.98	0.75	1	1-3	4
MB200	9	2.66	1.20	4.13	0.07	...	99	0.99	1.00	0.76	1	1-6	
MB205	4	2.37	1.02	3.67	0.07	...	99	0.99	1.00	0.76	1	1-6	
MA83	-2	2.35	1.00	3.18	0.08	...	99	0.99	0.55	0.38	1	1-3	

TABLE 9. (continued)

Star	$v_* - v_H$ km s^{-1}	$V_{HB} - V$ mag	$(B-V)_0$ mag	$\Sigma C a$ Å	$\sigma(\Sigma C a)$ Å	P_μ	P_v	f_p	f_r	w	N	Run-Night	Notes
MA57	−2	2.35	1.17	3.94	0.04	...	99	0.99	0.99	0.98	3	1-356	
MB118	−3	2.26	1.14	3.82	0.06	...	99	0.99	1.00	0.81	2	1-2	
MB85	−9	2.24	1.12	3.68	0.07	...	99	0.99	1.00	0.74	1	1-6	
MA90	5	2.13	1.11	3.76	0.06	...	99	0.99	1.00	0.84	3	1-3	
MA29	−15	2.09	1.03	3.51	0.06	...	99	0.99	1.00	0.87	5	1-2356	
MA60	−2	2.08	1.13	3.76	0.04	...	99	0.99	0.99	1.00	4	1-356	
MA27	−10	1.89	1.03	3.55	0.05	...	99	0.99	1.00	0.92	5	1-2356	
MB23	−42	1.84	0.99	3.42	0.07	...	98	0.98	1.00	0.71	1	1-6	
MB73	8	1.74	0.95	3.51	0.11	...	99	0.99	1.00	0.47	2	1-6	
MB77	12	1.68	0.87	3.14	0.09	...	99	0.99	0.99	0.58	2	1-2	
MB160	−18	1.54	0.87	3.06	0.13	...	99	0.99	1.00	0.35	1	1-6	
MA67	−24	1.43	1.00	2.92	0.11	...	99	0.99	0.98	0.42	2	1-3	
MB45	−63	1.34	0.86	3.47	0.12	...	61	0.61	0.96	0.24	1	1-6	
MB119	2	1.19	0.91	3.23	0.13	...	99	0.99	1.00	0.35	2	1-2	
MA62	−248	1.18	0.96	5.12	0.11	...	0	0.00	0.01	0.00	2	1-3	
MB33	0	1.06	0.89	2.87	0.15	...	99	0.99	1.00	0.30	2	1-3	
MB34	−159	0.96	1.23	5.04	0.15	...	0	0.00	0.02	0.00	2	1-2	
MB30	5	0.87	0.84	2.67	0.11	...	99	0.99	1.00	0.46	4	1-23	
MB67	−12	0.80	0.82	2.43	0.17	...	99	0.99	0.98	0.23	2	1-2	
MA84	−20	0.54	0.65	2.15	0.16	...	99	0.99	0.92	0.25	1	1-6	
MB70	−10	0.33	0.77	2.68	0.16	...	99	0.99	1.00	0.25	2	1-2	
MB94	−18	0.08	0.74	2.58	0.15	...	99	0.99	0.99	0.30	2	1-6	
NGC 5286													
H100	14	2.35	1.11	4.58	0.04	...	96	0.96	1.00	1.00	6	1-247	
H53	36	2.27	1.03	4.30	0.06	...	95	0.95	0.99	0.83	2	1-7	
H31	−70	2.22	1.09	5.35	0.15	...	1	0.01	0.45	0.00	1	1-7	
H116	−53	1.79	0.80	4.85	0.21	...	14	0.14	0.87	0.02	1	1-7	
H158	−93	1.79	0.95	5.02	0.09	...	0	0.00	0.30	0.00	3	1-27	
H110	6	1.75	0.87	4.93	0.20	...	96	1	1-7	0,10
H30	53	1.67	0.95	3.75	0.18	...	88	0.88	0.98	0.20	1	1-7	
H194	16	1.60	0.98	4.49	0.09	...	97	0.97	0.86	0.52	2	1-4	
H35	10	1.52	1.06	4.25	0.12	...	96	0.96	0.99	0.41	2	1-2	
H164	−8	1.43	0.84	3.60	0.10	...	93	0.93	0.94	0.48	4	1-47	

TABLE 9. (continued)

Star	$v_* - v_H$ km s ⁻¹	$V_{HB} - V$ mag	$(B-V)_0$ mag	ΣCa Å	$\sigma(\Sigma Ca)$ Å	P_μ	P_v	f_p	f_r	w	N	Run- Night	Notes
H77	0	1.33	0.83	3.92	0.08	...	95	0.95	1.00	0.62	3	1-4	
H160	-140	1.31	0.98	5.60	0.07	...	0	0.00	0.02	0.00	7	1-247	
H17	15	1.23	0.81	3.61	0.12	...	97	0.97	0.99	0.40	2	1-7	
H91	11	0.89	0.75	3.64	0.16	...	96	0.96	1.00	0.26	2	1-7	
H32	6	0.75	0.78	3.64	0.16	...	96	0.96	1.00	0.26	2	1-2	
H198	-16	0.58	0.73	3.52	0.16	...	90	0.90	1.00	0.24	2	1-4	
H78	-77	0.27	0.76	4.24	0.20	...	0	0.00	0.52	0.00	3	1-4	
NGC 5897													
S263	85	2.99	1.65	4.27	0.05	...	98	0.98	1.00	1.00	3	2-2	
S255	80	2.85	1.72	3.92	0.05	...	98	0.98	0.99	0.92	3	2-2	
S160	68	2.82	1.35	3.97	0.07	...	98	0.98	1.00	0.69	3	2-2	
S138	71	1.90	1.10	3.27	0.08	...	98	0.98	0.99	0.54	3	2-2	
S142	77	1.67	1.01	3.36	0.11	...	98	0.98	1.00	0.40	3	2-2	
S145	58	1.56	1.02	3.06	0.08	...	96	0.96	0.99	0.59	3	2-2	
S31	99	1.56	1.00	2.99	0.09	...	97	0.97	0.97	0.47	3	2-2	
S30	111	1.15	0.94	3.11	0.11	...	94	0.94	1.00	0.36	3	2-2	
S13	40	0.91	0.91	3.08	0.11	...	85	0.85	0.98	0.31	3	2-2	
S29	69	0.59	0.87	3.06	0.19	...	98	0.98	0.97	0.14	3	2-2	
S6	55	0.37	0.82	2.79	0.12	...	95	0.95	0.96	0.33	3	2-2	
S25	94	0.13	0.83	2.85	0.28	...	98	0.98	0.98	0.07	3	2-2	
S33	63	-0.09	0.84	2.86	0.18	...	97	3	2-2	
NGC 5904 = M 5													
BI68	44	2.69	1.49	5.34	0.10	99	85	0.85	1.00	0.19	1	1-6	
BIII114	30	2.46	1.38	5.35	0.09	...	94	0.94	1.00	0.27	1	1-5	
BIII36	15	2.27	1.31	5.17	0.09	99	97	0.97	1.00	0.31	1	1-5	
BI71	29	2.05	1.26	4.81	0.08	99	95	0.95	0.96	0.34	1	1-6	
BI39	27	2.03	1.26	4.88	0.06	99	95	0.95	0.99	0.49	2	1-6	
BII59	30	1.72	1.12	4.93	0.11	99	95	0.95	1.00	0.20	1	1-5	
BI61	24	1.69	1.14	4.88	0.03	99	96	0.96	1.00	1.00	12	1-1567	
BII106	1	1.64	1.08	4.81	0.06	...	96	0.96	1.00	0.47	2	1-5	
BII74	21	1.24	0.98	4.57	0.15	99	96	0.96	1.00	0.11	1	1-5	

TABLE 9. (continued)

Star	$v_* - v_H$ km s ⁻¹	$V_{HB} - V$ mag	$(B-V)_0$ mag	ΣCa Å	$\sigma(\Sigma Ca)$ Å	P_μ	P_v	f_p	f_r	w	N	Run- Night	Notes
BI98	-35	1.22	0.99	3.59	0.16	...	61	0.61	0.54	0.04	2	1-1	
BI2	42	1.19	0.99	4.26	0.14	99	87	0.87	0.99	0.12	2	1-1	
BI50	-27	1.15	0.94	3.87	0.23	99	80	0.80	0.96	0.04	2	1-2	9
BII50	5	1.14	0.93	4.46	0.07	99	97	0.97	1.00	0.42	4	1-25	
BI43	27	1.07	0.99	4.44	0.10	99	95	0.95	1.00	0.23	3	1-6	
BI80	6	1.06	1.05	4.40	0.12	98	97	0.97	1.00	0.17	2	1-6	
BI74	30	1.03	0.95	4.34	0.09	99	94	0.94	1.00	0.28	3	1-6	
BII51	-14	1.01	0.93	4.30	0.11	99	93	0.93	1.00	0.20	3	1-25	
BIII19	-5	0.86	0.91	4.49	0.12	99	95	0.95	1.00	0.18	1	1-5	
BII80	-5	0.75	0.88	4.49	0.10	...	96	0.96	0.98	0.23	3	1-7	
BII18	12	0.62	0.86	4.31	0.10	99	97	0.97	1.00	0.22	2	1-5	
BIII12	-1	0.46	0.85	4.27	0.19	99	96	0.96	1.00	0.07	1	1-5	
BI59	17	0.42	0.88	4.77	0.10	99	97	0.97	0.41	0.10	4	1-12	10
BII45	-10	0.31	0.79	3.83	0.17	99	94	0.94	1.00	0.09	3	1-5	
BIII147	-89	0.26	0.77	5.24	0.14	...	0	0.00	0.17	0.00	1	1-5	
BIII13	11	0.04	0.73	3.92	0.16	...	97	0.97	1.00	0.10	1	1-5	
BI44	-21	0.04	0.08	4.26	0.13	99	88	0.88	0.90	0.12	1	1-6	
BII16	2	-0.01	0.76	3.84	0.18	99	96	2	1-5	
BIII115	-28	-0.01	0.83	3.57	0.21	...	79	1	1-5	
BI146	-12	-0.06	0.52	2.99	0.16	...	93	2	1-1	0,5
BI64	-7	-0.11	0.80	4.22	0.15	99	95	2	1-1	
BI65	0	-0.13	0.79	3.67	0.10	99	96	10	1-1256	
BI92	-13	-0.32	0.75	2.24	0.31	...	93	5	1-125	0,9
NGC 5927													
M188	-17	2.17	1.76	6.20	0.07	...	98	0.98	1.00	0.80	3	2-1	
M190	-20	2.11	1.55	5.80	0.10	...	99	0.99	0.80	0.44	3	2-1	
M335	-43	1.96	1.47	5.96	0.05	...	99	0.99	1.00	0.96	3	2-1	
M65	-17	1.76	1.45	5.82	0.07	...	99	0.99	1.00	0.78	4	2-1	
M372	-24	1.74	1.64	6.09	0.05	...	99	0.99	0.96	1.00	3	2-1	
M133	-35	1.65	1.50	5.96	0.08	...	99	0.99	1.00	0.71	5	2-1	
M86	-18	1.23	1.37	5.44	0.12	...	99	0.99	1.00	0.43	4	2-1	
M69	-16	1.19	1.33	5.72	0.13	...	98	0.98	0.99	0.38	3	2-1	
M377	-12	1.17	1.38	5.56	0.10	...	98	0.98	1.00	0.56	3	2-1	

TABLE 9. (continued)

Star	$v_* - v_H$ km s ⁻¹	$V_{HB} - V$ mag	$(B-V)_0$ mag	ΣCa Å	$\sigma(\Sigma Ca)$ Å	P_μ	P_v	f_p	f_r	w	N	Run- Night	Notes
M37	-22	0.63	1.12	5.34	0.14	...	99	0.99	0.99	0.37	3	2-1	
M409	-25	0.61	1.17	5.12	0.16	...	99	0.99	1.00	0.29	3	2-1	
NGC 5986													
H156	-141	3.39	1.47	5.89	0.04	...	0	0.00	0.52	0.00	3	2-7	
H181	-126	2.46	1.27	5.93	0.04	...	0	0.00	0.05	0.00	7	2-78	
H166	9	2.39	1.18	4.79	0.07	...	97	0.97	1.00	1.00	3	2-7	
H185	-20	2.28	1.14	4.42	0.09	...	96	0.96	0.99	0.70	3	2-7	
H93	-52	2.08	0.95	4.05	0.14	...	59	0.59	0.90	0.23	3	2-7	
H158	-144	1.91	1.19	4.82	0.09	...	0	0.00	0.83	0.00	3	2-7	
H178	3	1.78	1.07	4.22	0.09	...	98	0.98	1.00	0.78	3	2-7	
H138	-118	1.67	0.90	3.73	0.12	...	0	0.00	0.79	0.00	3	2-7	
H155	-6	1.48	1.01	3.94	0.10	...	97	0.97	1.00	0.69	3	2-7	
H235	-7	1.05	0.81	4.05	0.11	...	97	0.97	0.99	0.56	3	2-8	
H228	-13	0.98	0.73	3.12	0.15	...	97	3	2-8	0,4
H201	54	0.40	0.74	3.76	0.19	...	59	0.59	0.98	0.16	4	2-8	
H194	-5	0.08	0.78	3.62	0.15	...	97	0.97	0.94	0.35	4	2-8	
NGC 6093 = M 80													
HI49	5	2.51	1.30	4.59	0.07	...	95	0.95	1.00	0.74	1	1-8	
HI170	16	2.33	1.24	4.62	0.10	...	94	0.94	0.96	0.50	1	1-6	
HI106	17	2.28	1.12	4.49	0.04	...	94	0.94	0.99	1.00	4	1-68	
HI138	17	2.15	1.21	4.28	0.09	...	94	0.94	1.00	0.55	1	1-6	
HI90	14	2.08	1.14	4.46	0.05	...	94	0.94	0.93	0.86	3	1-68	
HI67	10	1.93	0.93	3.83	0.10	...	94	0.94	0.96	0.46	1	1-8	
HI246	16	1.85	1.10	3.95	0.09	...	94	0.94	1.00	0.60	2	1-6	
HI51	11	1.80	1.01	3.98	0.13	...	94	0.94	1.00	0.35	1	1-8	
HI157	4	1.64	0.85	4.71	0.18	...	95	1	1-6	0,10
HI210	29	1.48	0.93	3.75	0.23	...	91	0.91	1.00	0.14	1	1-6	
HI130	-11	1.48	0.98	3.66	0.12	...	93	0.93	1.00	0.42	2	1-6	
HI275	-43	1.43	0.84	4.72	0.10	...	68	0.68	0.13	0.05	1	1-8	
HI72	4	1.33	0.82	3.47	0.10	...	95	0.95	0.97	0.49	2	1-68	
HI278	2	1.15	0.76	3.59	0.16	...	94	0.94	1.00	0.28	1	1-8	

TABLE 9. (continued)

Star	$v_* - v_H$ km s ⁻¹	$V_{HB} - V$ mag	$(B-V)_0$ mag	ΣCa Å	$\sigma(\Sigma Ca)$ Å	P_μ	P_v	f_p	f_r	w	N	Run- Night	Notes
HII25	-137	1.14	0.64	4.49	0.17	...	0	0.00	0.35	0.00	2	1-6	
HI124	15	1.09	0.85	3.20	0.14	...	94	0.94	0.93	0.30	2	1-6	
HI243	-26	0.92	0.86	3.26	0.18	...	88	0.88	1.00	0.20	2	1-6	
NGC 6101													
A9,M3777	173	3.26	1.56	4.40	0.07	...	99	0.99	0.94	0.77	3	2-7	10
A5,M7333	183	3.12	1.64	4.27	0.06	...	99	0.99	0.95	1.00	3	2-7	10
A2,M8739	158	2.56	1.23	3.49	0.17	...	99	0.99	1.00	0.18	3	2-7	
A12,M2727	176	2.40	1.17	3.23	0.10	...	99	0.99	0.99	0.47	3	2-7	
A28,M7051	154	2.38	1.14	3.20	0.12	...	99	0.99	0.99	0.35	3	2-7	
A41,M4581	176	2.30	1.10	3.57	0.09	...	99	0.99	1.00	0.53	3	2-8	
A39,M4374	172	2.28	1.14	3.27	0.09	...	99	0.99	1.00	0.56	3	2-8	
A13,M2800	185	2.21	1.12	3.34	0.12	...	99	0.99	1.00	0.32	3	2-7	
A33,M7592	180	2.00	1.08	2.68	0.15	...	99	0.99	0.95	0.22	3	2-7	
A7,M6231	150	2.00	0.93	2.34	0.18	...	99	3	2-7	0,4
A10,M3517	168	1.61	1.02	2.79	0.11	...	99	0.99	1.00	0.40	3	2-8	
A11,M3673	189	1.06	0.82	2.10	0.24	...	99	3	2-8	0,4
NGC 6121 = M 4													
L4511	-1	1.83	1.23	4.96	0.03	99	97	0.97	1.00	1.00	4	1-7,2-4	
L4201	5	1.74	1.02	4.58	0.03	99	97	0.97	0.87	0.89	5	1-57,2-4	
L4414	14	1.65	0.97	4.63	0.05	99	97	0.97	0.97	0.84	2	1-57	
L4633	4	1.65	1.00	4.53	0.07	99	97	0.97	0.92	0.60	1	1-7	
L1408	22	1.63	1.05	4.56	0.07	99	96	0.96	0.95	0.64	1	1-7	
L4310	-4	1.39	1.04	4.90	0.03	99	96	0.96	0.99	1.00	5	1-57,2-4	
L4208	5	1.37	1.07	4.72	0.03	99	97	0.97	1.00	0.99	4	1-5,2-4	
L1403	-1	1.32	1.10	4.74	0.08	99	97	0.97	1.00	0.59	1	1-7	
L4630	14	1.26	1.06	4.82	0.06	99	97	0.97	0.99	0.78	2	1-7	
L4207	-1	0.98	0.95	4.40	0.03	99	97	0.97	1.00	0.99	4	1-5,2-4	
L4415	20	0.88	1.02	4.30	0.04	99	96	0.96	1.00	0.90	3	1-57	
L2301	-31	0.82	1.17	5.39	0.04	...	79	0.00	0.11	0.00	4	1-7,2-4	
L4413	-6	0.80	0.94	4.30	0.08	99	97	0.97	1.00	0.59	1	1-5	
L4416	20	0.54	0.98	4.26	0.07	99	96	0.96	1.00	0.66	2	1-57	

TABLE 9. (continued)

Star	$v_* - v_H$ km s ⁻¹	$V_{HB} - V$ mag	$(B-V)_0$ mag	ΣCa Å	$\sigma(\Sigma Ca)$ Å	P_μ	P_v	f_p	f_r	w	N	Run- Night	Notes
L4508	-14	0.51	0.94	4.41	0.03	99	95	0.95	0.97	0.96	5	1-7,2-4	
L4509	-7	0.47	0.95	4.34	0.04	99	96	0.96	0.99	0.93	4	1-7,2-4	
L2305	0	0.39	1.02	4.25	0.04	99	97	0.97	1.00	0.92	4	1-7,2-4	
L3419	3	0.38	0.95	4.36	0.05	99	97	0.97	0.96	0.81	3	2-4	
L2404	1	0.37	0.94	4.16	0.04	99	97	0.97	1.00	0.91	3	2-4	
NGC 6144													
A89	38	2.84	1.33	4.15	0.04	...	99	0.99	0.98	1.00	3	2-1	
A97	42	2.36	1.12	3.57	0.09	...	99	0.99	0.97	0.58	3	2-1	
A75	29	1.92	1.13	3.48	0.09	...	99	0.99	1.00	0.61	3	2-1	
A59	-139	1.73	1.21	5.12	0.09	...	0	0.00	0.00	0.00	3	2-1	
A66	-194	1.29	0.92	4.91	0.11	...	0	0.00	0.00	0.00	3	2-1	
A67	30	1.27	0.94	3.17	0.12	...	99	0.99	0.99	0.40	3	2-1	
A9	-220	1.08	0.93	4.82	0.12	...	0	0.00	0.00	0.00	4	2-1	
A10	37	0.91	0.83	2.65	0.11	...	99	0.99	0.98	0.49	4	2-1	
A56	17	0.60	0.90	2.55	0.13	...	99	0.99	1.00	0.39	3	2-1	
A57	-73	0.48	0.84	3.21	0.20	...	0	0.00	0.33	0.00	3	2-1	
NGC 6171 = M 107													
SC	-14	3.91	0.84	5.05	0.14	94	94	1	1-8	0,6
SF	11	2.31	1.37	5.45	0.09	98	95	0.95	1.00	0.83	1	1-5	
SH	-5	1.86	1.28	5.16	0.09	97	96	0.96	1.00	0.76	1	1-5	
SI	-4	1.81	1.13	5.15	0.09	97	96	0.96	1.00	0.78	2	1-58	
S62	17	1.73	1.29	5.13	0.07	97	94	0.94	1.00	1.00	2	1-58	
SJ	3	1.73	1.25	5.25	0.13	94	96	0.96	1.00	0.50	1	1-8	
SK	10	1.66	1.15	4.93	0.10	98	95	0.95	0.99	0.74	1	1-5	
SL	-19	1.66	1.14	4.75	0.11	98	93	0.93	0.88	0.54	1	1-5	
S278	5	1.56	1.15	4.98	0.12	98	96	0.96	1.00	0.55	1	1-5	
S100	-2	1.49	1.07	4.96	0.09	97	96	0.96	1.00	0.81	1	1-8	
SO	-30	1.32	1.11	4.83	0.12	94	86	0.86	1.00	0.53	1	1-5	
S205	23	1.14	1.12	4.96	0.15	96	92	0.92	0.98	0.38	1	1-8	
SR	22	1.04	0.95	4.27	0.14	97	93	0.93	0.83	0.36	1	1-5	
S63	25	0.96	1.02	4.72	0.10	96	91	0.91	1.00	0.69	2	1-58	

TABLE 9. (continued)

Star	$v_* - v_H$ km s ⁻¹	$V_{HB} - V$ mag	$(B-V)_0$ mag	ΣCa Å	$\sigma(\Sigma Ca)$ Å	P_μ	P_v	f_p	f_r	w	N	Run- Night	Notes
SU	-9	0.92	0.95	4.44	0.22	97	95	0.95	1.00	0.21	1	1-8	
SS	4	0.91	1.07	4.88	0.15	83	96	0.96	0.94	0.40	1	1-5	
S203	15	0.48	0.99	4.61	0.19	96	95	0.95	0.96	0.27	1	1-8	
S70	-7	-0.15	0.85	4.50	0.18	96	95	1	1-5	
NGC 6218 = M 12													
RI-3-06	3	2.39	1.15	5.20	0.07	...	96	0.96	1.00	0.85	1	1-4	
RII-2-47	13	1.94	0.93	4.98	0.07	...	95	0.95	1.00	0.88	1	1-7	
RI-2-65	27	1.53	0.90	4.81	0.05	...	92	0.92	1.00	1.00	3	1-14	
RI-2-86	-80	1.31	0.91	5.26	0.06	...	0	0.00	0.73	0.00	5	1-147	
RI-2-42	72	1.14	0.96	5.11	0.11	...	5	0.05	0.89	0.02	1	1-4	
RI-2-91	-4	0.87	0.91	4.31	0.06	...	96	0.96	1.00	0.94	5	1-147	
RII-2-55	1	0.47	0.90	4.51	0.11	...	96	0.96	0.97	0.52	1	1-7	
RII-2-54	-13	0.39	0.83	4.41	0.13	...	94	0.94	0.99	0.43	1	1-7	
RI-3-37	47	0.12	0.75	3.50	0.17	...	67	0.67	0.98	0.20	2	1-1	
RI-3-36	3	0.10	0.83	3.75	0.12	...	96	0.96	1.00	0.46	3	1-14	
RI-2-49	42	0.10	0.82	4.61	0.18	...	77	0.77	0.88	0.18	1	1-4	
RI-2-96	1	-0.01	0.83	3.91	0.14	...	96	2	1-1	
RI-3-57	15	-0.01	0.72	3.99	0.15	...	95	2	1-1	
RI-3-54	-8	-0.02	0.67	4.84	0.18	...	95	2	1-1	0,5,10
RI-3-43	-49	-0.13	0.79	4.01	0.16	...	38	2	1-7	
RI-3-42	-6	-0.30	0.71	3.96	0.15	...	95	2	1-1	
RI-2-87	5	-0.37	0.75	3.95	0.17	...	96	2	1-1	
RII-2-44	-3	-0.47	0.77	3.45	0.19	...	96	1	1-7	
RI-4-28	-25	-0.57	0.68	3.92	0.20	...	89	2	1-7	
RI-3-15	58	-1.85	0.53	4.20	0.22	...	34	1	1-4	0
NGC 6235													
L71	-19	2.26	1.27	5.35	0.09	...	94	0.94	0.94	0.79	3	2-3	
L75	16	2.08	1.20	4.92	0.08	...	97	0.97	1.00	1.00	3	2-3	
L12	33	1.76	0.95	4.48	0.08	...	96	0.96	0.99	0.93	3	2-3	
L37	81	1.45	0.89	4.04	0.12	...	41	0.41	0.92	0.23	3	2-3	
L69	83	1.30	1.00	4.63	0.09	...	35	0.35	0.99	0.30	3	2-3	

TABLE 9. (continued)

Star	$v_* - v_H$ km s ⁻¹	$V_{HB} - V$ mag	$(B-V)_0$ mag	$\Sigma C a$ Å	$\sigma(\Sigma C a)$ Å	P_μ	P_v	f_p	f_r	w	N	Run- Night	Notes
L53	89	1.15	0.98	5.18	0.12	...	20	0.20	0.38	0.05	3	2-3	
L72	-64	1.05	0.61	4.66	0.20	...	25	0.25	0.97	0.07	3	2-3	4
L74	-28	1.02	0.62	4.07	0.13	...	91	0.91	1.00	0.51	3	2-3	4
L125	-76	0.85	0.89	5.17	0.12	...	6	0.06	0.24	0.01	3	2-3	
L160	-190	0.80	0.78	5.16	0.15	...	0	0.00	0.30	0.00	3	2-3	
L104	-199	0.57	0.92	2.96	0.12	...	0	0.00	0.35	0.00	3	2-3	
L101	60	0.28	0.86	3.46	0.14	...	84	0.84	0.99	0.43	3	2-3	
L102	-152	0.10	0.65	4.94	0.17	...	0	0.00	0.21	0.00	3	2-3	
NGC 6254 = M 10													
HI367	19	2.20	1.23	4.59	0.07	...	97	0.97	0.99	0.77	1	1-7	
III217	10	1.72	1.15	4.48	0.07	...	97	0.97	1.00	0.78	1	1-7	
HI115	9	1.68	1.09	4.51	0.05	...	97	0.97	1.00	0.93	3	1-47	
HI222	7	1.67	1.08	4.51	0.07	...	97	0.97	1.00	0.78	1	1-4	
HI251	14	1.65	1.17	4.70	0.04	...	97	0.97	0.99	1.00	3	1-47	
HI246	14	1.38	0.94	3.85	0.07	...	97	0.97	0.87	0.67	2	1-47	
HI363	11	1.30	1.05	4.63	0.07	...	97	0.97	0.94	0.73	1	1-7	
HI113	8	1.11	1.01	4.03	0.07	...	97	0.97	1.00	0.79	3	1-47	
HI199	6	0.79	0.95	4.24	0.06	...	97	0.97	0.97	0.85	2	1-4	
HI166	-2	0.70	0.89	3.75	0.07	...	97	0.97	1.00	0.76	2	1-4	
HI174	7	0.69	0.84	3.72	0.07	...	97	0.97	1.00	0.74	2	1-4	
HI361	3	0.64	0.93	3.93	0.11	...	97	0.97	1.00	0.49	1	1-7	
III139	10	0.58	0.81	3.48	0.12	...	97	0.97	0.99	0.40	1	1-4	
III154	17	0.39	0.93	3.60	0.09	...	97	0.97	1.00	0.59	1	1-4	
III103	-5	0.26	0.88	4.00	0.07	...	96	0.96	0.92	0.69	3	1-4	
NGC 6266 = M 62													
A7	-16	2.97	1.54	5.84	0.04	...	95	0.95	1.00	0.95	3	2-6	
A5	-2	2.91	1.58	5.73	0.04	...	96	0.96	1.00	1.00	3	2-6	
A124	31	1.84	1.13	4.95	0.08	...	91	0.91	1.00	0.59	3	1-6	
A14	26	1.70	1.13	5.29	0.11	...	93	0.93	0.99	0.41	2	1-6	
A27	-10	1.66	0.96	4.70	0.06	...	96	0.96	0.96	0.73	5	1-6,2-6	
A195	41	1.61	1.02	5.11	0.11	...	85	0.85	1.00	0.39	2	1-6	

TABLE 9. (continued)

Star	$v_* - v_H$ km s ⁻¹	$V_{HB} - V$ mag	$(B-V)_0$ mag	ΣCa Å	$\sigma(\Sigma Ca)$ Å	P_μ	P_v	f_p	f_r	w	N	Run-Night	Notes
A191	176	1.55	0.95	4.73	0.12	...	0	0.00	1.00	0.00	2	1-6	
A115	-1	1.53	1.09	4.99	0.08	...	96	0.96	1.00	0.64	3	1-6	
A199	5	1.52	0.90	4.42	0.14	...	96	0.96	0.92	0.30	2	1-6	
A131	21	1.38	1.12	4.60	0.10	...	94	0.94	0.99	0.51	2	1-6	
A206	-16	1.32	1.02	5.14	0.07	...	94	0.94	0.95	0.66	10	1-6,2-6	
A24	-23	1.30	1.07	4.85	0.07	...	93	0.93	1.00	0.73	5	1-6,2-6	
A44	26	0.99	0.95	4.41	0.06	...	96	0.96	1.00	0.82	6	1-6,2-6	
A178	-84	0.55	1.06	5.91	0.13	...	7	0.07	0.09	0.00	2	1-6	
A201	39	0.55	0.35	4.61	0.18	...	86	0.86	0.99	0.20	3	2-6	
A147	0	0.40	0.50	3.09	0.14	...	96	3	2-6	0,9
A42	-23	0.35	0.99	4.59	0.08	...	92	0.92	0.91	0.54	6	1-6,2-6	
A188	12	0.19	0.85	4.39	0.19	...	95	0.95	0.99	0.19	2	1-6	
A140	3	-0.39	0.78	4.70	0.13	...	96	3	2-6	0,10
NGC 6273 = M 19													
H63	2	2.85	1.35	4.12	0.04	...	99	0.99	0.94	1.00	3	2-5	
H75	-191	2.69	1.56	6.89	0.08	...	0	0.00	0.02	0.00	3	2-5	
H458	-28	2.24	1.17	3.92	0.09	...	90	0.90	1.00	0.54	3	2-5	
H504	29	2.14	0.90	3.82	0.05	...	99	0.99	0.99	0.95	3	2-5	
H72	-5	2.12	1.27	4.25	0.05	...	98	0.98	1.00	0.96	3	2-5	
H444	-22	2.00	1.18	4.30	0.08	...	95	0.95	0.98	0.69	3	2-5	
H486	25	1.84	0.85	4.11	0.06	...	99	0.99	0.99	0.87	3	2-5	
H120	42	1.35	1.05	3.63	0.09	...	98	0.98	1.00	0.65	3	2-5	
H77	36	1.05	0.77	2.87	0.16	...	99	0.99	0.97	0.29	3	2-5	
H493	-17	1.03	0.83	3.32	0.07	...	96	0.96	1.00	0.74	3	2-5	
H415	-158	0.97	0.84	5.05	0.10	...	0	0.00	0.09	0.00	3	2-5	
H438	21	0.85	1.03	3.62	0.09	...	99	0.99	0.97	0.63	3	2-5	
NGC 6304													
H1232	-2	1.64	1.45	5.81	0.07	...	98	0.98	1.00	1.00	3	2-6	
H3244	-17	1.58	1.32	5.61	0.10	...	98	0.98	0.94	0.62	3	2-6	
H1208	-3	1.52	1.48	6.06	0.09	...	98	0.98	0.94	0.72	3	2-6	
H3238	88	1.26	1.40	6.03	0.10	...	0	0.00	0.76	0.00	3	2-6	

TABLE 9. (continued)

Star	$v_* - v_H$ km s ⁻¹	$V_{HB} - V$ mag	$(B-V)_0$ mag	ΣCa Å	$\sigma(\Sigma Ca)$ Å	P_μ	P_v	f_p	f_r	w	N	Run- Night	Notes
H1235	109	1.16	0.50	3.38	0.16	...	0	0.00	0.01	0.00	3	2-6	
H4220	6	1.14	1.34	5.84	0.09	...	98	0.98	0.92	0.69	3	2-6	
H3213	-16	1.07	1.11	5.42	0.10	...	98	0.98	1.00	0.69	3	2-6	
H4232	-2	0.99	1.21	5.52	0.08	...	98	0.98	1.00	0.82	3	2-6	
H1209	-24	0.91	1.11	5.60	0.11	...	98	0.98	0.99	0.60	3	2-6	
H4106	-4	0.89	1.27	5.43	0.11	...	98	0.98	1.00	0.57	3	2-6	
H3224	31	0.51	0.93	5.05	0.12	...	87	0.87	1.00	0.44	3	2-6	
H3223	-23	0.50	1.19	5.02	0.14	...	98	0.98	1.00	0.44	3	2-6	
H4243	8	0.05	1.01	4.94	0.13	...	98	0.98	1.00	0.45	3	2-6	
H4244	33	0.03	1.00	4.70	0.12	...	85	0.85	0.99	0.44	3	2-6	
H1213	-60	-0.07	0.92	5.68	0.33	...	70	2	2-6	
NGC 6352													
A1	116	3.49	1.23	7.22	0.05	...	0	2	1-58	0,3
A10	190	2.96	0.75	5.83	0.07	...	0	2	1-58	0,2
A181,H37	-23	2.06	1.52	5.79	0.05	...	99	0.99	0.97	0.97	3	2-8	
A166,H55	-18	1.99	1.47	5.79	0.05	...	99	0.99	0.98	1.00	3	2-8	
A7,H113	-7	1.89	1.59	6.08	0.03	...	99	7	1-35,2-8	0,3
A35	-1	1.36	1.20	5.81	0.06	...	98	0.98	0.99	0.85	4	1-358	
A118,H161	18	1.36	1.25	5.55	0.13	...	95	0.95	1.00	0.39	2	1-3	
S126,H72	-5	0.88	1.14	5.16	0.13	...	99	0.99	1.00	0.38	1	1-8	
A4,H129	-29	0.87	0.99	5.32	0.14	...	99	0.99	1.00	0.35	1	1-5	
S27,A140,H142	-3	0.80	1.17	5.59	0.05	...	98	0.98	0.93	0.89	6	1-58,2-8	
S15,A119,H162	-12	0.76	1.22	4.93	0.08	...	99	0.99	0.97	0.65	3	1-35	
A9,H111	-19	0.67	1.01	5.31	0.08	...	99	0.99	1.00	0.67	3	1-58	
S204,A73,H211	-14	0.46	1.20	5.28	0.09	...	99	0.99	0.99	0.64	4	1-35	
S101,A101,H186	-11	0.35	1.07	4.85	0.11	...	99	0.99	1.00	0.50	3	1-35	
S9,A120,H163	78	0.35	1.09	5.19	0.10	...	0	0.00	0.99	0.00	3	1-35	
S173,A172,H48	15	0.32	1.11	4.99	0.14	...	96	0.96	1.00	0.34	2	1-8	
S213,A72,H213	-25	0.17	0.97	4.80	0.11	...	99	0.99	1.00	0.47	4	1-35	
S74,A187,H33	5	0.08	1.02	4.53	0.13	...	98	0.98	0.99	0.39	2	1-8	
A6,H118	-13	0.01	0.89	5.34	0.16	...	99	0.99	0.86	0.25	2	1-3	
A11	-15	-0.14	0.74	5.10	0.21	...	99	2	1-3	0,5
A5,H125	0	-0.15	0.62	4.79	0.18	...	98	2	1-3	0,5

TABLE 9. (continued)

Star	$v_* - v_H$ km s ⁻¹	$V_{HB} - V$ mag	$(B-V)_0$ mag	ΣCa Å	$\sigma(\Sigma Ca)$ Å	P_μ	P_v	f_p	f_r	w	N	Run- Night	Notes
NGC 6366													
P301	-61	1.40	1.06	4.95	0.15	...	24	0.24	0.40	0.03	1	1-4	
P168	15	1.21	1.40	5.23	0.09	...	98	0.98	0.90	0.66	1	1-4	
P118	-2	0.92	1.16	5.18	0.11	...	99	0.99	1.00	0.53	1	1-4	
P224	8	0.72	1.05	5.15	0.11	...	99	0.99	1.00	0.58	1	1-4	
P465	13	0.31	1.10	4.88	0.07	...	98	0.98	1.00	1.00	2	1-4	
P423	-9	0.25	0.96	5.07	0.09	...	98	0.98	0.95	0.73	2	1-4	
P266	1	0.24	0.96	4.84	0.14	...	99	0.99	1.00	0.40	1	1-4	
P215	32	0.23	0.93	4.72	0.11	...	95	0.95	0.99	0.55	2	1-4	
P330	22	0.19	0.94	4.88	0.16	...	98	0.98	1.00	0.31	1	1-4	
P467	18	0.11	0.98	4.86	0.16	...	98	0.98	1.00	0.29	1	1-4	
P229	0	0.09	0.95	5.11	0.17	...	99	0.99	0.92	0.25	1	1-4	
P333	24	0.03	0.96	4.90	0.18	...	97	0.97	0.99	0.25	1	1-4	
P430	2	-0.01	1.00	4.91	0.22	...	99	1	1-4	
P438	-15	-0.03	0.98	4.64	0.20	...	98	1	1-4	
P322	14	-0.32	0.87	4.05	0.20	...	98	1	1-4	
NGC 6362													
A36	11	2.61	1.44	5.73	0.07	...	94	0.94	1.00	0.96	1	1-6	
A35	-6	2.20	1.29	5.50	0.07	...	95	0.95	1.00	1.00	1	1-6	
A6	-2	2.11	1.26	5.08	0.08	...	95	0.95	0.99	0.87	3	1-6	
A4	-4	2.02	1.16	4.76	0.09	...	96	0.96	0.82	0.62	1	1-6	
A44	-7	1.85	1.09	4.83	0.09	...	95	0.95	0.97	0.72	1	1-6	
A40	8	1.61	1.16	5.18	0.14	...	95	0.95	0.99	0.46	1	1-6	
A49	-1	1.50	1.21	5.19	0.10	...	95	0.95	0.97	0.66	1	1-6	
A43	0	1.33	1.16	4.94	0.13	...	95	0.95	1.00	0.51	1	1-6	
A55	-8	1.21	0.99	4.50	0.17	...	95	0.95	1.00	0.34	2	1-6	
A93	-5	1.21	1.16	4.88	0.17	...	96	0.96	1.00	0.32	1	1-6	
A73	-14	1.06	1.05	4.64	0.18	...	95	0.95	1.00	0.29	1	1-6	
A46	-8	1.06	1.00	4.84	0.15	...	95	0.95	0.99	0.39	1	1-6	
A47	-21	0.94	0.91	4.20	0.16	...	94	0.94	0.98	0.34	1	1-6	
A42	3	0.86	1.19	4.59	0.18	...	95	0.95	1.00	0.28	1	1-6	

TABLE 9. (continued)

Star	$v_* - v_H$ km s ⁻¹	$V_{HB} - V$ mag	$(B-V)_0$ mag	ΣCa Å	$\sigma(\Sigma Ca)$ Å	P_μ	P_v	f_p	f_r	w	N	Run- Night	Notes
NGC 6397													
A340,AB1119	7	2.82	1.13	5.90	0.10	...	95	1	1-2	0,10
A366,AB380	-31	2.14	1.00	3.32	0.05	...	85	0.85	0.91	0.83	2	1-2	
A269,AB769	2	1.64	0.89	3.34	0.08	...	96	0.96	1.00	0.56	1	1-2	
A272,AB841	-11	1.34	0.83	3.12	0.08	...	95	0.95	1.00	0.57	1	1-2	
A343,AB958,C428	26	1.32	0.85	2.98	0.07	...	90	0.90	1.00	0.61	1	1-2	
A305,AB1635	15	1.20	0.81	2.70	0.10	...	94	0.94	0.98	0.34	1	1-2	
A361,AB630	-3	1.09	0.81	2.88	0.05	...	96	0.96	1.00	1.00	2	1-2	
A322,AB1441	-5	0.97	0.78	2.76	0.05	...	95	0.95	1.00	0.99	2	1-2	
A258,AB443,C75	11	0.76	0.65	2.46	0.07	...	95	0.95	0.96	0.68	2	1-2	4
A328,AB1344	-6	0.73	0.78	2.83	0.08	...	95	0.95	1.00	0.52	2	1-2	
A256,AB439	2	0.48	0.74	2.69	0.05	...	96	0.96	0.99	0.98	2	1-2	
A169,AB797	11	0.22	0.73	2.69	0.13	...	95	0.95	0.98	0.23	1	1-2	
A264,AB574	-14	0.20	0.71	2.55	0.07	...	94	0.94	0.98	0.63	3	1-2	
A326,AB1642	7	0.13	0.76	2.56	0.11	...	95	0.95	0.98	0.31	2	1-2	
A319,AB1450	-24	-0.20	0.77	4.52	0.13	...	91	2	1-2	0,10
A365,AB424	-14	-0.28	0.68	2.22	0.10	...	94	2	1-2	
A387,AB501	-35	-0.57	0.66	2.08	0.12	...	81	3	1-2	
NGC 6496													
A213,R7	-35	1.57	1.39	5.57	0.11	...	99	0.99	0.99	0.91	1	1-7	
A50,R48	-29	1.40	1.17	5.51	0.12	...	98	0.98	1.00	0.78	2	1-7	
A67,R20	-25	1.36	1.26	5.76	0.14	...	98	0.98	0.98	0.63	2	1-7	
A168,R111/112	-35	1.33	1.27	5.64	0.11	...	99	0.99	1.00	1.00	1	1-7	
NGC 6522													
A15	-25	2.43	1.39	4.98	0.05	...	94	0.94	1.00	1.00	3	2-2	
A97	23	2.16	1.11	4.87	0.04	...	84	0.84	1.00	0.94	3	2-2	
A110	-33	1.84	1.06	4.88	0.06	...	92	0.92	0.99	0.85	3	2-2	
A116	71	1.58	0.95	4.59	0.05	...	1	3	2-2	0,1
A158	-22	1.13	0.72	3.78	0.08	...	95	0.95	0.92	0.67	3	2-2	

TABLE 9. (continued)

Star	$v_* - v_H$ km s ⁻¹	$V_{HB} - V$ mag	$(B-V)_0$ mag	ΣCa Å	$\sigma(\Sigma Ca)$ Å	P_μ	P_v	f_p	f_r	w	N	Run- Night	Notes
A27	-31	1.02	0.94	3.99	0.09	...	93	0.93	1.00	0.61	3	2-2	
A24	-19	1.01	0.92	4.53	0.08	...	95	0.95	0.93	0.66	3	2-2	
A148	-6	0.91	0.82	3.85	0.07	...	95	0.95	0.99	0.81	3	2-2	
A107	108	0.72	1.11	5.62	0.10	...	0	0.00	0.06	0.00	3	2-2	
A129	-7	0.70	1.17	3.87	0.08	...	95	0.95	1.00	0.73	3	2-2	
A46	-24	0.60	0.80	4.13	0.09	...	94	0.94	0.99	0.58	3	2-2	
NGC 6535													
L13,S304	53	2.17	1.22	3.97	0.07	...	96	0.96	1.00	1.00	1	1-7	
L63,S132	207	0.78	0.86	4.32	0.13	...	0	0.00	0.83	0.00	2	1-7	
L16,S252	7	0.70	0.94	3.45	0.19	...	99	0.99	1.00	0.24	1	1-7	
L56,S474	25	0.62	0.75	2.65	0.13	...	99	0.99	0.99	0.44	2	1-7	4
L20,S250	25	0.09	0.90	3.62	0.15	...	99	0.99	0.96	0.32	2	1-7	
L9,S400	-19	-0.08	0.85	2.86	0.16	...	99	2	1-7	
L39,S219	-14	-0.16	0.86	2.80	0.16	...	99	2	1-7	
NGC 6528													
VYII-7,O251	-230	1.50	1.34	5.84	0.08	...	0	0.00	0.91	0.00	3	2-3	
VYII-8,O355	40	1.39	1.33	6.14	0.08	...	99	0.99	1.00	1.00	3	2-3	
VYII-39,O335	-117	1.22	1.40	6.22	0.09	...	0	0.00	1.00	0.00	3	2-3	
VYI-40,O351	46	1.18	1.24	5.78	0.08	...	99	0.99	0.98	0.88	3	2-3	
VYII-4,O745	-229	0.96	0.94	5.22	0.09	...	0	0.00	0.73	0.00	3	2-3	
VYII-35,O752	-18	0.84	1.24	6.05	0.08	...	40	0.40	1.00	0.40	6	2-3	
VYII-41,O232	56	0.83	1.18	6.13	0.12	...	99	0.99	1.00	0.53	3	2-3	
VYI-36,O344	41	0.70	1.20	5.85	0.12	...	99	0.99	1.00	0.53	3	2-3	
VYI-42,O354	57	0.68	1.24	6.36	0.10	...	99	0.99	0.95	0.62	3	2-3	
VYI-37,O302	-259	0.60	1.22	5.89	0.10	...	0	0.00	1.00	0.00	3	2-3	
VYII-54,O262	-234	0.54	1.18	6.41	0.15	...	0	0.00	0.95	0.00	3	2-3	
VYII-48,O227	-337	0.50	1.21	4.97	0.11	...	0	0.00	0.83	0.00	3	2-3	
VYI-35,O380	19	0.46	1.13	5.29	0.11	...	99	0.99	0.98	0.55	3	2-3	
VYII-42	56	0.40	0.95	6.04	0.11	...	99	0.99	0.99	0.59	3	2-3	5

TABLE 9. (continued)

Star	$v_* - v_H$ km s ⁻¹	$V_{HB} - V$ mag	$(B-V)_0$ mag	ΣCa Å	$\sigma(\Sigma Ca)$ Å	P_μ	P_v	f_p	f_r	w	N	Run- Night	Notes
NGC 6544													
A37	-11	1.34	1.22	4.65	0.07	...	95	0.95	0.99	1.00	1	1-8	
A33	-13	0.87	0.85	3.59	0.08	...	95	0.95	0.84	0.76	1	1-8	
A74	-17	0.78	0.98	4.09	0.10	...	96	0.96	1.00	0.78	1	1-8	
A67	-13	0.77	0.81	3.67	0.14	...	95	0.95	0.98	0.51	1	1-8	
A92	-20	0.63	0.84	3.85	0.10	...	96	0.96	1.00	0.74	1	1-8	
A46	-33	0.34	0.62	3.60	0.11	...	94	0.94	1.00	0.67	1	1-8	
A38	8	0.14	0.73	3.77	0.12	...	90	0.90	1.00	0.59	1	1-8	
A59	-15	0.11	1.05	4.00	0.07	...	96	0.96	0.93	0.93	1	1-8	
A88	-21	0.10	0.73	3.66	0.11	...	96	0.96	1.00	0.67	1	1-8	
A48	-43	0.01	0.68	3.42	0.15	...	92	0.92	1.00	0.47	1	1-8	
A49	-2	0.00	0.77	3.68	0.16	...	94	0.94	1.00	0.43	1	1-8	
NGC 6541													
AII-76	-14	2.65	1.26	4.52	0.07	...	99	0.99	1.00	1.00	1	1-7	
AI-66	-5	2.26	1.08	4.07	0.07	...	99	0.99	0.99	1.00	1	1-7	
AII-72	-15	2.09	1.04	4.02	0.10	...	99	0.99	1.00	0.58	1	1-7	
AII-10	2	1.93	1.07	3.66	0.12	...	99	0.99	0.86	0.38	1	1-7	
AII-49	-15	1.83	1.03	3.95	0.10	...	99	0.99	1.00	0.58	1	1-7	
AII-47	-5	1.70	0.98	4.02	0.12	...	99	0.99	0.96	0.44	1	1-7	
AII-65	155	1.67	1.12	5.71	0.14	...	0	0.00	0.01	0.00	1	1-7	
AI-65	-10	1.53	0.94	3.90	0.17	...	99	0.99	0.99	0.24	1	1-7	
AII-33	-25	1.25	0.83	3.47	0.18	...	99	0.99	1.00	0.24	1	1-7	
AII-36	-1	1.14	0.83	3.42	0.14	...	99	0.99	1.00	0.36	1	1-7	
NGC 6553													
III-44,O665	33	1.73	1.38	6.18	0.07	...	95	0.95	1.00	0.89	3	2-8	
III-33,O1253	67	1.63	1.24	6.37	0.11	...	85	0.85	1.00	0.52	3	2-8	
III-17,O85	18	1.58	1.48	5.97	0.09	...	93	0.93	1.00	0.64	3	2-8	
III-51,O110	37	1.37	1.44	6.17	0.06	...	95	0.95	1.00	1.00	5	2-8	
III-48,O118	35	1.37	1.48	6.38	0.11	...	95	0.95	0.95	0.54	2	2-8	

TABLE 9. (continued)

Star	$v_* - v_H$ km s ⁻¹	$V_{HB} - V$ mag	$(B-V)_0$ mag	$\Sigma C a$ Å	$\sigma(\Sigma C a)$ Å	P_μ	P_v	f_p	f_r	w	N	Run- Night	Notes
HIV-11,O429	44	1.31	1.47	5.66	0.10	...	95	0.95	0.97	0.60	3	2-8	
HII-54,O117	83	1.05	1.18	5.28	0.13	...	51	0.51	0.88	0.20	3	2-8	
HII-92,O77	39	0.79	1.14	5.47	0.13	...	95	0.95	1.00	0.42	3	2-8	
HII-91,O71	70	0.78	1.17	6.02	0.16	...	81	0.81	0.97	0.27	3	2-8	
HII-32,O390	200	-0.14	1.77	6.08	0.14	...	0	2	2-8	0,3
NGC 6624													
LIV34,R545	1	1.60	1.18	5.68	0.12	...	95	0.95	1.00	0.55	1	1-5	
LIV150	-55	1.43	0.85	5.09	0.10	...	70	0.70	0.43	0.23	2	1-4	
LIV21,R520	-45	1.36	1.18	4.70	0.17	...	86	2	1-5	0,7,8
LII36,R56	5	1.21	1.01	5.46	0.12	...	94	0.94	1.00	0.60	2	1-45	
LIII7,R50	-8	1.21	1.10	5.48	0.13	...	96	0.96	1.00	0.51	2	1-4	
LI33,R485	6	1.02	1.05	5.18	0.16	...	94	0.94	1.00	0.34	1	1-5	
LII111,R129	-3	1.01	1.01	5.36	0.10	...	95	0.95	1.00	0.71	2	1-5	7
LIV122,R566	-27	0.96	0.93	5.03	0.20	...	95	0.95	0.99	0.24	1	1-5	
Le,R18	-128	0.87	0.91	5.17	0.18	...	0	0.00	1.00	0.00	1	1-4	
LIII27,R159	11	0.86	1.01	5.48	0.14	...	91	0.91	0.95	0.39	2	1-5	
LI141,R483	-20	0.85	0.90	5.08	0.15	...	96	0.96	1.00	0.37	2	1-4	
LII43,R54	-9	0.71	0.97	5.34	0.08	...	96	0.96	0.91	1.00	3	1-45	
LI34,R477	3	0.61	0.83	4.97	0.21	...	94	0.94	1.00	0.21	1	1-5	
LI127,R600	-10	0.53	0.92	4.74	0.15	...	96	0.96	0.96	0.38	2	1-4	
LI153,R332	15	0.37	0.88	5.18	0.17	...	90	0.90	0.96	0.29	2	1-4	
LIII22,R102	12	0.27	0.99	4.61	0.20	...	91	0.91	0.99	0.23	2	1-5	
LI102	-19	0.19	1.03	4.61	0.18	...	96	0.96	1.00	0.30	2	1-4	
LII110,R147	-50	0.13	0.89	5.05	0.17	...	80	0.80	0.95	0.24	2	1-5	
LII45,R51	-45	-0.17	0.61	4.47	0.25	...	86	1	1-5	0,1,5
NGC 6626													
A2-11	11	2.04	1.14	4.32	0.09	...	94	1	1-8	0,9
A2-36	12	1.57	1.10	5.14	0.11	...	94	0.94	1.00	0.67	1	1-8	
2-127	-4	1.33	1.01	4.42	0.13	...	86	0.86	0.84	0.39	1	1-8	
A2-121	37	1.24	1.05	4.71	0.10	...	95	0.95	1.00	0.77	2	1-8	
A1-30	40	1.23	0.96	5.16	0.13	...	95	0.95	0.97	0.47	1	1-8	

TABLE 9. (continued)

Star	$v_* - v_H$ km s ⁻¹	$V_{HB} - V$ mag	$(B - V)_0$ mag	$\Sigma C a$ Å	$\sigma(\Sigma C a)$ Å	P_μ	P_v	f_p	f_r	w	N	Run- Night	Notes
A2-76	30	1.13	0.98	4.55	0.08	...	96	0.96	0.98	1.00	2	1-8	
A2-69	47	0.94	0.84	4.74	0.21	...	94	0.94	1.00	0.22	1	1-8	
A2-12	-29	0.93	0.98	5.60	0.16	...	32	0.32	0.39	0.05	1	1-8	
A2-109	45	0.81	1.04	4.64	0.13	...	95	0.95	1.00	0.50	2	1-8	
A1-50	32	0.68	0.87	4.41	0.19	...	96	0.96	1.00	0.28	1	1-8	
A1-80	8	0.46	0.80	4.53	0.15	...	93	0.93	1.00	0.40	2	1-8	
A2-101	26	0.26	0.64	4.55	0.14	...	96	0.96	0.97	0.45	2	1-8	
A2-125	-2	0.06	0.78	4.00	0.15	...	88	0.88	1.00	0.38	2	1-8	
NGC 6638													
A26	24	2.22	1.36	5.55	0.08	...	95	0.95	1.00	0.94	1	1-8	
A53	25	1.89	1.35	5.40	0.11	...	95	0.95	1.00	0.72	1	1-8	
A148	113	1.65	0.98	6.16	0.19	...	0	0.00	0.78	0.00	1	1-8	
A108	-4	1.49	1.15	5.19	0.08	...	93	0.93	1.00	1.00	2	1-8	
A175	-69	1.33	1.11	5.52	0.17	...	1	0.01	0.99	0.00	1	1-8	
A161	-10	1.31	1.11	4.97	0.15	...	91	0.91	1.00	0.41	1	1-8	
A123	34	1.18	0.94	5.08	0.18	...	93	0.93	1.00	0.32	1	1-8	
A126	17	1.04	0.87	4.98	0.19	...	95	0.95	1.00	0.30	1	1-8	
A14	19	0.95	0.91	4.62	0.14	...	95	0.95	0.99	0.48	2	1-8	
A11	12	0.93	1.05	5.47	0.12	...	95	0.95	0.83	0.53	2	1-8	10
A91	37	0.93	1.08	5.39	0.12	...	92	0.92	0.91	0.53	2	1-8	10
A117	-64	0.65	1.10	4.30	0.13	...	2	0.02	0.95	0.01	3	1-8	
A120	-22	0.61	0.85	4.63	0.15	...	82	0.82	1.00	0.40	3	1-8	
NGC 6637 = M 69													
HIIn-43,R345	19	2.33	1.55	6.52	0.05	...	95	3	2-5	0,2
HIIn-42,R409	47	2.26	1.64	6.25	0.06	...	64	3	2-5	0,2
HIIn-14,S72	-13	2.19	1.53	5.99	0.04	...	94	0.94	1.00	1.00	3	2-4	
HI-41	39	1.95	1.66	5.75	0.07	...	81	3	2-4	0,1
HIIn-41,S406	-45	1.94	1.51	4.74	0.09	...	51	0.51	0.14	0.04	3	2-4	
HIIn-42,S74	-30	1.86	1.38	5.90	0.06	...	85	0.85	0.97	0.71	3	2-4	
HIVn-11,R108	-4	1.76	1.55	5.56	0.04	...	96	3	2-4	0,3
HIV-47,R107	-1	1.56	1.22	5.29	0.08	...	96	0.96	0.99	0.61	3	2-4	

TABLE 9. (continued)

Star	$v_* - v_H$ km s ⁻¹	$V_{HB} - V$ mag	$(B - V)_0$ mag	$\Sigma C a$ Å	$\sigma(\Sigma C a)$ Å	P_μ	P_v	f_p	f_r	w	N	Run- Night	Notes
HIV-34,R62	-2	1.46	1.16	5.21	0.10	...	96	0.96	0.99	0.42	3	2-4	
R116	8	1.41	1.19	5.15	0.06	...	96	0.96	0.96	0.82	3	2-4	
HIn-23,R72	-14	1.32	1.07	5.47	0.09	...	94	0.94	1.00	0.45	3	2-4	
HII-10,S60	3	1.30	1.21	5.39	0.05	...	96	0.96	1.00	0.99	8	2-45	
HIV-15,R67	-84	0.89	1.00	5.44	0.13	...	0	0.00	0.94	0.00	3	2-4	
HIV-19,R44	2	0.89	0.99	5.04	0.14	...	96	0.96	1.00	0.25	3	2-4	
HI-38,R26	-3	0.88	1.02	4.80	0.14	...	96	0.96	0.99	0.24	3	2-4	
HIn-1,S57	-4	0.77	1.08	5.29	0.10	...	96	0.96	0.95	0.41	3	2-5	
HI-12,S29	-10	0.67	0.68	4.96	0.12	...	95	3	2-5	0,4
HI-20	2	0.66	1.38	5.43	0.11	...	96	3	2-5	0,1
HI-8	1	0.20	0.85	4.61	0.10	...	96	8	2-45	0,1
HI-19,S24	16	-0.03	0.75	5.26	0.13	...	95	8	2-45	0,5
HI-11	8	-0.27	0.91	5.14	0.10	...	96	8	2-45	0,1
NGC 6681 = M 70													
H166	0	2.04	1.40	4.51	0.05	...	99	0.99	1.00	1.00	3	2-8	0,3
H153	-250	1.82	0.99	6.63	0.06	...	0	3	2-8	
H137	-259	1.53	1.13	5.76	0.24	...	0	0.00	0.01	0.00	1	2-8	
H127	-159	1.30	1.20	6.10	0.26	...	0	0.00	0.00	0.00	1	2-8	
H102	10	0.78	0.93	3.54	0.10	...	99	0.99	0.98	0.46	3	2-8	
H118	-154	0.40	1.05	4.57	0.11	...	0	0.00	0.00	0.00	3	2-8	
H83	-9	0.19	0.96	3.29	0.10	...	99	0.99	1.00	0.44	4	2-8	
H197	-227	-0.03	1.06	4.53	0.13	...	0	3	2-8	
H30	11	-0.13	0.93	3.25	0.20	...	99	5	2-8	
H193	-22	-0.17	0.85	2.77	0.18	...	99	3	2-8	
H82	-272	-0.35	0.98	4.31	0.21	...	0	2	2-8	
NGC 6712													
SB66	1	2.22	1.41	5.32	0.04	...	98	0.98	0.95	1.00	3	2-7	
SA51	5	1.98	1.30	5.34	0.06	...	98	0.98	1.00	0.79	3	2-7	
SA38	-2	1.39	1.14	5.25	0.06	...	98	0.98	0.94	0.74	3	2-7	
SA44	7	1.28	1.11	5.08	0.08	...	98	0.98	1.00	0.55	3	2-7	
SA46	7	1.04	0.84	4.80	0.06	...	98	0.98	1.00	0.78	6	2-78	

TABLE 9. (continued)

Star	$v_* - v_H$ km s ⁻¹	$V_{HB} - V$ mag	$(B-V)_0$ mag	ΣCa Å	$\sigma(\Sigma Ca)$ Å	P_μ	P_v	f_p	f_r	w	N	Run- Night	Notes
SA36	2	0.92	0.89	4.73	0.08	...	98	0.98	1.00	0.58	3	2-7	1,4
SB67	-15	0.91	0.77	4.41	0.09	...	98	0.98	0.94	0.48	3	2-7	
SB55	8	0.65	0.89	4.50	0.11	...	98	0.98	1.00	0.35	3	2-8	
SA34	152	0.06	0.96	4.89	0.14	...	0	0.00	0.50	0.00	3	2-7	
SB75	-9	0.05	0.84	4.37	0.13	...	98	0.98	0.99	0.26	3	2-7	
NGC 6717 = Pal 9													
G35	37	3.25	1.18	5.18	0.04	...	95	3	2-8	0,8
G17	19	2.95	1.23	5.53	0.05	...	95	0.95	1.00	1.00	3	2-8	
G18	-11	2.55	0.52	4.71	0.10	...	72	0.72	0.68	0.32	3	2-8	
G21	29	1.82	0.99	4.99	0.12	...	96	0.96	1.00	0.55	3	2-8	
G16	22	1.32	0.85	4.51	0.15	...	95	0.95	1.00	0.39	6	2-8	
G22	8	0.70	0.73	4.52	0.06	...	92	0.92	0.98	0.83	4	2-8	
G20	18	0.66	0.79	3.79	0.16	...	95	0.95	0.97	0.35	3	2-8	
G23	40	0.47	0.79	4.29	0.09	...	95	0.95	1.00	0.69	4	2-8	
G15	16	0.33	0.84	4.49	0.15	...	95	0.95	0.94	0.36	4	2-8	
G24	9	-0.02	0.66	4.08	0.10	...	93	4	2-8	
G14	19	-0.13	0.80	4.25	0.13	...	95	3	2-8	
NGC 6723													
MIH-45	88	2.81	1.03	5.25	0.07	...	0	0.00	0.49	0.00	3	2-5	0,1
MIV-8	-23	2.57	1.37	4.92	0.08	...	98	3	2-5	
MI-71	-22	2.55	1.52	5.71	0.04	...	98	0.98	1.00	1.00	3	2-5	
MII-9	-1	2.48	1.31	5.50	0.05	...	96	0.96	0.99	0.84	3	2-5	
MII-14	-23	2.39	1.38	5.50	0.05	...	98	0.98	1.00	0.83	3	2-5	
MII-5	8	1.51	1.06	4.99	0.08	...	93	0.93	1.00	0.48	3	2-5	0,4
MII-12	-8	1.49	1.27	5.16	0.09	...	97	0.97	1.00	0.43	3	2-5	
MI-40	-12	1.08	0.72	4.18	0.09	...	98	3	2-5	
MII-96	-2	0.97	0.97	4.50	0.10	...	96	0.96	0.99	0.38	3	2-5	
MII-38	-23	0.68	0.95	4.69	0.07	...	98	0.98	0.99	0.59	3	2-5	
MII-7	-35	0.40	0.15	5.17	0.13	...	98	3	2-5	0,5
MII-27	-4	0.06	0.89	4.68	0.13	...	97	0.97	0.83	0.21	3	2-5	10
MII-63	-39	0.01	0.56	4.07	0.25	...	98	3	2-5	0,5

TABLE 9. (continued)

Star	$v_* - v_H$ km s ⁻¹	$V_{HB} - V$ mag	$(B-V)_0$ mag	$\Sigma C a$ Å	$\sigma(\Sigma C a)$ Å	P_μ	P_v	f_p	f_r	w	N	Run- Night	Notes
MIV-45	-30	-0.10	0.85	4.12	0.17	...	98	3	2-5	
NGC 6752													
A9,B2403	16	2.58	1.16	4.54	0.07	...	95	1	1-2	0,1
A12,B2113	-8	2.46	1.31	5.11	0.08	...	95	0.95	1.00	0.64	1	1-2	
A29,B1518	8	1.86	1.10	4.59	0.07	...	95	0.95	1.00	0.81	1	1-2	
A8,B2580	5	1.71	1.08	4.40	0.06	...	95	0.95	0.98	0.89	2	1-2	
A30,B1285	6	1.55	1.02	4.22	0.09	...	95	0.95	0.94	0.53	1	1-2	
C123,B435	6	1.46	1.03	4.49	0.10	...	95	0.95	0.99	0.47	1	1-2	
A55,B2892	19	1.46	1.01	4.53	0.07	...	94	0.94	0.96	0.69	1	1-2	
A33,B1868	33	1.45	0.98	4.17	0.20	...	88	0.88	0.99	0.14	1	1-2	
C107,B4991	-2	1.36	1.05	4.29	0.05	...	95	0.95	1.00	1.00	2	1-2	
C122,B360	14	0.98	0.96	4.10	0.15	...	95	0.95	1.00	0.25	1	1-2	
C119,B758	-9	0.71	0.89	3.71	0.10	...	94	0.94	0.98	0.46	2	1-2	
A48,B2482	-1	0.70	0.90	3.95	0.13	...	95	0.95	1.00	0.31	1	1-2	
C106,B5021	-19	0.12	0.82	3.76	0.14	...	91	0.91	0.94	0.27	2	1-2	
NGC 6809 = M 55													
L2441	0	2.68	1.26	4.27	0.04	...	99	0.99	0.98	0.85	3	2-1	
L2437	-16	2.65	1.24	4.29	0.04	...	99	0.99	1.00	0.86	3	2-1	
L1317	14	2.49	1.18	3.71	0.04	...	99	3	2-1	0,9
L2420	-9	1.92	1.09	3.97	0.04	...	99	0.99	1.00	0.87	3	2-1	
L1212	-4	1.53	1.02	3.64	0.03	...	99	0.99	1.00	1.00	6	2-12	
L2313	-50	1.37	0.90	2.82	0.08	...	95	3	2-1	0,4,9
L1113	-8	1.15	0.93	3.56	0.03	...	99	0.99	0.99	0.97	6	2-12	
L4426	-11	1.12	0.93	3.64	0.04	...	99	0.99	0.91	0.78	3	2-1	
L2314	-19	0.84	0.88	3.08	0.05	...	99	0.99	0.98	0.72	3	2-1	
L2315	-34	0.57	0.86	3.09	0.05	...	99	0.99	1.00	0.71	3	2-1	
NGC 6981 = M 72													
D6	-45	2.65	1.34	5.11	0.05	...	99	0.99	1.00	1.00	8	2-23	
D12	-66	2.32	1.21	4.70	0.06	...	99	0.99	0.96	0.82	8	2-23	

TABLE 9. (continued)

Star	$v_* - v_H$ km s ⁻¹	$V_{HB} - V$ mag	$(B-V)_0$ mag	ΣCa Å	$\sigma(\Sigma Ca)$ Å	P_μ	P_v	f_p	f_r	w	N	Run- Night	Notes
D19	-37	1.72	0.95	4.55	0.11	...	99	0.99	1.00	0.41	8	2-23	
D38	-56	1.68	1.02	4.64	0.10	...	99	0.99	1.00	0.44	3	2-3	
D47	-90	1.61	1.01	4.50	0.12	...	99	0.99	1.00	0.34	3	2-3	
D108	-63	1.61	0.94	4.28	0.13	...	99	0.99	0.99	0.29	3	2-2	
D110	-68	1.09	0.90	4.22	0.16	...	99	0.99	1.00	0.20	3	2-2	
D46	-64	0.98	0.76	4.26	0.16	...	99	0.99	1.00	0.21	3	2-2	
D48	-70	0.77	0.88	4.07	0.16	...	99	0.99	1.00	0.20	3	2-2	
D115	-71	0.53	0.86	4.43	0.15	...	99	0.99	0.95	0.21	4	2-2	10
D119	-87	0.21	0.85	4.46	0.23	...	99	0.99	0.94	0.10	4	2-2	10
D54	-59	0.14	0.80	4.36	0.16	...	99	0.99	0.86	0.19	3	2-2	10
NGC 7089 = M 2													
HI-103	9	2.56	1.25	4.75	0.06	...	95	0.95	0.99	1.00	3	2-7	
HI-104	9	2.13	1.12	4.41	0.10	...	95	0.95	0.99	0.58	3	2-7	
HI-298	8	2.04	1.13	5.09	0.13	...	95	0.95	0.91	0.32	3	2-7	
HI-8	13	1.63	1.04	4.73	0.14	...	95	0.95	0.96	0.32	2	2-8	
HI-586	18	1.14	0.84	4.14	0.11	...	95	0.95	1.00	0.50	5	2-78	
HI-53	23	1.09	0.91	3.85	0.12	...	94	0.94	1.00	0.42	3	2-7	
HI-20	-13	0.87	0.88	3.78	0.14	...	91	0.91	1.00	0.33	3	2-7	
HI-583	27	0.77	0.67	3.34	0.29	...	93	0.93	0.99	0.08	3	2-7	
HI-100	32	0.49	0.78	3.86	0.27	...	92	0.92	1.00	0.10	3	2-7	
NGC 7099 = M 30													
DP18	-19	2.51	1.19	3.48	0.04	...	99	0.99	1.00	0.99	6	2-8	
DP17	-9	2.49	1.17	3.03	0.05	...	99	0.99	0.96	0.82	6	2-8	8
DP19,AF	-6	1.96	1.00	2.91	0.04	...	99	0.99	1.00	1.00	9	2-8	
DP10,AH	-16	1.50	0.97	3.04	0.14	...	99	0.99	0.99	0.21	1	2-8	
D62,A68	178	0.78	0.68	5.06	0.12	...	0	0.00	0.01	0.00	4	2-8	
D57,A72	57	0.17	0.69	2.21	0.19	...	86	0.86	0.99	0.11	4	2-8	
D35	84	-0.23	0.64	3.68	0.30	...	13	2	2-8	

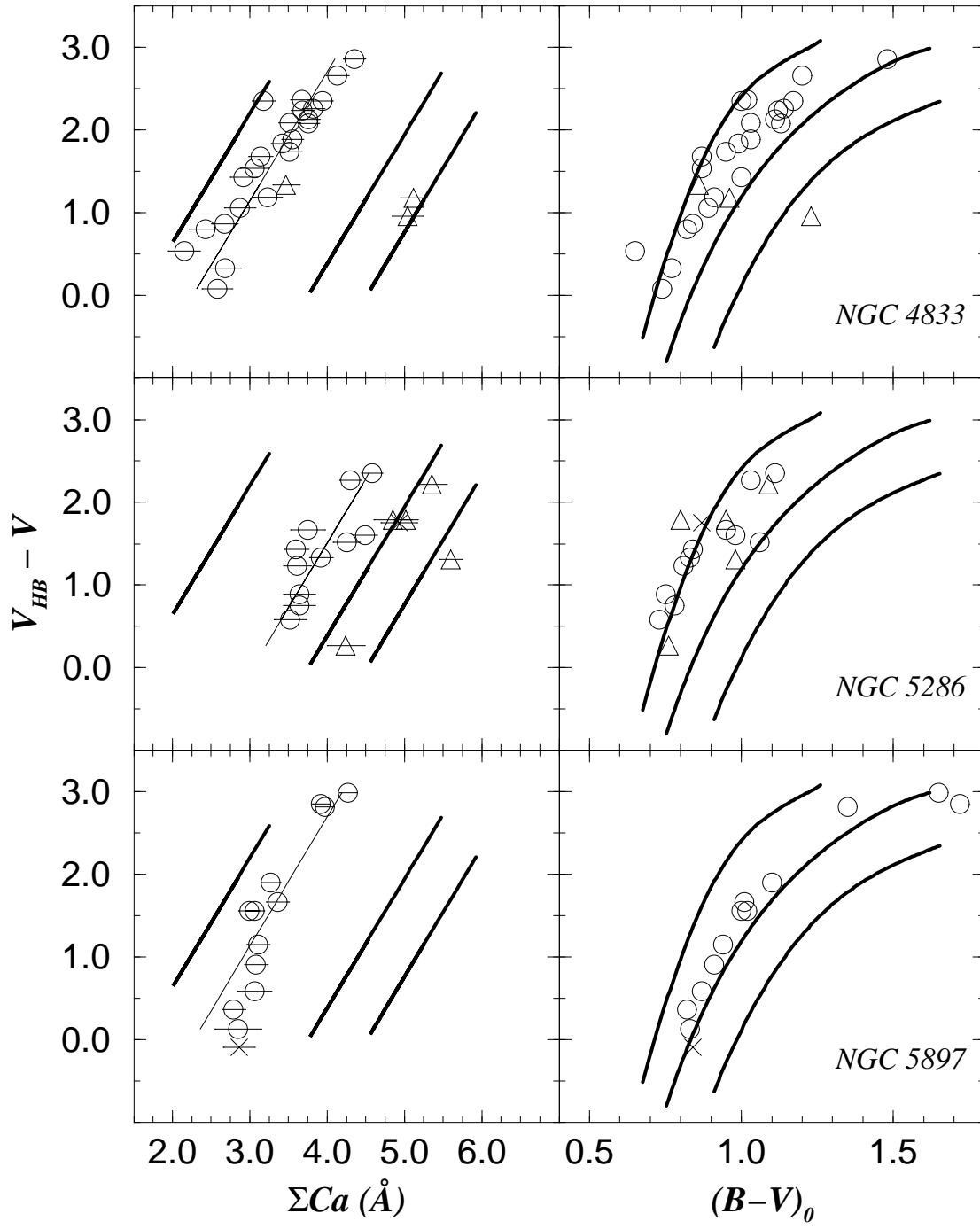
TABLE 9. (continued)

Star	$v_* - v_H$ kms ⁻¹	$V_{HB} - V$ mag	$(B-V)_0$ mag	ΣCa Å	$\sigma(\Sigma Ca)$ Å	P_μ	P_v	f_p	f_r	w	N	Run- Night	Notes
NGC 7492													
CT,B458	-25	1.95	1.15	3.80	0.12	...	99	0.99	0.98	1.00	3	2-1	
CJ,B624	-18	1.71	1.14	3.70	0.13	...	99	0.99	0.99	0.81	6	2-13	
C1-1-6,B542	10	1.49	1.04	4.32	0.13	...	99	0.99	0.99	0.88	3	2-1	
CU,B523	-71	1.40	0.99	3.71	0.18	...	99	0.99	1.00	0.48	3	2-1	
CR	11	1.25	1.10	4.17	0.13	...	98	0.98	0.99	0.85	3	2-1	8
C2-3-11,B858	-36	1.17	0.97	3.25	0.18	...	99	0.99	0.99	0.46	3	2-3	
C1-4-12,B490	-38	0.82	0.82	3.62	0.21	...	99	0.99	1.00	0.37	3	2-3	
C1-3-7,B1093	-33	0.29	0.82	3.82	0.17	...	99	0.99	0.96	0.51	3	2-3	
Pal 12													
S1118	-7	2.30	1.45	5.95	0.07	...	94	0.94	1.00	1.00	3	2-5	
S1128	-19	1.70	1.24	5.54	0.08	...	94	0.94	1.00	0.88	7	2-5	
S1305	-26	1.27	1.06	5.39	0.14	...	94	0.94	1.00	0.31	3	2-5	
H4122	-86	1.25	0.81	5.02	0.27	...	14	0.14	1.00	0.01	3	2-5	
S1337	-32	0.46	0.87	5.47	0.21	...	93	0.93	0.98	0.14	4	2-5	4,7
S1317	3	0.24	0.92	5.52	0.22	...	93	0.93	0.95	0.12	2	2-5	

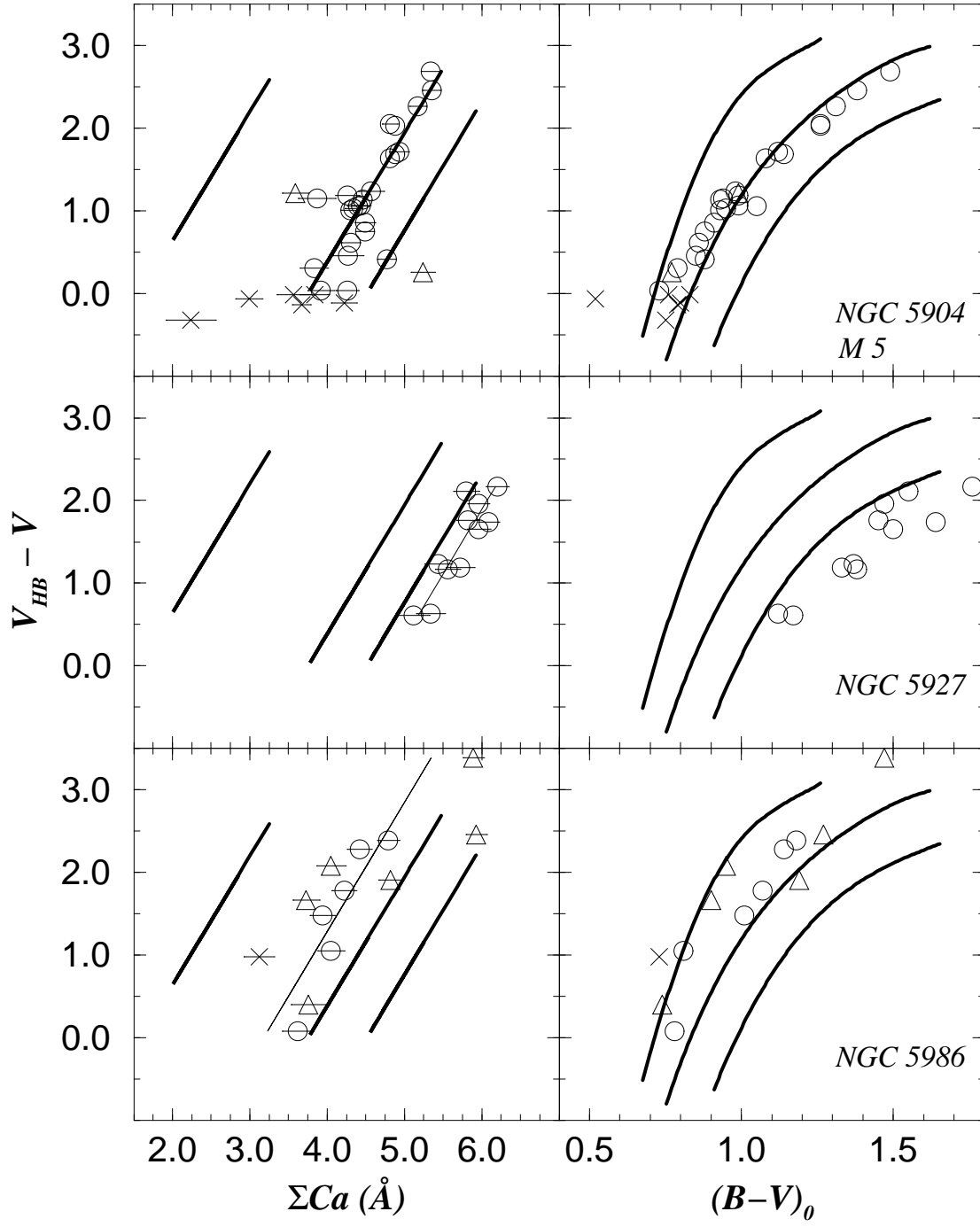
Notes to Table 9.

0. Star not used to compute reduced EW for cluster, 1. See cluster notes in Appendix A, 2. Weak TiO present, 3. Strong TiO present, 4. Possible AGB star, 5. Possible HB star, 6. Non-cluster member based on position in CMD, 7. Crowded field, 8. Uncertain ID, 9. Star has weak ΣCa for $V_{HB} - V$ position, 10. Star has strong ΣCa for $V_{HB} - V$ position, 11. SK96 suggest that line strength is variable.

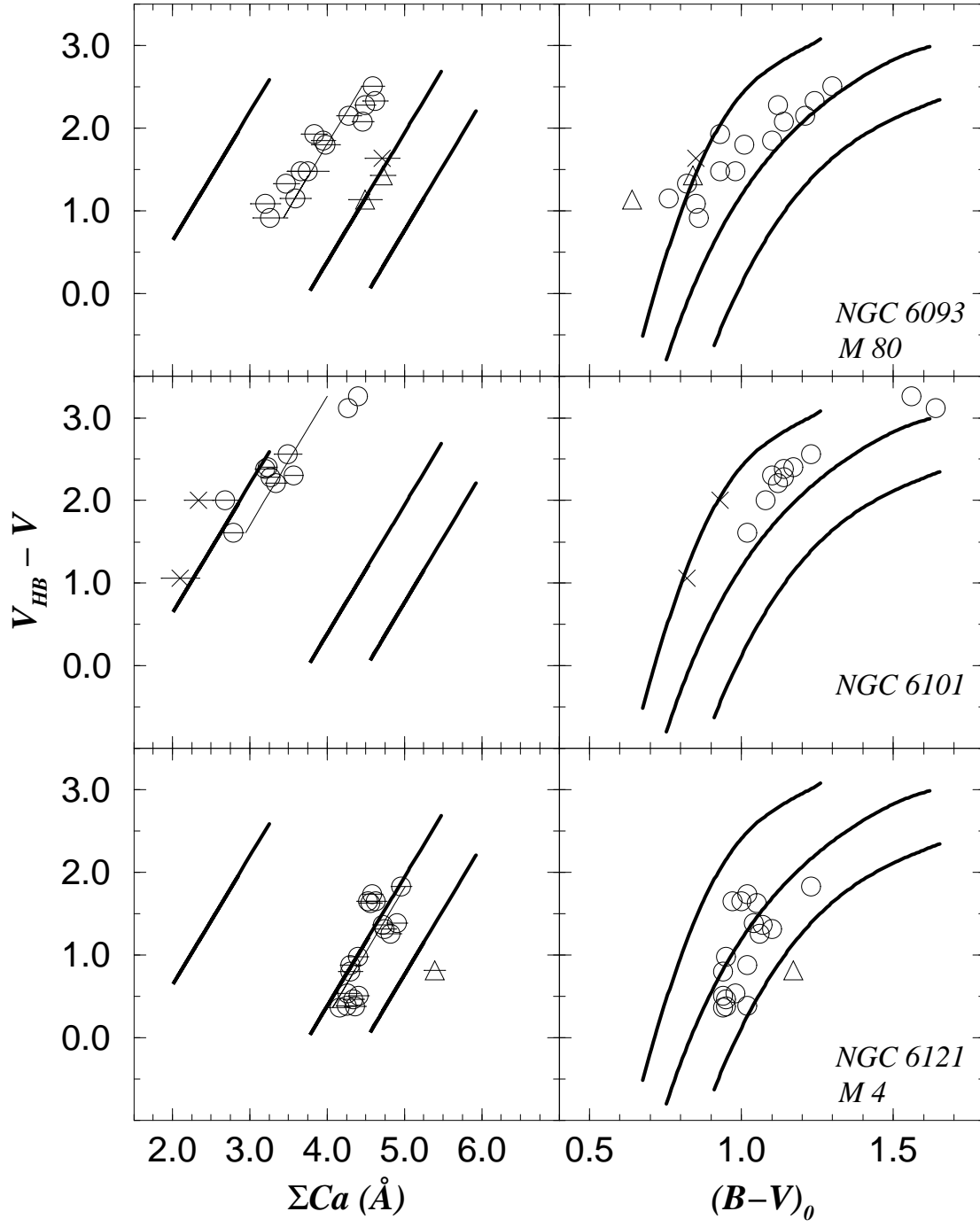
Rutledge et al.: GGC CaII Metallicity Scale -- Figure 7.



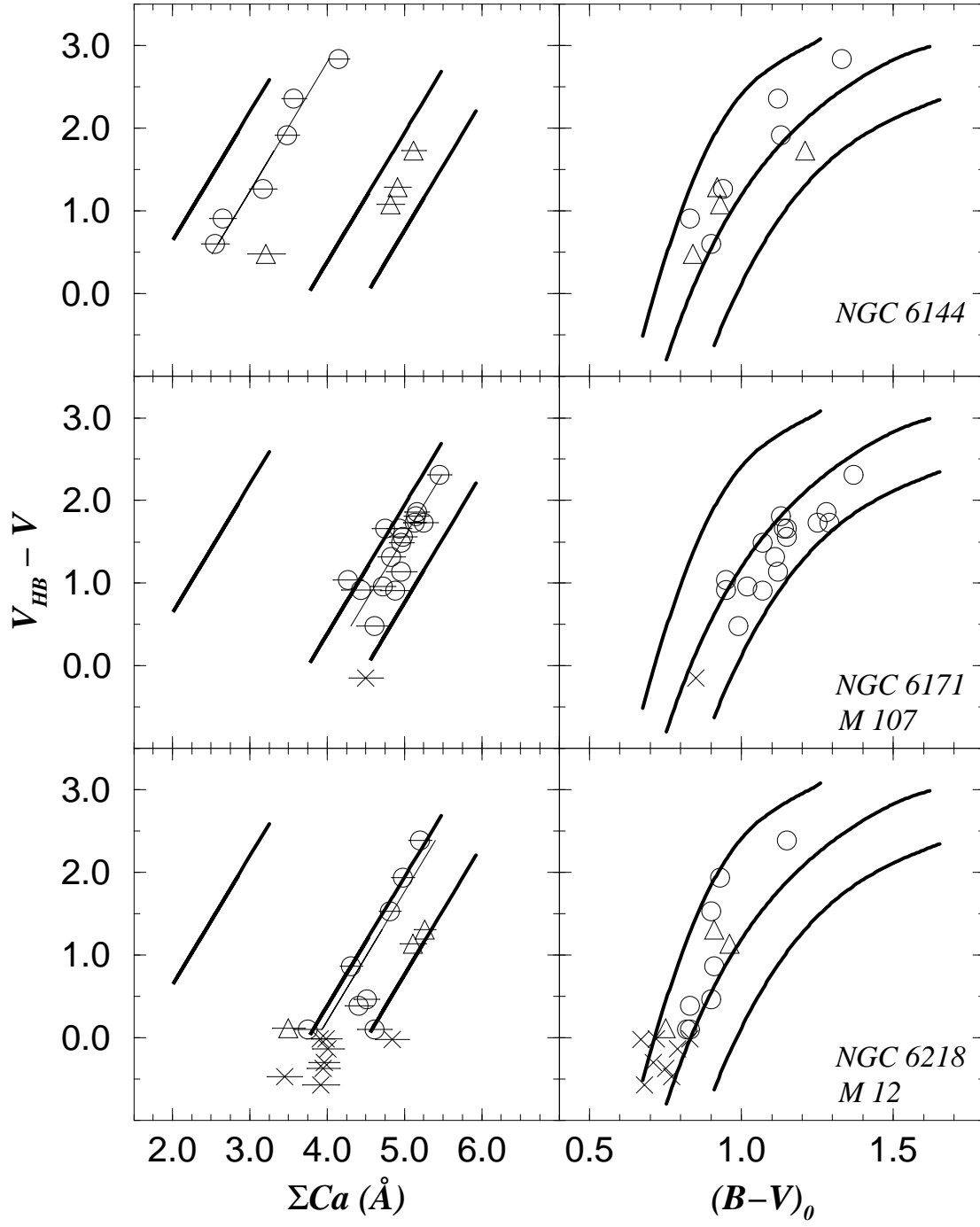
Rutledge et al.: GGC CaII Metallicity Scale -- Figure 7.



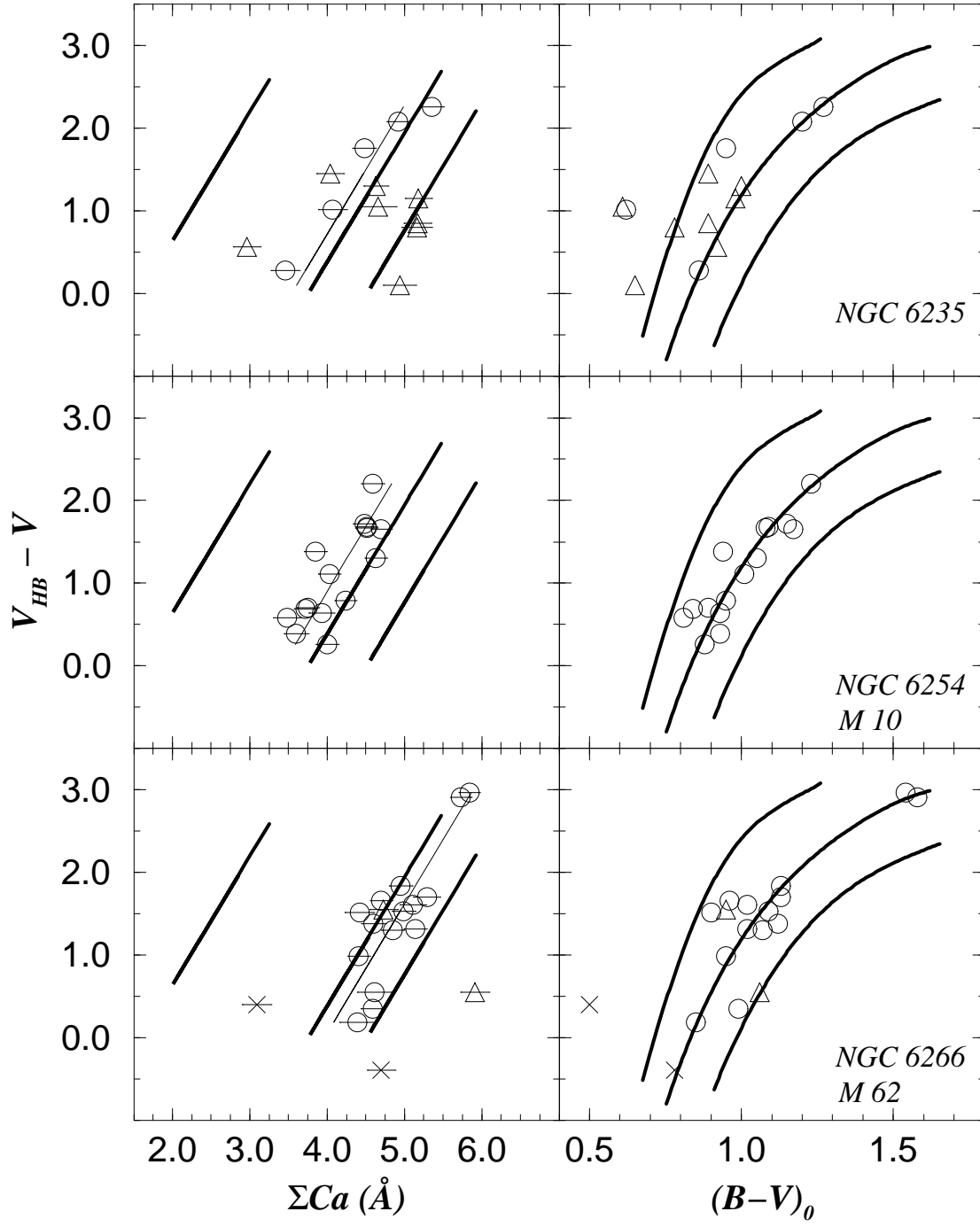
Rutledge et al.: GGC CaII Metallicity Scale -- Figure 7.



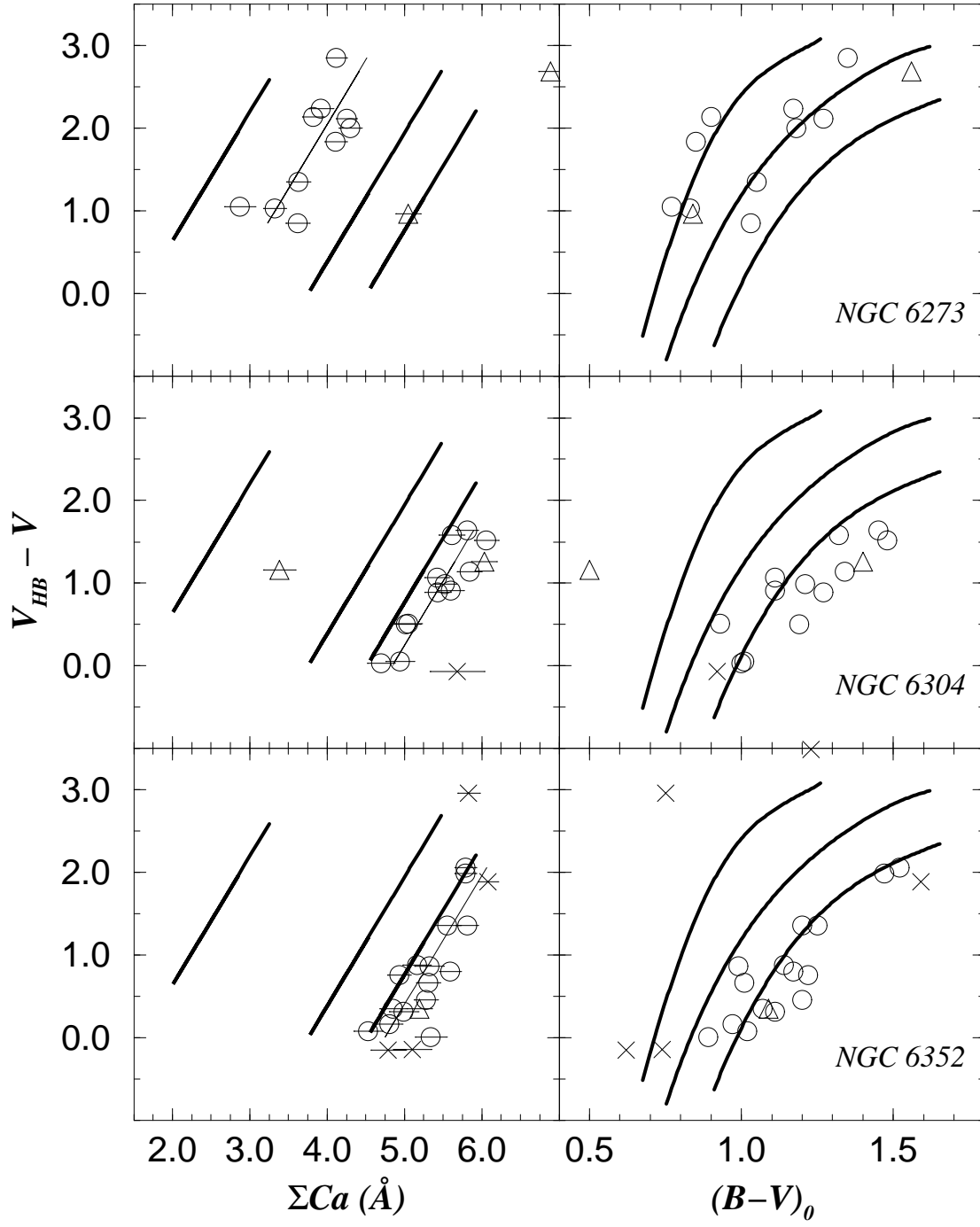
Rutledge et al.: GGC CaII Metallicity Scale -- Figure 7.



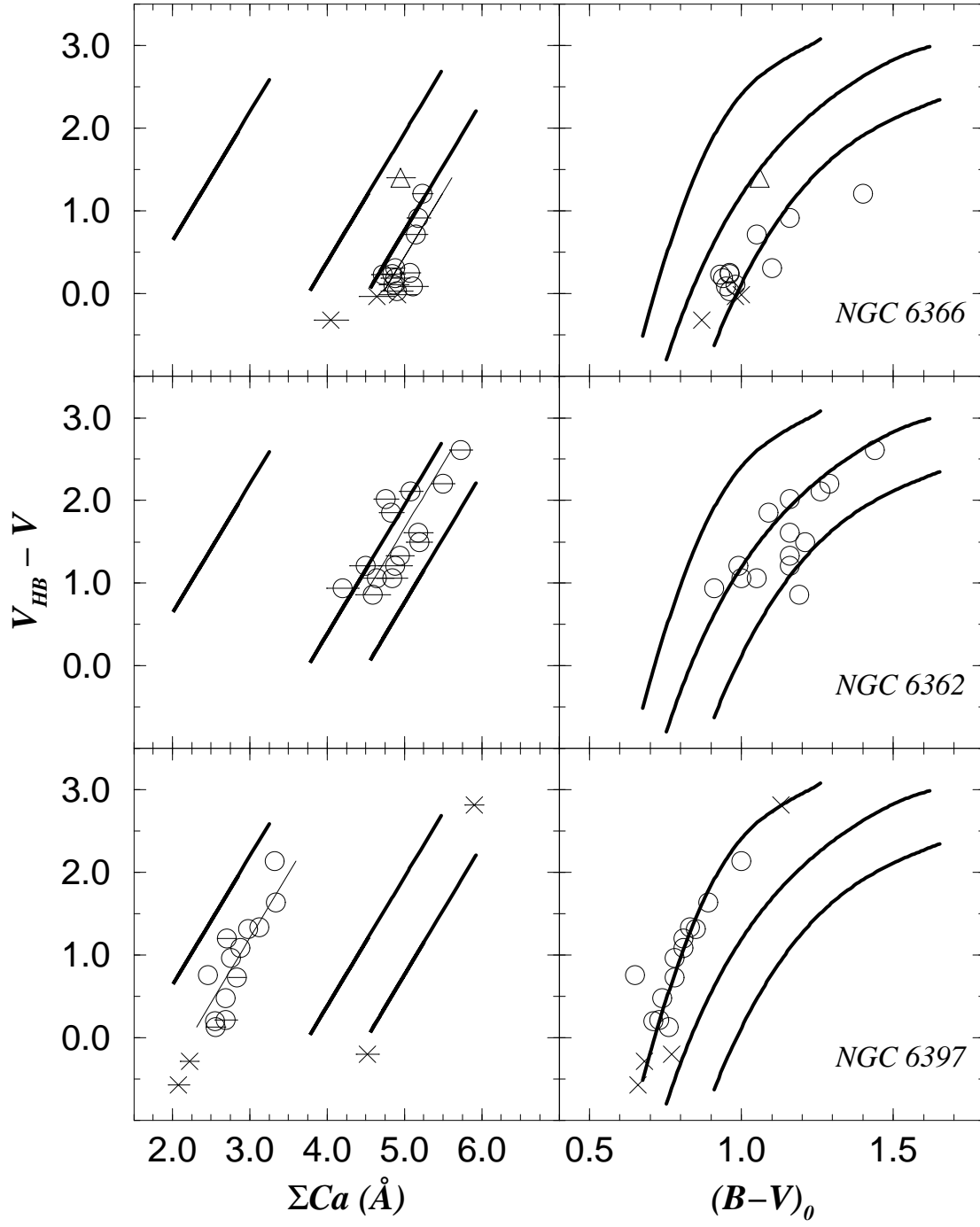
Rutledge et al.: GGC CaII Metallicity Scale -- Figure 7.



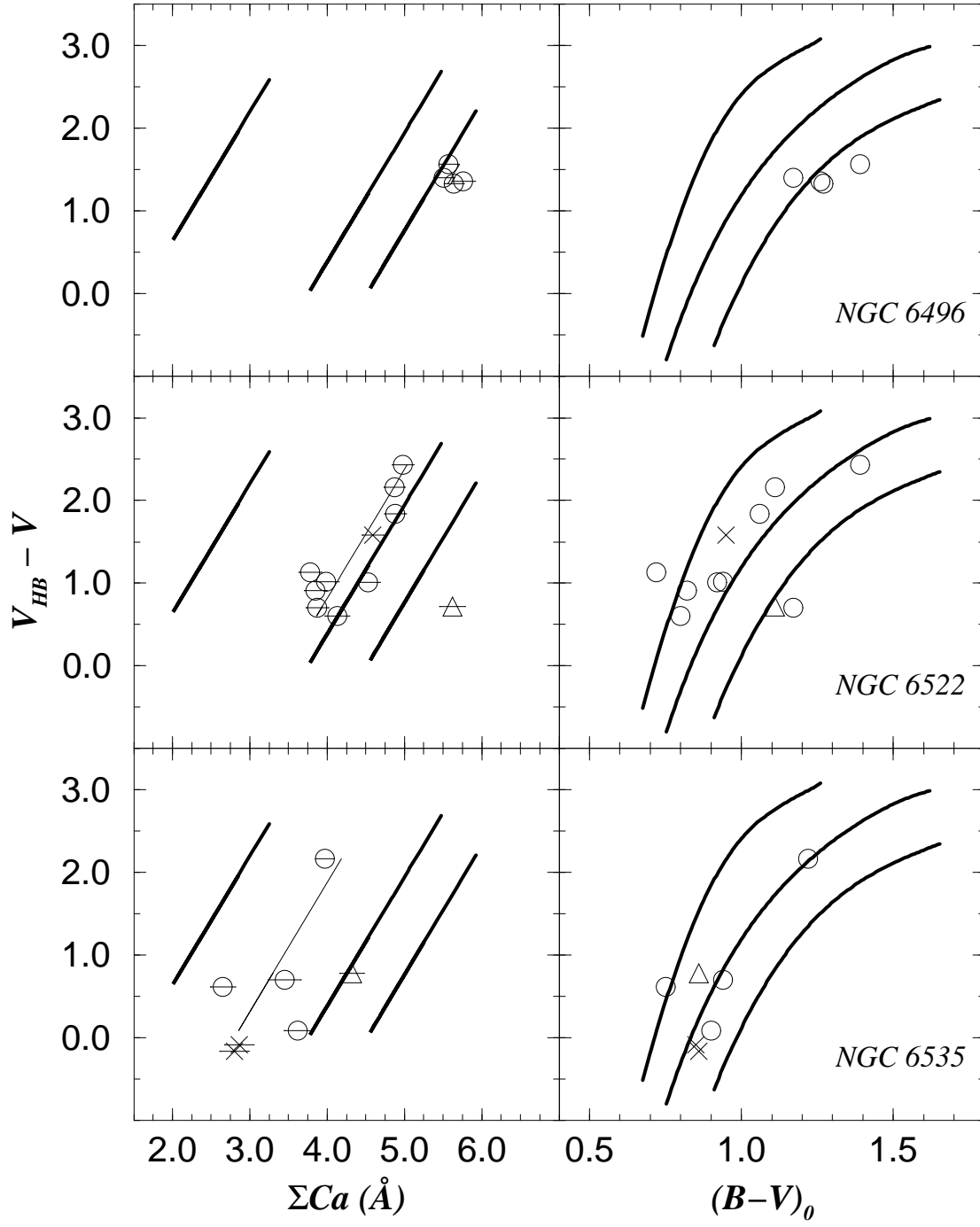
Rutledge et al.: GGC CaII Metallicity Scale -- Figure 7.



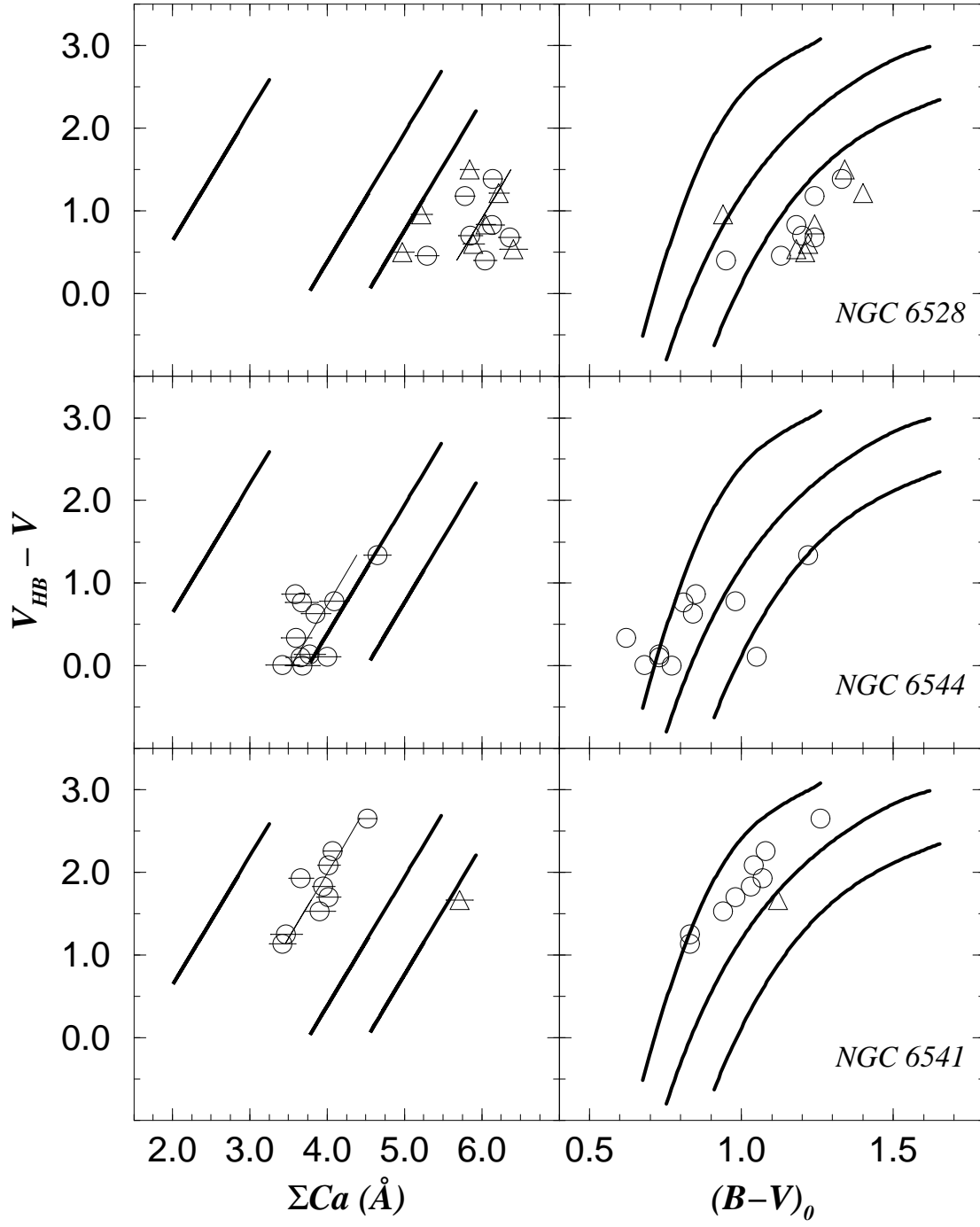
Rutledge et al.: GGC CaII Metallicity Scale -- Figure 7.



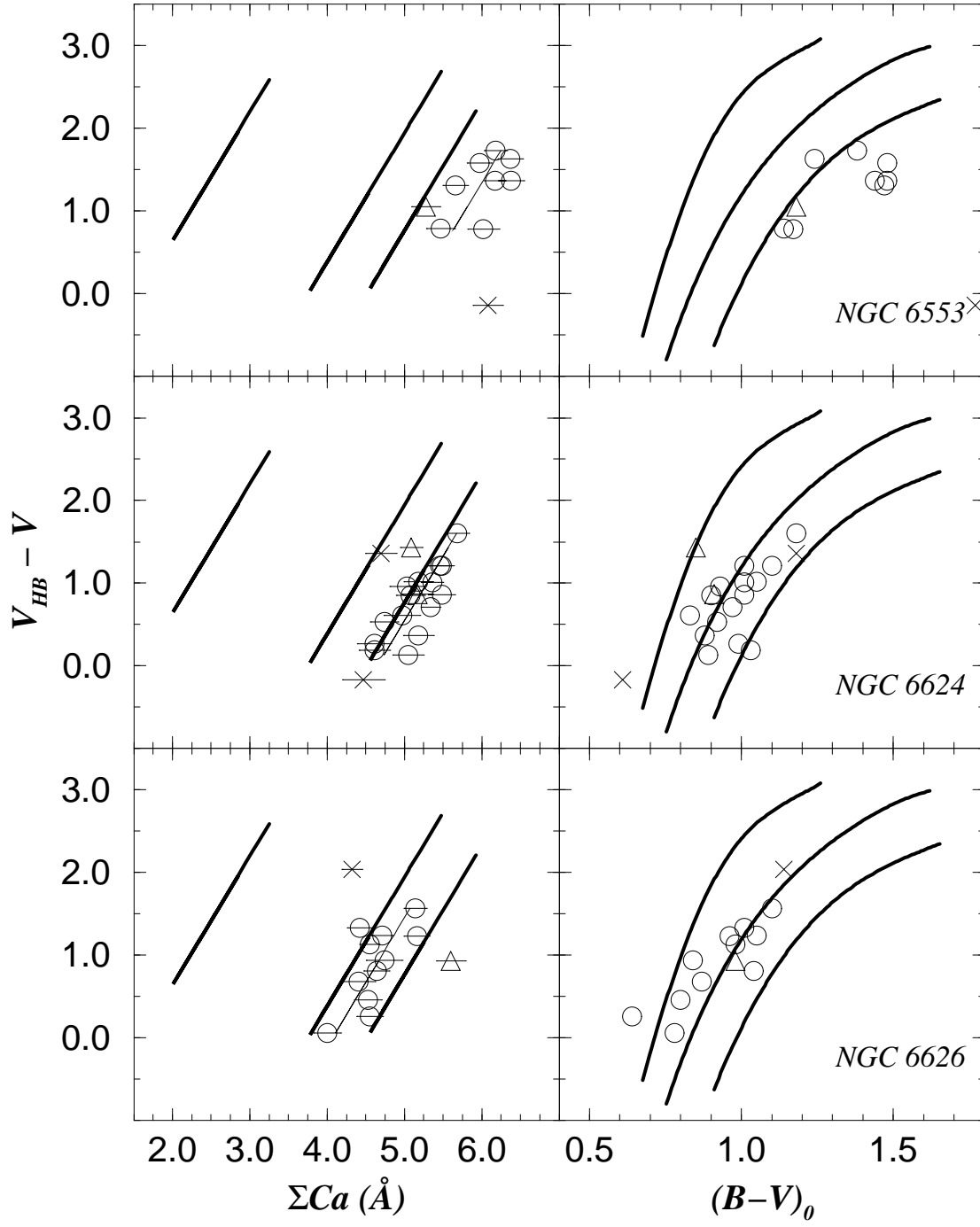
Rutledge et al.: GGC CaII Metallicity Scale -- Figure 7.



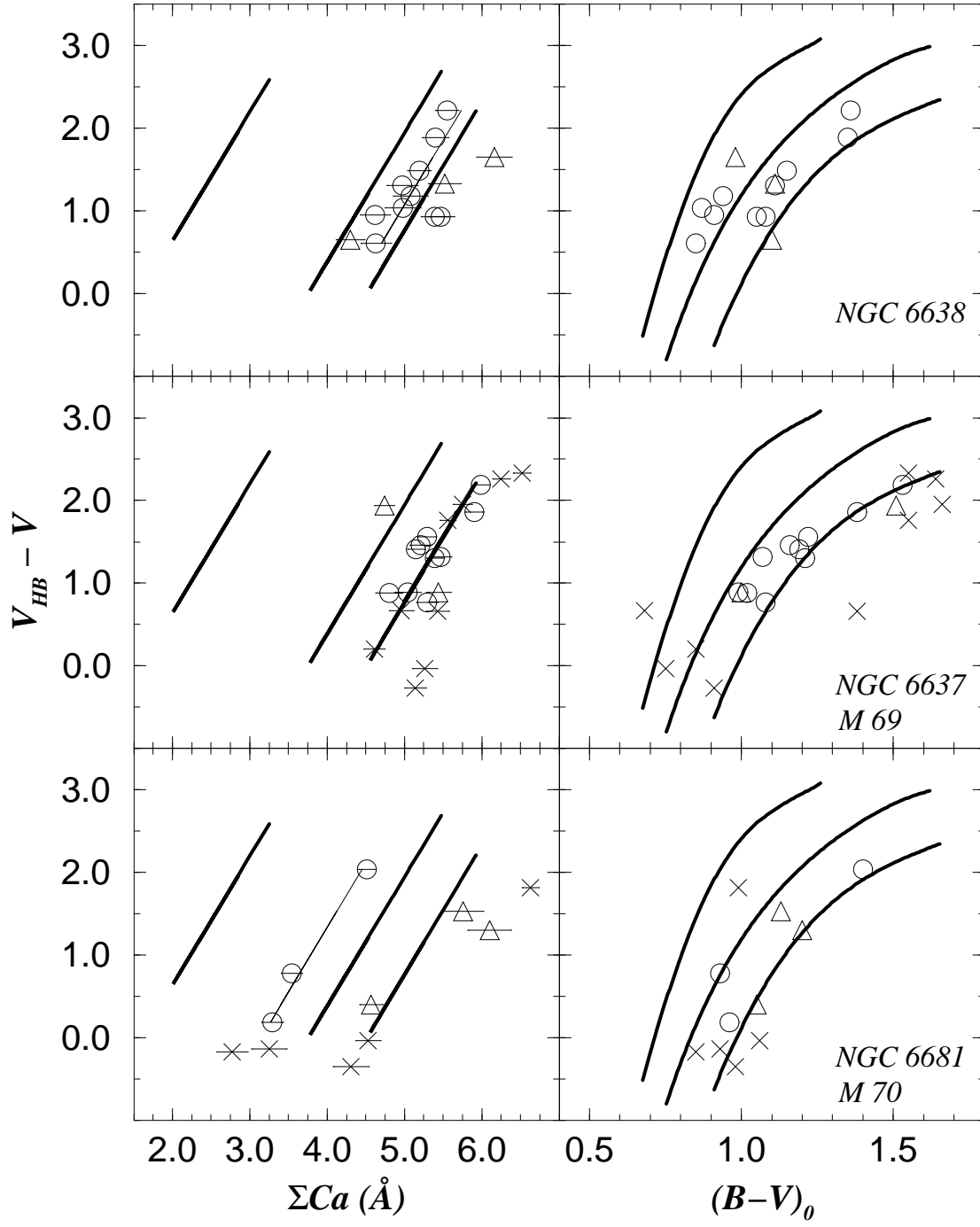
Rutledge et al.: GGC CaII Metallicity Scale -- Figure 7.



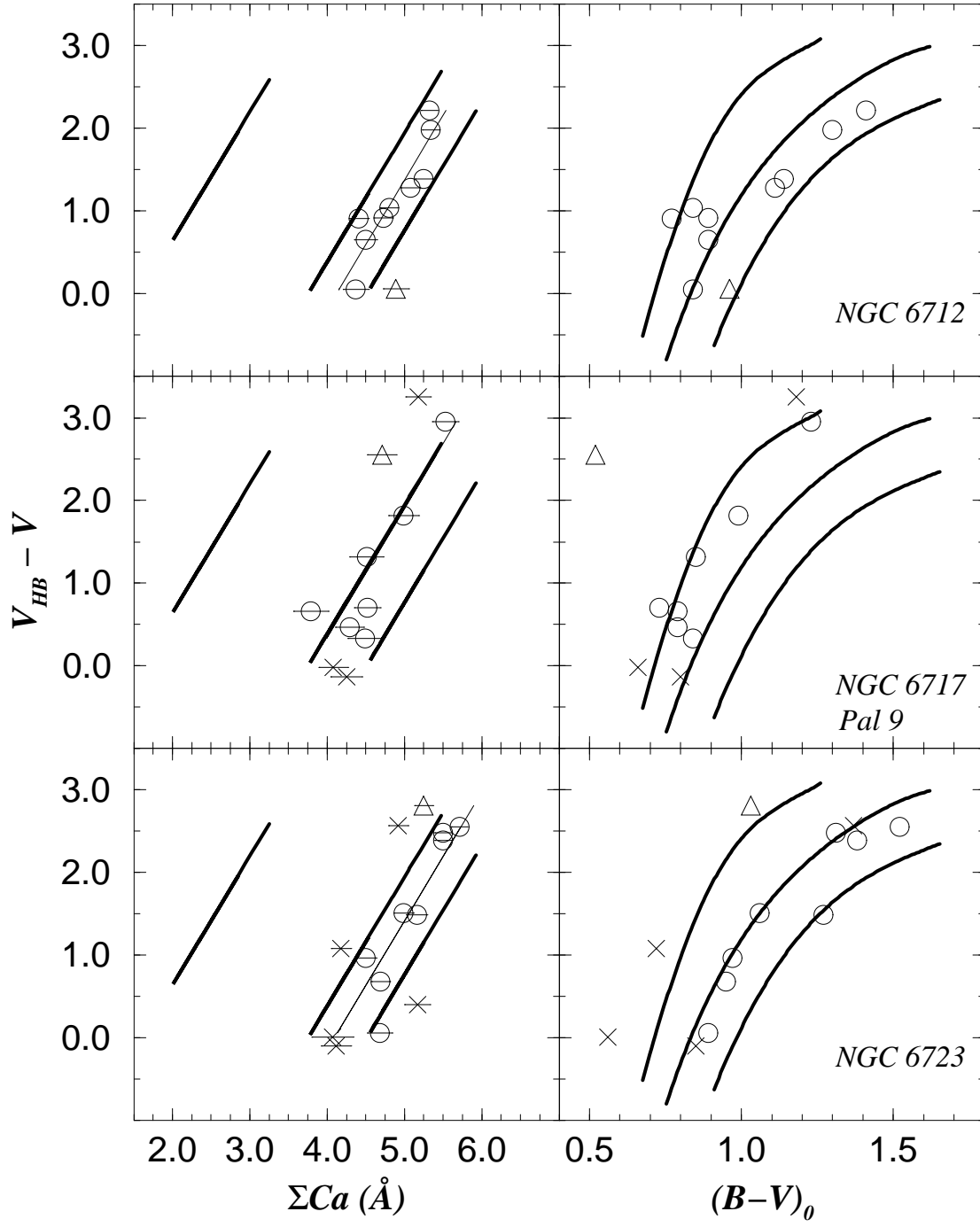
Rutledge et al.: GGC CaII Metallicity Scale -- Figure 7.



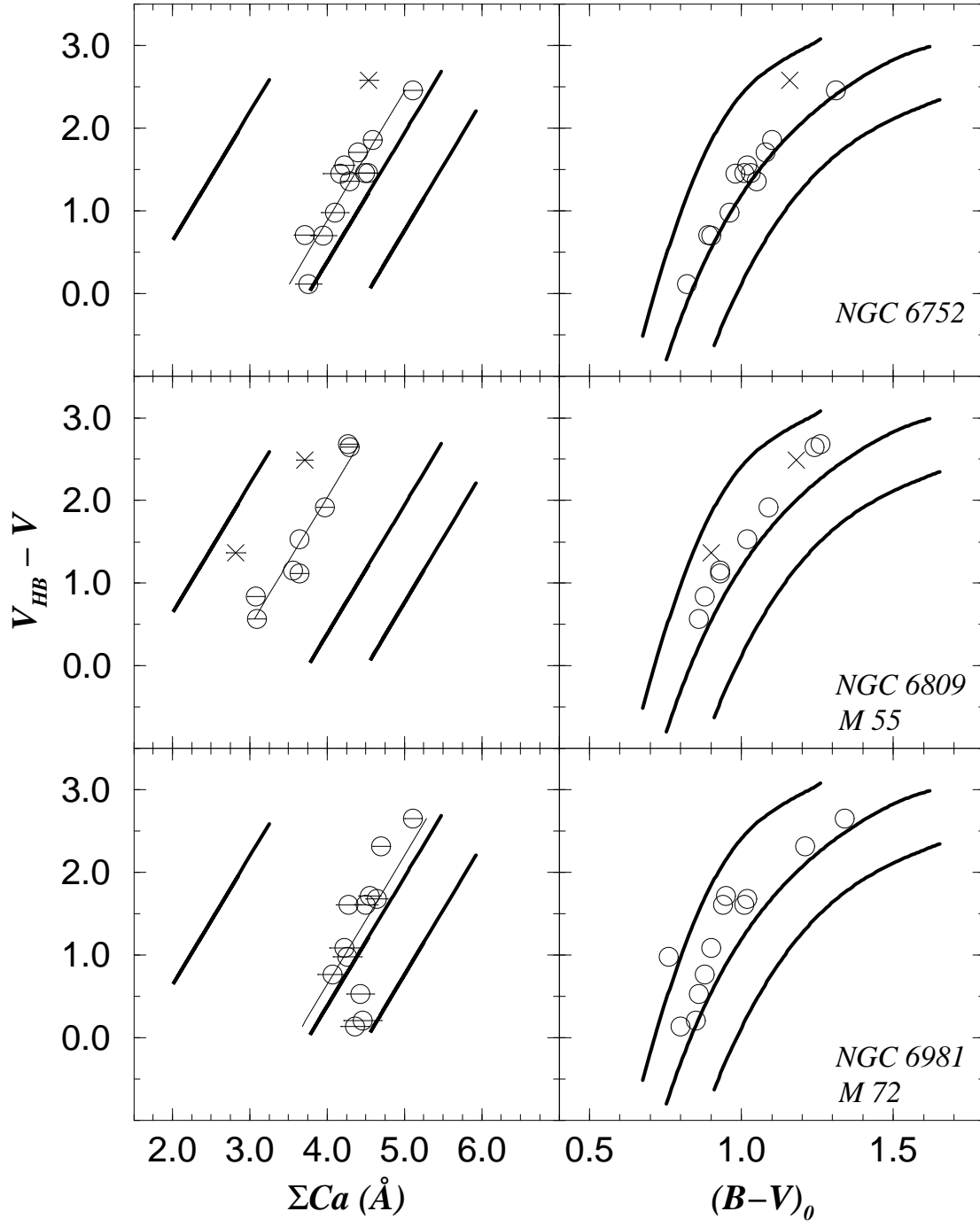
Rutledge et al.: GGC CaII Metallicity Scale -- Figure 7.



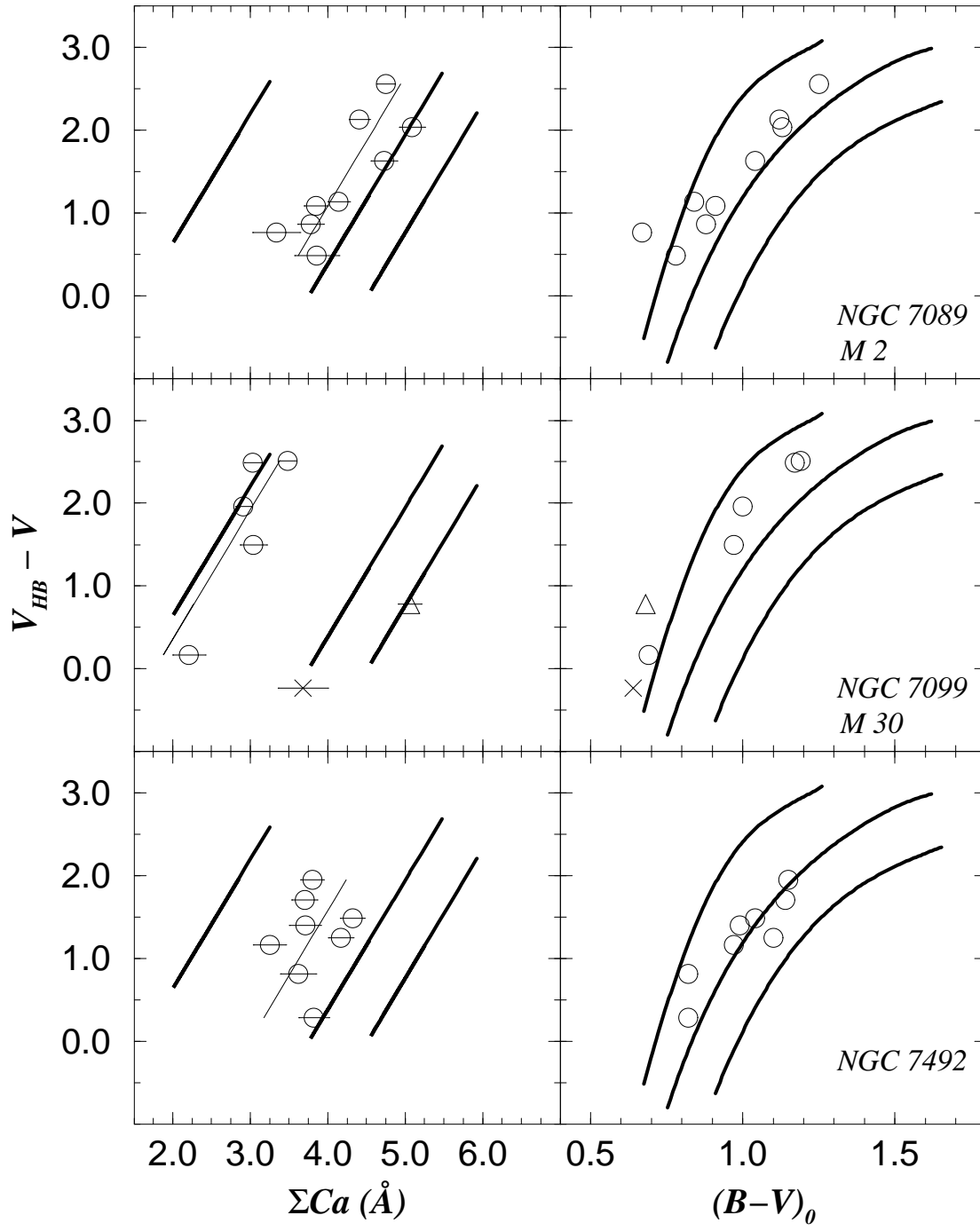
Rutledge et al.: GGC CaII Metallicity Scale -- Figure 7.



Rutledge et al.: GGC CaII Metallicity Scale -- Figure 7.



Rutledge et al.: GGC CaII Metallicity Scale -- Figure 7.



Rutledge et al.: GGC CaII Metallicity Scale -- Figure 7.

